2038-5625

Italian Journal of Agrometeorology

Rivista Italiana di Agrometeorologia

n. 2 – 2019

Poste Italiane spa - Tassa pagata - Piego di libro
Aut. n. 072/DCB/FI1/VF del 31.03.2005

FIRENZE UNIVERSITY PRESS

Italian Journal of Agrometeorology

n. 2 - 2019

Firenze University Press

The ***Italian Journal of Agrometeorology*** (***IJAm - Rivista Italiana di Agrometeorologia***) is the official periodical of the Italian Association of Agrometeorology (AIAM) and aims to publish original scientific contributions in English on agrometerology, as a science that studies the interactions of hydrological and meteorological factors with the agricultural and forest ecosystems, and with agriculture in its broadest sense (including livestock and fisheries).

SUBSCRIPTION INFORMATION
IJAm articles are freely available online, but print editions are available to paying subscribers. Subscription rates are in Eur and are applicable worldwide.
Annual Subscription: € 50,00 Single Issue: € 25,00

CONTACT INFORMATION
Please contact ordini@fupress.com, if you have any questions about your subscription or if you would like to place an order for the print edition. Information on payment methods will be provided after your initial correspondence.

Published by
Firenze University Press – University of Florence, Italy
Via Cittadella, 7 - 50144 Florence - Italy
http://www.fupress.com/ijam

Italian Journal of Agrometeorology
Rivista Italiana di Agrometeorologia

Firenze University Press
www.fupress.com/ijam

Citation: L. Verdi, M. Mancini, M. Napoli, S. Orlandini, A. Dalla Marta (2019) Soil carbon emissions from maize under different fertilization methods in an extremely dry summer in Italy. *Italian Journal of Agrometeorology* (2): 3-10. doi: 10.13128/ijam-648

Received: November 10, 2018

Accepted: March 20, 2019

Published: October 29, 2019

Data Availability Statement: All relevant data are within the paper and its Supporting Information files.

Competing Interests: The Author(s) declare(s) no conflict of interest.

Soil carbon emissions from maize under different fertilization methods in an extremely dry summer in Italy

Emissioni di carbonio dal suolo in una coltivazione di mais da insilato in condizioni di estrema siccità estiva in Italia

Leonardo Verdi*, Marco Mancini, Marco Napoli, Roberto Vivoli, Andrea Pardini, Simone Orlandini, Anna Dalla Marta

Department of Agriculture, Food, Environment and Forestry (DAGRI) - University of Florence, Italy
*Corresponding author e-mail: leonardo.verdi@unifi.it

Abstract. During the last decades, climate change and variability are increasingly and negatively affecting agriculture. To ensure satisfactory and stable food production, agriculture is intensifying the adoption of external input with environmental consequences such as the emission of greenhouse gases. In this experiment, we monitored CO_2 and CH_4 emission dynamics from cultivation of maize for silage grown under different fertilization treatments: (i) liquid fraction of digestate from pig slurries, (ii) urea, and (iii) no fertilization (control), in an extremely dry summer in Central Italy. Results show that the use of the liquid-organic fertilizer (digestate) significantly increased CO_2 emissions from soil (685.29 kg-C ha^{-1}) compared to the conventional fertilizer (urea) (391.60 kg-C ha^{-1}). However, CH_4 emissions were comparable between the two fertilizers and almost negligible compared to those of CO_2. In both treatments CH_4 emissions were enhanced by the only precipitation event, coupled with an increase of air temperature. Effectiveness of tested fertilizers was assessed through a yield analysis, and proved that digestate may represent a viable alternative to urea (6.97 and 6.48 t ha^{-1}). Nevertheless, considering CO_2 emissions from digestate and the numerous passes in field needed for its spreading, the use of this fertilizer in extreme dry conditions requires specific considerations.

Keywords. Carbon dioxide, Methane, Maize, Digestate, Drought.

Abstract. Il recente sviluppo del fenomeno dei cambiamenti climatici ha negativamente influenzato numerosi settori produttivi tra i quali quello agricolo. Per assicurare una produzione alimentare soddisfacente a livello globale, l'agricoltura ha dovuto incrementare il ricorso ad input esterni di sintesi con notevoli risvolti negativi a livello ambientale, come l'aumento delle emissioni di gas serra. In questo studio sono state monitorate le emissioni di CO_2 e CH_4 dal suolo in una coltivazione di mais da insilato con differenti strategie di concimazione: (i) frazione liquida del digestato da reflui suini, (ii) urea e (iii) un controllo non concimato, durante una stagione estiva (2017) estremamente siccitosa nell'Italia Centrale. Dall'analisi dei risultati è possibile affermare che l'utilizzo di un concime liquido-organico (digestato) determina un aumento significativo delle emissioni di CO_2 (685.29 kg-C ha^{-1}) rispetto all'urea (391.60 kg-C ha^{-1}). Al contrario, le emissioni di CH_4 sono risultate confrontabili fra i due trattamenti con produzioni trascurabili rispetto alla CO_2. In entrambi i trattamenti le emissioni di CH_4 sono state favorite dall'unico evento piovoso, seguito da un aumento delle temperature. L'efficacia dei due concimi è stata valutata attraverso l'analisi delle rese in termini di insilato di mais confermando che l'utilizzo del digestato rappresenta un'interessante alternativa all'urea (6.97 e 6.48 t ha^{-1}, rispettivamente). Tuttavia, alla luce dei livelli di emissioni di CO_2 e dai numerosi passaggi in campo che si richiedono in fase di distribuzione, l'utilizzo del digestato, in condizioni di estrema siccità, richiede specifiche considerazioni.

Parole chiave. Anidride carbonica, Metano, Mais, Digestato, Siccità.

1. INTRODUCTION

Climate change and extreme weather conditions are among the most important threats affecting crop production and management in agriculture (Gobin *et al.*, 2013). Extreme climatic phenomena, especially drought, determine fluctuations in crop production and affect the economic stability of farmers. In particular, as affirmed by Li *et al.* (2009), since 1960s the areas affected by drought, based on Palmer Drought Severity Index (PDSI) (Palmer, 1965), increased approximately from 5-10% to 15-25%. Comparisons between climate model simulations and observed data suggest that anthropogenic greenhouse gases emissions (GHGs) are the main driver of such trend (Burke *et al.*, 2006; IPCC, 2007; Gornall *et al.*, 2010). The combination of prolonged high temperature and absence of rainfall has a relevant impact on agricultural systems from different points of view, including soil microbiological activity, water availability, crop growth and yields. In particular, prolonged drought spells negatively affect soil microbial community that may reduce or, in extreme cases even dramatically compromise, the biological activity with a strong reduction of their metabolisms. Moreover, the effect of drought on activity of soil microorganisms results in an alteration of gas exchanges, such as CO_2 and CH_4, in the soil-atmosphere system following the modification of carbon (C) and nitrogen (N) availability in the soil (Forster *et al.*, 2007; Davidson *et al.*, 2008). As affirmed by Muñoz *et al.* (2010), Krištof *et al.* (2014), Lu *et al.* (2015) and Rutkowska *et al.* (2018) the reduction of CO_2 emissions by changes in agricultural practices is still small. This is mainly due to the complex interactions of factors affecting C emissions from soil, including agronomic practices, meteorological conditions and microbiological activity. However, technologies for their reduction are continuously under development.

One opportunity to reduce the environmental impact of human activities, including agriculture, is represented by the production of renewable energies. In this regard, biogas is one of the most interesting strategy (Alburquerque *et al.*, 2012) for reducing the negative environmental impact of current agricultural practices, and also represents an additional source of income for farmers (Carrosio, 2013).

Furthermore, digestate, which is a by-product of biogas production, represents an interesting alternative N source for crops. Although the production process ensures a lower environmental impacts of digestate compared to synthetic fertilizers, uncertainties remain regarding the direct emissions from its use in the field (Ahlgren *et al.*, 2010; Hasler *et al.*, 2015). Digestate has high level of macro and micro nutrients easily available for plants and, as an organic fertilizer, it stimulates soil microbial activities and emission dynamics from the soil. However, depending on the agricultural management, nutrients can be made available for the crops or lost through leaching or volatilization (Alburquerque *et al.*, 2012; Pezzolla *et al.*, 2012; Nkoa, 2014; Maucieri *et al.*, 2016). Therefore, beside the nutritional requirements of the crop, the environment conditions must be considered. Climate plays a key role affecting numerous soil dynamics such as water content, temperature, organic matter mineralization rate, root systems and soil microbial community development. The fluctuations in climate with extreme phenomena, such as drought or heat waves, may produce different effects based on location and agricultural systems. After a long dry period, gas exchanges between soil and atmosphere are extremely reduced by substantial modification of soil water content and soil aeration (Davidson *et al.*, 2008). In this sense, a reduced thickness in soil water films may reduce the diffusion of roots exudates with a net reduction of available soluble organic-C substrates for crops (Davidson and Janssens, 2006). However, in specific areas such as the Mediterranean and Southern Europe, a rewetting after drought through precipitation or irrigation, promotes an intense pulse of C emission flux from soil (Birch, 1964; Jarvis *et al.*, 2007; Unger *et al.*, 2010). Thereafter, organic matter decomposition, mineralization and release of inorganic N, CO_2 and CH_4 suddenly occurs. If in water-saturated soils the organic matter may accumulate producing layers of peat, in severe dry conditions an addition of organic fertilizers may produce an intense CO_2 flux from soil as consequence of microbial community stimulation (Luo *et al.*, 2001; Francaviglia *et al.*, 2018). For these reasons, the assessment of relations between drought and C emissions represents a key factor for future agricultural sector evolutions in dry climates.

The aim of this research was to evaluate CO_2 and CH_4 emission dynamics from the soil in the short period immediately after fertilization. Experimentation was carried out on a cultivation of maize for silage under different fertilization treatments: (i) liquid fraction of digestate from pig slurries, (ii) urea, and (iii) no fertilization (control), in an extreme dry summer in Central Italy.

2. MATERIALS AND METHODS

An experiment was conducted in Florence (Tuscany), Central Italy (43°47'02.3"N, 11°13'13.4"E). Twelve tanks of 1 m^3 each, equipped with a leachate collecting system to control eventual nutrient losses, were positioned in two rows on a supporting structure made by reinforced concrete poles and soil. Under the tanks a plastic mulching film was placed to reduce weed development and to favor measuring and management operations. The tanks were filled with soil from the experimental site of CREA-ABP located in Scarperia, Florence (43°58'56" N, 11°20'53" E). A silty-clay soil was used and soil layers (0 to 30; 30 to 60; 60 to 90 cm of depth) were kept divided to reproduce as much as possible the natural soil profile. Maize for silage (var. Ronaldinio) was planted on 20th June 2017 with a density of 12.000 plants/ha (13 seeds per tank). Fertilization treatments were (i) liquid fraction of digestate from pig slurries (DIG); (ii) urea (URE); (iii) no fertilization as control (CON), organized in a randomized block design, including four replicates for each treatment. All field operations were performed by hand replacing mechanical ones in field. Digestate was obtained from the biogas plant of "Marchesi de' Frescobaldi, Tenuta di Corte" farm (43°58'29" N, 11°23'21" E) from a mesophilic fermentation process of pig slurries and different kinds of agricultural by-products such as straw, olive cake and sorghum silage. Solid and liquid fractions of digestate were manually separated. Topdressing fertilization at a rate of 150 kg N ha^{-1}, was performed at the beginning of the growth stage (27 days after sowing). Based on methods adopted by local farmers, digestate was injected at a depth of 20 cm while urea was spread on soil surface. The N content of digestate was determined by a Kjeldhal analysis, and NH_4^+ and NO_3^- were determined using the method described in "Regione Piemonte Metodi di analisi del Compost Met. C.7.3 and EPA 9056A 2007". Based on fertilizers characteristics (Tab. 1), the organic C supplied was 1420.06 kg/ha and 65.22 kg/ha for DIG and URE, respectively, through the application of 150 kg N/ha of each fertilizer. GHGs emissions were monitored using a static chamber method and the portable gas analyzer XCGM 400 (Madur Sensonic). Twelve static chambers, one per each tank, were constructed as described by Verdi *et al.* (2019) following USDA-ARS GRACEnet Project Protocols (Parkin and Venterea, 2010). Chambers were made by two parts: an anchor system and the lid. The anchor system was made by a PVC cylinder of 20 cm diameter to be inserted into the soil for approximately 15 cm. The anchor ensures the support for the lid of the chamber during samplings. For the lid of the chamber a PVC cylinder of 20 cm diameter and 15 cm height, and a PVC stopper sealed with silicon glue were used. The chamber was completely covered by reflective Mylar tape to reduce the influence of solar radiation. Moreover, on the top of the chamber a hole (13.2 mm) was drilled approximately halfway between the center of the circle and the outside edge. A butyl rubber septum of 20 mm of diameter was fixed into the hole to allow sampling operations. To connect the chamber lid to the anchor system, a strip of tire tube was used (7 cm). Strip was put around the lid and fixed with silicon glue. Exceeding part of the strip (approximately 5 cm) was kept folded back on the lid of the chamber and then folded down to connect the lid to the anchor during sampling. The anchor system was placed into the soil immediately after sowing between plant rows to reduce roots disturbance. It was removed only during fertilization (digestate injection) and then reinstalled immediately at the same location. Temperature was monitored by two thermocouples placed in each chamber. In addition, an automatic meteorological station located 20 m away from the experimental field was used to monitor air temperature, atmospheric pressure and precipitations. The XCGM 400 Madur Sensonic gas analyzer uses nondispersive infrared (NDIR) sensors for the analysis of CO_2 and CH_4 concentrations in the air sample. Emission measurements lasted for three consecutive weeks after fertilization. Samplings were performed (daily in the first week and twice a week during the second and the third) by holding the sensor inside the chamber for 1 minute after chamber closing (T1) and then repeating the procedure at 1 hour interval (T2) from T1. Interpolation was used to obtain missing data from the days were measurements were not performed (eg. the weekend). Gas fluxes were calculated starting from the gas concentration into the chamber (ppm) (the difference between T2 – T1), chamber dimensions (area and volume), closing time and molecular weight of each gas. Through this calculation, it was possible to quantify C losses as kg of C emitted per hectare. As temperature had a similar trend inside each chamber (data not shown), the whole experiment was assumed to be at standard temperature and pressure (STP) conditions and the molar volume of the air was assumed as 22.4 liters. Parametric and non-parametric statistical tests were used to analyze C emissions data.

Tab. 1. Elemental characterization of fertilizers.
Tab. 1. Caratterizzazione elementare dei fertilizzanti.

	Urea	Digestate
Organic C %	20	3.02
Total N %	46	0.319
N-NH_4^+ %	-	0.284
N-NO_3^- %	-	0.035
Total P %	-	1.84
Total K %	-	6.94

3. RESULTS AND DISCUSSION

3.1 Carbon dioxide emissions

Soil under DIG treatment emitted roughly twice CO_2 than URE (685.29 and 391.60 kg C-CO_2 ha^{-1} 17 days^{-1}, respectively). Treatments comparison was performed with both a parametric (Bonferroni test) and a non-parametric (Kruskal-Wallis test) analysis (Bonferroni, 1936; Kruskal and Wallis, 1952). Both tests confirmed that DIG produced higher CO_2 emissions than URE. In addition, no significant differences were observed between URE and CON, confirming the low contribution of URE to soil CO_2 emissions compared to DIG. Highest emissions from soil mainly occurred during the first days after fertilization until the end of the first week. In particular, we observed that immediately after fertilization (AF) (24 hours) CO_2 emissions from DIG were eight times higher than those from URE (Fig. 1). This result is in accordance to Maucieri *et al.* (2016) that observed the highest soil CO_2 emissions during the first 24 hours after digestate spreading.

From the second day AF, differences among treatments were strongly reduced, and from the second week until the end of the experiment significant differences were no longer observed (Fig. 1). Nevertheless, it should be noticed that from day 3 to 5 AF average daily temperature increased by 2 °C and CO_2 emissions from soil increased also (Fig. 1 and Fig. 2). This phenomenon was defined by Luo *et al.* (2001) as "acclimatization" of soil respiration to warming, that represents a proper modification on microorganism's population to altered environmental conditions. In addition, the similarity of soil CO_2 emission trends between DIG and URE from day 2 AF until the end of the experiment suggests that after a short period (24-48h) urea decomposition occurred and soil microbial community increased its metabolic activity (Black *et al.*, 1987). As described by Xu *et al.* (1993) a positive correlation exists between the rate of urea hydrolysis and temperature. This is in accordance to our observations where soil CO_2 emission peaks were observed at days 2 and 5 AF when the highest air temperature of the first week was registered (Fig. 2).

Our observations are also in accordance to Johansen *et al.* (2013) and Verdi *et al.* (2018), affirming that the use of fertilizers with high organic C content strongly encourages a fast-growing soil microbial community with an intense oxygen demand to support microbial metabolisms (Parkin, 1987; Petersen *et al.*, 1996) and a consequent increase in soil CO_2 emissions. The high water content of digestate ensured its homogenous infiltration into the soil, thus increasing the availability of C for microorganisms. This contributed to CO_2 flux immediately after fertilization. Similar experiments performed in open fields in non-drought conditions and in soil

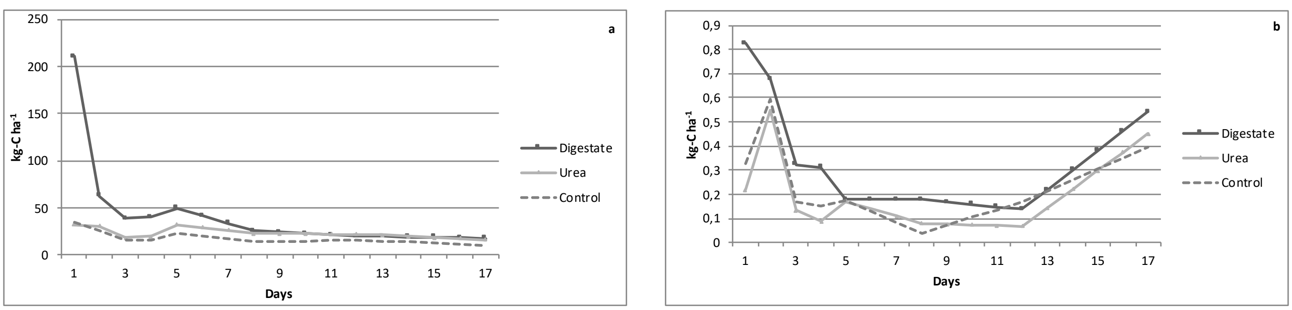

Fig. 1. CO_2 (a) and CH_4 (b) emission trends of digestate (DIG), urea (URE) and control (CON) treatments.
Fig. 1. Andamento delle emissioni di CO_2 (a) e CH_4 (b) da digestato (DIG), urea (URE) e controllo (CON).

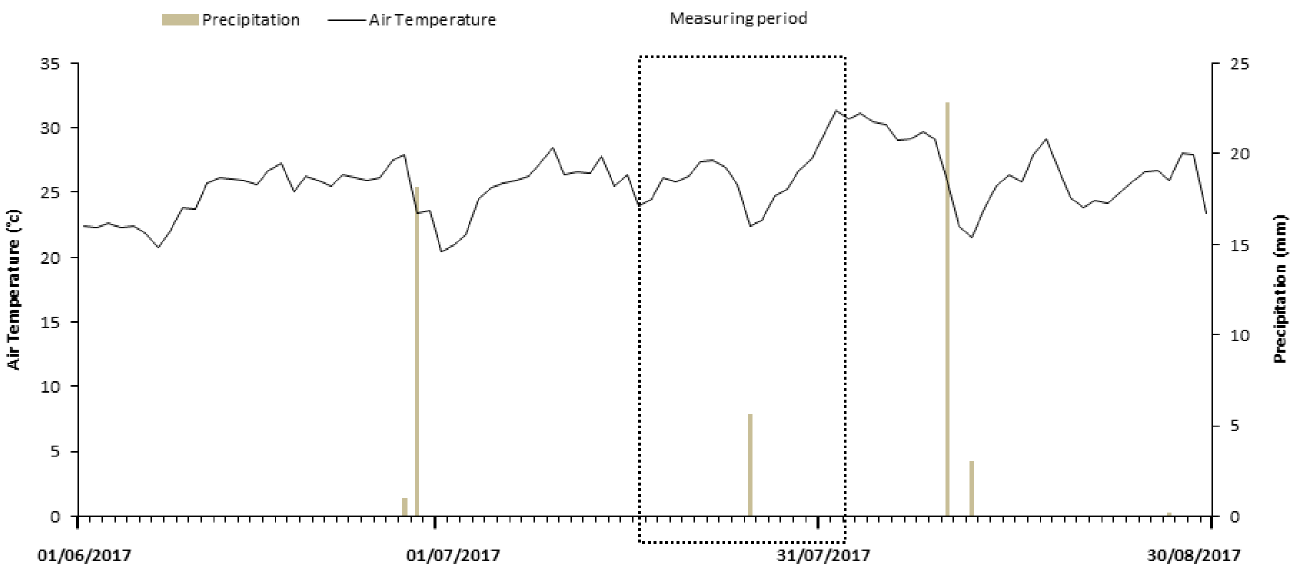

Fig. 2. Average air temperature and precipitation during the experiment (measurement period is indicated by the box).
Fig. 2. Andamento della temperatura media dell'aria e delle precipitazioni (nel riquadro è evidenziato il periodo di monitoraggio delle emissioni).

columns at field capacity (Sänger *et al.*, 2011; Severin *et al.*, 2015; Luoro *et al.*, 2016;), found 25 to 50% more soil CO_2 emissions than our study. This confirms that environmental conditions, more specifically drought, highly affect C emission dynamics. However, the emissions peak observed in the first 24-48 hours AF is confirmed by literature (Severin *et al.*, 2015; Askri *et al.*, 2016).

Despite higher soil C emissions compared to URE, DIG showed better performances in terms of fertilization potential by increasing soil organic matter (SOM). In fact, 1420.06 kg of organic C per hectare were spread with DIG in front of 690.65 kg C/ha (corresponding to about 48.6% of the distributed organic C) lost through emissions (CO_2+CH_4, Tab.2). On the contrary, URE provided only 65.22 kg of organic C/ha against 394.86 kg C/ha (CO_2+CH_4, Tab.2) lost as emissions. Probably, URE stimulated the soil microbial activity determining an increase in soil C emissions 6.05 times higher than the provided organic C. This corresponds to a depletion of soil organic carbon of about 329.64 kg/ha. This fact indicates that the use of organic fertilizers, such as DIG, contributes to an increase or at least maintenance of SOM.

3.2. Methane emissions

No significant differences in CH_4 emissions from soil were observed between treatments (Tab. 2). At day 1 AF, CH_4 emissions from DIG were significantly higher (p=0.001) compared to URE and CON also due to the intrinsic content of methanogenic bacteria of DIG. However, from day 2 AF the amount of C emitted as CH_4 from soil treated with DIG quickly decreased (Fig. 1) probably due to the fast proliferation of soil bacteria that consumed the available soil organic C for their metabolisms (Bernet *et al.*, 2000; Norberg *et al.*, 2016; Verdi *et al.*, 2018). Apparently, methanogenic population of DIG was negatively affected by the extreme dry conditions occurred during the experimentation. During the last days AF (days 12-17) soil CH_4 emissions increased in all treatments (including CON). This fact was observed, and is in accordance to Le Mer and Roger (2001), in correspondence to the warmest period of the experiment that followed the only rainy event (5.6 mm) (Fig. 2). The combined effect of increasing soil water content and atmospheric temperature encouraged soil CH_4 emissions in the last day of measurements.

3.3. Yields

Performances of the tested treatments (DIG, URE and CON) were analyzed in terms of final yields (Tab. 3). A preliminary ANOVA analysis was performed, followed by Bonferroni and Kruskal-Wallis tests. Both tests proved the effectiveness of DIG as fertilizer that provided yields comparable to those obtained under URE treatment (6.97 t ha^{-1} and 6.48 t ha^{-1}, respectively). As observed by Lotter *et al.* (2003), the use of organic fer-

Tab. 2. Measured soil CO_2 and CH_4 emissions from digestate (DIG), urea (URE) and control (CON).
Tab. 2. Emissioni cumulate di CO_2 e CH_4 da digestato (DIG), urea (URE) e controllo (CON).

	CO_2 (kg C ha^{-1} 17 days^{-1})	CH_4 (kg C ha^{-1} 17 days^{-1})
DIG	685.29 (± 75.49)^a	5.36 (± 1.61)^c
URE	391.60 (± 79.26)^b	3.26 (± 1.02)^c
CON	286.79 (± 32.64)^b	3.69 (± 0.52)^c

Standard deviations of the four replicates per each treatment are in brackets.
Values marked with the same letter do not differ significantly.
Deviazione standard delle quattro repliche per ogni trattamento è indicata tra parentesi.
I valori contraddistinti dalla stessa lettera non evidenziano differenze significative.

Tab. 3. Silage maize yields in digestate (DIG), urea (URE) and control (CON), DM= dry matter.
Tab. 3. Produzione di insilato di mais da digestato (DIG), urea (URE) e controllo (CON).

	Yields (t DM ha^{-1})
DIG	6.97 (± 0.56)^a
URE	6.48 (± 0.85)^a
CON	4.49 (± 0.25)^b

Standard deviations of the four replicates per each treatment are in brackets.
Values marked with the same letter do not differ significantly.
Deviazione standard delle quattro repliche per ogni trattamento è indicata tra parentesi.
I valori contraddistinti dalla stessa lettera non evidenziano differenze significative.

tilizers on maize ensures higher or similar yields compared to urea. This is due to the improvement of soil's water-holding capacity, infiltration rate and water capture efficiency of soils treated with organic fertilizers that allow to maintain more available water into the crop root zone. Furthermore, as observed by Alburquerque *et al.* (2012), DIG provides similar yields than urea due to the significant amount of ammonium N that is rapidly nitrified, becoming available for crops. During the experiment, characterized by extremely dry (5.6 mm of cumulated precipitation) and warm (average temperature of 26.55 °C) conditions, these two effects of DIG were particularly evident: on one hand, more available water was retained in the root zone, and on the other the absence of rainfall reduced the risk of N-based compounds leaching which were therefore available for crops. Nevertheless, yields obtained from this experiment were affected by drought conditions showing a strong reduction compared to national average data in well irrigated and fertilized systems (Borrelli *et al.*, 2014).

4. CONCLUSIONS

Based on the obtained results, we can conclude that C emissions from cultivated soil depend not only on the fertilizer but also on the environmental conditions. In particular, the increased CO_2 emissions from soil observed in DIG, compared to URE, were principally due to the combined effect of the high temperatures and drought that occurred during the experimentation, and the high water content of DIG. These two factors encouraged soil bacteria proliferation with a consequent increase in soil respiration. This is in accordance to Sainju *et al.* (2008) that observed an increase of 13% of soil CO_2 emissions from irrigated maize fields, compared to rainfed conditions. However, the same conditions blocked methanogenic bacteria proliferation with a sensible reduction of CH_4 production in all treatments. From a productive point of view, our analysis confirmed that DIG may represent an effective alternative to URE for maize, as similar yields were obtained. In addition, considering that digestate is a by-product of biogas, its production has a better environmental performance compared urea. Zegada-Lizarazu *et al.* (2010) reported that to produce 1 kg of urea 76-78 MJ of energy are needed, with consequent emissions from the system. Nevertheless, the use of DIG in dry summer conditions may represent a critical factor due to its higher impacts on CO_2 emissions. This aspect should be carefully considered especially under the view of global warming trends. In addition, due to its low N content, a large amount of DIG is required to satisfy the nutrient demand of crops, involving an intensive and repeated use of fossil fuel-based machinery for fertilization field operations. Thus, further experiments focused on full life cycle analysis are suggested for a more in-depth understanding of environmental impacts from DIG and URE.

AUTHOR CONTRIBUTIONS

Conceptualization, Leonardo Verdi, Simone Orlandini and Anna Dalla Marta; Data curation, Leonardo Verdi; Formal analysis, Marco Napoli; Investigation, Leonardo Verdi; Methodology, Leonardo Verdi and Marco Mancini; Project administration, Simone Orlandini; Supervision, Simone Orlandini; Writing – original draft, Leonardo Verdi; Writing – review & editing, Anna Dalla Marta.

FUNDING

This research was funded by H2020-TWINN-2015 SERBIA FOR EXCELL project. This project has received founding from the European Union's Horizon 2020 research and innovation program under grant agreement No. 691998.

ACKNOWLEDGEMENTS

The authors want to thank *Azienda Agricola Marchese De' Frescobaldi, Fattoria di Corte* for kindly providing the digestate.

REFERENCES

Ahlgren S., Bernesson S., Nordberg Å., Hansson P.-A., 2010. Nitrogen fertiliser production based on biogas – Energy input, environmental impact and land use. Bioresource Technol., 101: 7181–7184.

Alburquerque J.A., de la Fuente C., Campoy M., Carrasco L., Nájera I., Baixauli C., Caravaca F., Roldán A., Cegarra J., Bernal M.P., 2012. Agricultural use of digestate for horticultural crop production and improvement of soil properties. Eur. J. Agron., 43: 119–128.

Askri A., Laville P., Trémier A., Houot S., 2016. Influence of origin and post-treatment on greenhouse gas emissions after anaerobic digestate application to soil. Waste Biomass Valor., 7: 293–306.

Bernet N., Delgenes N., Akunna J.C., Delgenes J.P., Moletta R., 2000. Combined anaerobic–aerobic SBR for the treatment of piggery wastewater. Water Res., 34(2): 611–619.

Birch H.F., 1964. Mineralisation of plant nitrogen following alternate wet and dry conditions. Plant Soil., 2: 43–49.

Black A.S., Sherlock R.R., Smith N.P., 1987. Effect of timing of simulated rainfall on ammonia volatilization from urea, applied to soil of varying moisture content. Eur. J. Soil Sci., 38: 679–687.

Bonferroni C.E., 1936. Teoria statistica delle classi e calcolo delle probabilità. Pubblicazioni del R Istituto Superiore di Scienze Economiche e Commerciali di Firenze 1936.

Borrelli L., Castelli F., Ceotto E., Cabassi G., Tomasoni C., 2014. Maize grain and silage yield and yield stability in a long-term cropping system experiment in Northern Italy. Europ. J. Agronomy, 55: 12–19.

Burke E.J., Brown S.J., Christidis N., 2006. Modeling the recent evolution of global drought and projections for the twenty-first century with the Hadley Centre climate model. J. Hydrometeorol., 7: 1113–1125.

Carrosio G., 2013. Energy production from biogas in the Italian countryside: Policies and organizational models. Energ Policy 2013,63: 3-9.

Davidson E.A., Janssens I.A., 2006. Temperature sensitivity of soil carbon decomposition and feedbacks to climate change. Nature, 440: 165–173.

Davidson E.A., Nepstad D.C., Ishida F.Y., Brando P.M., 2008. Effects of an experimental drought and recovery on soil emissions of carbon dioxide, methane, nitrous oxide, and nitric oxide in a moist tropical forest. Glob Change Biol., 14: 2582–2590.

Forster P., Ramaswamy V., Artaxo P., *et al.*, 2007. Changes in atmospheric constituents and in radiative forcing. In: Climate Change 2007: The Physical Science Basis. Contribution of Working Group 1 to the Fourth Assessment Report of the Intergovernmental Panel on Climate Change (eds Solomon S, Qin D, Manning M, Chen Z, Marquis M, Averyt KB, Tignor M, Miller HL), pp. 129– 234. Cambridge University Press, Cambridge, UK/New York, NY, USA.

Francaviglia R., Ledda L., Farina R., 2018. Organic Carbon and Ecosystem Services in Agricultural Soils of the Mediterranean Basin. In: Gaba S., Smith B., Lichtfouse E. (eds) Sustainable Agriculture Reviews 28. Sustainable Agriculture Reviews, 28. Springer, Cham.

Gobin A., Tarquis A.M., Dalezios N.R., 2013. Weather-related hazards and risks in agriculture preface. Nat Hazards Earth Syst Sci., 13(10): 2599–2603.

Gornall J., Betts R., Burke E., Clark R., Camp J., Willett K., Wiltshire A., 2010. Implications of climate change for agricultural productivity in the early twenty-first century. Phil. Trans. R. Soc. B., 365: 2973–2989.

Hasler K., Bröring S., Omta S.W.F., Olfs H.-W., 2015. Life cycle assessment (LCA) of different fertilizer product types. Eur. J. Agron., 69: 41–51.

IPCC. Climate change 2007: the physical science basis. Contribution of Working Group I to the Fourth Assessment Report of the Intergovernmental Panel on Climate Change. Cambridge, UK: Cambridge University Press.

Jarvis P.G., Rey A., Petsikos C., Wingate L., Rayment M., Pereira J., Banza J., David J., Miglietta F., Borghetti M., Manca G., Valentini R., 2007. Drying and wetting of Mediterranean soils stimulates decomposition and carbon dioxide emission: the 'birch effect'. Tree Physiol., 27: 929–940.

Johansen A., Carter M.S., Jensen E.S., Hauggard-Nielsen H., Ambus P., 2013. Effects of digestate from anaerobically digested cattle slurry and plant materials on soil microbial community and emission of CO2 and

N2O. Appl Soil Ecol., 63: 36–44.

Krištof K., Šima T., Nozdrovický L, Findura P., 2014. The effect of soil tillage intensity on carbon dioxide emissions released from soil into the atmosphere. Agron. Res., 12(1): 115–120.

Kruskal W.H., Wallis W.A., 1952. Use of ranks in one-criterion variance analysis. J. Am Stat. Assoc., 47 (260).

Le Mer J., Roger P., 2001. Production, oxidation, emission and consumption of methane by soils: a review. Eur. J. Soil Biol., 37: 25–50.

Li Y.P., Ye W., Wang M., Yan X.D., 2009. Climate change and drought: a risk assessment of crop-yield impacts. Clim. Res., 39: 31–46.

Lotter D.W., Seidel R., Liebhardt W., 2003. The performance of organic and conventional cropping systems in an extreme climate year. Am J Alternative Agr., 18: 146–154.

Lu X., Lu X., Khan S., Xiaoxia T., Liao W., Liao Y., 2015. Effects on tillage management on soil CO2 emission and wheat yield under rain-fed conditions. Soil Res., 54(1): 38–48.

Luo Y., Wan S., Hui D., Wallace L.L., 2001. Acclimatization of soil respiration to warming in a tall grass prairie. Nature., 413: 622–625.

Luoro A., Cárdenas L.M., Garcia M.I., Báez D., 2016. Greenhouse gas fluxes from grazed grassland soil after slutty injections and mineral fertilizer applications under the Atlantic climatic conditions of NW Spain. Sci. Total Environ., 573: 258–269.

Maucieri C., Barbera A.C., Borin M., 2016. Effect of injection depth of digestate liquid fraction on soil carbon dioxide emission and maize biomass production. Ital. J. Agron., 11: 6-11.

Muñoz C., Paulino L., Monreal C., Zagal E., 2010. Greenhouse gas (CO2 and N2O) emissions from soil: a review. Chil. J. Agric. Res., 70(3): 485–497.

Nkoa R., 2014. Agricultural benefits and environmental risks of soil fertilization with anaerobic digestates: a review. Agron. Sustain. Dev., 34: 473–492.

Norberg L., Berglund O., Berglund K., 2016. Nitrous oxide and methane fluxes during the growing season from cultivated peat soils, peaty marl and gyttja clay under different cropping systems. Acta Agr. Scand. B-S P., 66: 602–612.

Palmer W.C., 1965. Meteorological drought. Research paper 45. Washington, DC: US Weather Bureau, 1965.

Parkin T.B., 1987. Soil microsites as a source of denitrification variability. Soil Sci. Soc. Am. J., 51: 1194–1199.

Parkin T.B., Venterea R.T., 2010. USDA-ARS GRACEnet Project Protocols, Chapter 3. Chamber-Based Trace Gas Flux Measurements. (Replace original version of April 2003).

Petersen S.O., Nielsen T.H., Frostegard A., Olesen T., 1996. O2 uptake, C metabolism and denitrification associated with manure hot-spots. Soil Biol. Biochem., 28: 341–349.

Pezzolla D., Bol R., Gigliotti G., Sawamoto T., Lopez A.L., Cardenas L., Chadwick D., 2012. Greenhouse gas (GHG) emissions from soils amended with digestate derived from anaerobic treatment of food waste. Rapid Commun. Mass Sp., 26: 2422–2430.

Rutkowska B., Szulc W., Sosulski T., Skowrońska M., Szczepaniak J., 2018. Impact of reduced tillage on CO2 emission from soil under maize cultivation. Soil Till. Res., 180: 21–28.

Sainju U.M., Jabro J.D., Stevens W.B., 2008. Soil carbon dioxide emissions and carbon content as affected by irrigation, tillage, cropping system, and nitrogen fertilization. J. Environ. Qual., 37: 98–106.

Sänger A., Geisseler D., Ludwing B., 2011. Effects of moisture and temperature on greenhouse gas emissions and C and N leaching losses in soil treated with biogas slurry. Biol. Fertil. Soils., 47: 249–259.

Severin M., Fuß R., Well R., Garlipp F., Van den Weghe H., 2015. Soil, slurry and application effects on greenhouse gas emissions. Plant Soil Environ., 61(8): 344–351.

Unger S., Máguas C., Pereira J.S., David T.S., Werner C., 2010. The influence of precipitation pulses on soil respiration – assessing the "birch effect" by stable carbon isotopes. Soil Biol. Biochem., 42: 1800–1810.

Verdi L., Mancini M., Ljubojevic M., Orlandini S., Dalla Marta A., 2018. Greenhouse gas and ammonia emissions from soil: The effect of organic matter and fertilisation method. Ital. J. Agron., 13: 260–266.

Verdi L., Kuikman P.J., Orlandini S., Mancini M., Napoli M., Dalla Marta A., 2019. Does the use of digestate to replace mineral fertilizers have less emissions of N2O and NH3? Agric. For. Meteorol., 269: 112-118.

Xu J.G., Heeraman D.A., Wang Y., 1993. Fertilizer and temperature effects on urea hydrolysis in undisturbed soil. Biol fert soils., 16: 63–65.

Zegada-Lizarazu W., Matteucci D., Monti A., 2010. Critical review on energy balance of agricultural systems. Biofuels, Bioprod. Bioref., 4: 423–446.

Italian Journal of Agrometeorology
Rivista Italiana di Agrometeorologia

Firenze University Press
www.fupress.com/ijam

OPEN ACCESS

Citation: A. Baldi, G. Brandani, M. Petralli, A. Messeri, S. Cecchi, R. Vivoli, M. Mancini (2019) Termo-pluviometric Variability of Val d'Orcia Olive Orchards area (Italy). *Italian Journal of Agrometeorology* (2): 11-20. doi: 10.13128/ijam-649

Received: July 31, 2018

Accepted: March 25, 2019

Published: October 29, 2019

Data Availability Statement: All relevant data are within the paper and its Supporting Information files.

Competing Interests: The Author(s) declare(s) no conflict of interest.

Termo-pluviometric Variability of Val d'Orcia Olive Orchards area (Italy)

Variabilità termo-pluviometrica degli oliveti della Val d'Orcia (Italia)

Ada Baldi[1], Giada Brandani[1,2], Martina Petralli[1,*], Alessandro Messeri[1], Stefano Cecchi[2], Roberto Vivoli[1], Marco Mancini[1,2]

[1] *Department of Agriculture, Food, Environment and Forestry (DAGRI), University of Florence, Italy*
[2] *Fondazione Clima e Sostenibilità, Florence, Italy*
*Corresponding author e-mail: martina.petralli@unifi.it

Abstract. In a context of climate change, the knowledge of local meteorological trend and variability is a very useful tool in precision farming for improving crop production and quality. The aim of this study is to analyze the thermo-pluviometric variability of Val d'Orcia olive orchards area (Tuscany, Italy), a hilly region characterized by a great orographic variability that lacs of historical termo-pluviometric information. The trend of thermo-pluviometric indices (TX, TN, TG, FD, RR and GDD) for the period 2012-2017 in three weather stations located at different altitude and orientation in the Val d'Orcia area are presented. During the study period, yearly extra virgin olive oil (EVO) yield was also analyzed. The variability observed in precipitation confirms the strong influence of topography and atmospheric circulation on local precipitation distribution. While the analysis of thermal regimes and frost days evidence the strong presence of thermal inversion phenomenon in this area. A strong relationship was found between yearly EVO yield and GDD during the vegetative period.

Keywords. Olive orchards, microclimate, agrometeorology.

Abstract. Nell'attuale contesto di cambiamento climatico, aumentare le informazioni disponibili in merito ai trend ed alla variabilità meteorologica locale costituisce un utile strumento all'agricoltura di precisione volta al miglioramento della produttività e della qualità dei prodotti agricoli. Lo scopo di questo studio è di analizzare la variabilità termo-pluviometrica dei territori della Val d'Orcia (Toscana) a vocazione olivicola, un'area collinare caratterizzata da una elevata variabilità orografica e che manca di serie storie di questo tipo. In questo studio sono quindi presentati alcuni indici termo-pluviometrici (TX, TN, TG, FD e RR) ed alcuni indici legati alla fenologia dell'Olivo, come i GDD di tre stazioni localizzate a diverse altitudini e con diversa esposizione nel territorio della Val d'Orcia, nel periodo 2009 – 2017. Nello stesso periodo sono state analizzate le rese in olio extra-vergine di oliva (EVO). I risultati mostrano una forte variabilità pluviometrica legata all'orografia del territorio, mentre le analisi degli indici di temperatura evidenzia la presenza nell'area di una forte escursione termica. Infine, una forte relazione è stata osservata tra i GDD nel periodo vegetativo e la resa annuale in olio delle olive.

Parole chiave. Oliveti, microclima, agrometeorologia

INTRODUCTION

Agrometeorology deals with the influence of climate on agriculture. Two of the most important agrometeorological variables influencing crop growth and development are air temperature and precipitation which have also a direct influence on pest and disease incidence (Rosenzweig *et al.*, 2001).

Many studies highlighted that a general increase in extreme events such as frequency and persistence of high temperatures and changes in total precipitation and rainy days are among the most impact-relevant consequences of climate warming (Brunetti *et al.*, 2001; Manton *et al.*, 2001; Yan *et al.*, 2002; Beniston and Stephenson, 2004). Therefore, knowing the meteoclimatic trend and in particular the interseasonal and interannual variability of air temperature and precipitation could be decisive for adopting climate change mitigation and adaptation strategies in agriculture techniques.

Olive (*Olea europaea* L.) is considered a good indicator of the ongoing climate change in Mediterranean area where is one of the most important socio-economic crop (Osborne *et al.*, 2000; Orlandi *et al.*, 2005; Loumou and Giourga, 2003). Air temperature and precipitation have a significant influence on the timing of olive trees phenological stages. A low temperature period prior to bud development is essential to reach the base temperature and interrupt dormancy, then the plant accumulates heat until flowering starts (Galán *et al.*, 2001). As olive trees produce allergenic pollen, the effects of temperatures on olive trees flowering can also affect human health (Murray and Galán, 2016; Massetti *et al.*, 2015). Despite its tolerance to drought stress by means of morphological, physiological and biochemical adaptations for optimal yield olive needs of a relative wet period during anthesis and fruits ripening (Sofo *et al.*, 2008). On the contrary, precipitation and high relative humidity during anthesis tending to reduce pollen airborne concentrations (Recio *et al.*,1996).

The role of olive orchards in maintaining the traditional Tuscan (Italy) agricultural landscape is indisputable especially in Val d'Orcia (southern-east Tuscany), a hilly region characterized by a great orographic variability, where olive trees are cultivated on the slopes and hilltops from the seventh century AD (Milanesi *et al.*, 2011). Recent studies on the seasonal and annual variability of air temperature and precipitation over Tuscany has shown a general increase in minimum and maximum temperatures and extreme temperature events, a decrease in wet days and an increase in precipitation fraction (Bartolini *et al.,* 2008; Bartolini *et al.,* 2014).

Having weather-climatic information as specific as possible together with the monitoring of temperature and precipitation variability, it could be helpful to optimize some crop management practices like foliar fertilization, phytosanitary treatments, olive fly control. Before now, no specific agroclimatic analysis have been conducted in the Val d'Orcia olive orchards.

According to these premises, the aim of this study is to analyse and characterize the agroclimatic variability of Val d'Orcia olive orchards applying unifactorial bioclimatic indices in order to improve olive management techniques introducing the most advanced precision farming techniques.

MATERIALS AND METHODS

Study area

The Val d'Orcia is a valley crossed by the Orcia river in central-western Italy at about latitude 43°4'0"N, and longitude 11°33'0"E. It is approximately 669 km^2 and is located in the central-southern part of Tuscany (Fig. 1). It is geographically defined by the border of five Communities (Castiglione d'Orcia, Montalcino, Pienza, Radi-

Fig. 1. Localization of Val d'Orcia area in Tuscany (in yellow) and in Italy.

Fig. 1. Localizzazione della Val d'Orcia in Toscana (in giallo) ed in Italia.

cofani, and San Quirico d'Orcia) of the province of Siena. The area is characterized by a hilly morphology with slopes from weak (5-10%) to moderate (10-15%). The elevation of this area ranged from 160 to 690 m a.s.l..

Basing on the Köppen-Geiger (1936) climate classification system, which is useful for climate classification in terms of geographical area, the Val d'Orcia is characterized by a temperate climate of the sublittoral types.

Val d'Orcia is a predominantly agricultural area, and dedicated to agricultural tourism thanks to its typical landscapes. The main crops cultivated in Val d'Orcia are cereals, vines and, above all, olives. The most important olive cultivars in Val d'Orcia are 'Frantoio', 'Moraiolo', 'Leccino', and the autochthonous 'Olivastra Seggianese'.

Meteorological data

No historical termo-pluviometric series are available for the Val d'Orcia. Validated and continuous data are provided by the Regional Hydrological Sector of Tuscany (SIR) and are available only from 2012. The SIR meteorological stations collect hourly temperature and precipitation data that are made available as daily data of minimum, maximum, average temperature and cumulative precipitation. Three of them meteorological stations are located in olive orchards area (Tab. 1).

In order to analyze meteoclimatic trend, and interseasonal and interannual thermos-pluviometric variability of Val d'Orcia olive orchard area, Walter end Lieth climate diagrams were performed as a mean of station for the entire period in exam and annually for each single station (Walter and Lieth, 1960).

Indices

Aiming at defining the agro-meteorological resources of the area and the limitations imposed by climate to agricultural practice, an agro-climatic characterization was carried out using agro-meteorological techniques. Considering daily temperature and rainfall values recorded in the period 2009-2017 and 2012-2017 respectively, general and specific unifactorial bioclimatic indices were calculated according to the European Climate Assessment (ECA) indices definition (Peterson *et al.*, 2001):
TX - monthly mean of daily maximum temperature (°C)
TN - monthly mean of daily minimum temperature (°C)
TG - monthly mean of daily mean temperature (°C)
FD - frost Days: days with minimum temperature lower than 0 °C
RR - sum of days with precipitation higher than 0 mm

Furthermore, air temperature data was used to calculate the Growing Degree Days (GDD) by the following formula: GDD = S (T daily mean temperature – T threshold). T threshold is the minimum temperature for olive biothermic accumulation and it is assumed to be 7.5°C (Bonofiglio *et al.*, 2008).
GDD_{VP} were calculated for the whole olive vegetative period (from 1st of march to 31st of October) and separately for each season:
GDD_{MAM} - between 1st of March to 31 of May (Spring);
GDD_{JJA} - between 1st of June to 31 of August (Summer);
GDD_{SO} - between 1st of September to 31st of October (Autumn).

Yearly EVO yield (Y, %) was calculated from 2009 to 2017 by data provided by the Val d'Orcia Oil Mill, located in Castiglione d'Orcia (SI) .

RESULTS AND DISCUSSION

The analysis of thermo-pluviometric data, as a mean of the three stations for the period 2012-2017, confirms that Val d'Orcia olive orchard area is characterized by a temperate climate of the sublittoral types according to Koppen-Geiger climate classification system. The area has an average annual temperatures of 14.2 °C, an average temperature of the coldest month of 5.8 °C, three months with thermal averages above 20 °C, and annual temperature range (difference between average tempera-

Tab. 1. Meteorological station of Regional Hydrological Sector of Tuscany (SIR) in Val d'Orcia olive orchards area.
Tab. 1. Lista e localizzazione delle stazioni meteorologiche localizzate in oliveti della Val d'Orcia del Servizio Idrogeologico Regionale della Toscana (SIR).

Number	Meteorological station code	Meteorological station name	Altitude m a.s.l.	WGS84 Coordinates	
				Lat.	Long.
1	TOS11000067	Buonconvento	188	43.092	11.439
2	TOS11000059	Ripa d'Orcia	506	43.027	11.582
3	TOS11000058	Castiglione d'Orcia	672	42.961	11.618

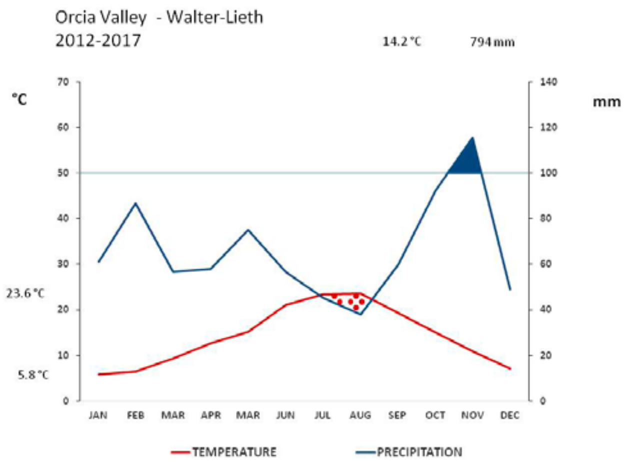

Fig. 2. Walter and Lieth climate diagram of Val d'Orcia for the period 2012-2017.
Fig. 2. Diagramma di Walter e Lieth della Val d'Orcia per il periodo 2012-2017.

ture of the coldest month and of the warmest one) equal to 17.8 °C (Fig. 2).

The mean rainfall of the area is 794 mm and it is distributed fairly evenly throughout the year, with a peak during autumn. The wettest period coincides with the autumn months with the 35% of the average annual rainfall; the wettest month is November, with an average value of 117 mm of rainfall. Summer results to be the less rainy season with 18% of the total average rainfall. Finally, rainfall is equally spread in spring and winter with an average annual rainfall of about 23% in both seasons. August seems to be the driest month with about 40 mm of monthly cumulative precipitation (Fig. 2).

Walter end Lieth climate diagram were also annually performed for each single station. The monthly temperature and precipitation trend was similar between stations and no differences were observed in interseasonal trend (data not shown). On the contrary, during the study period interannual differences were observed; as no differences in temperature and precipitation trend were observed according to altitude, annual Walter and Lieth climate diagram were shown only for station 2 (Ripa d'Orcia) (Fig. 3).

The years 2012, 2013, 2014, and 2016 were characterized by wet periods: in 2012, 2013, and 2014 the wet period was recorded during the autumn, in 2013 during the fall with the addition of the month of May, while in 2016 in February and June. The wettest year was 2014, with 908 mm, while 2017 was the driest (409 mm) characterized by the largest number of consecutive dry months (5 months). Also 2012 and 2015 were very dry years, with 6 dry months. The dry period is usually concentrated in summer and occasionally in the other seasons: in 2012 during winter, in 2015 during autumn and winter, in 2017 during spring and autumn. In 2013 no dry months were observed, while only one dry month (August) and two dry months (July and August) were observed in 2014 and 2016, respectively. Annual temperature range varied from 13.6 °C in 2014 and 23.6 °C in 2012. Although the difference between the average annual temperatures was 1 °C between the coldest (2013) and the warmest (2017) years, marked differences were observed between years in the mean temperature values of the warmest month (between 26.6 °C in 2017 and 21.4 °C in 2014) and the average temperature of the coldest one (between 2.3 °C in 2012 and 7.8 °C in 2014) (Fig. 3).

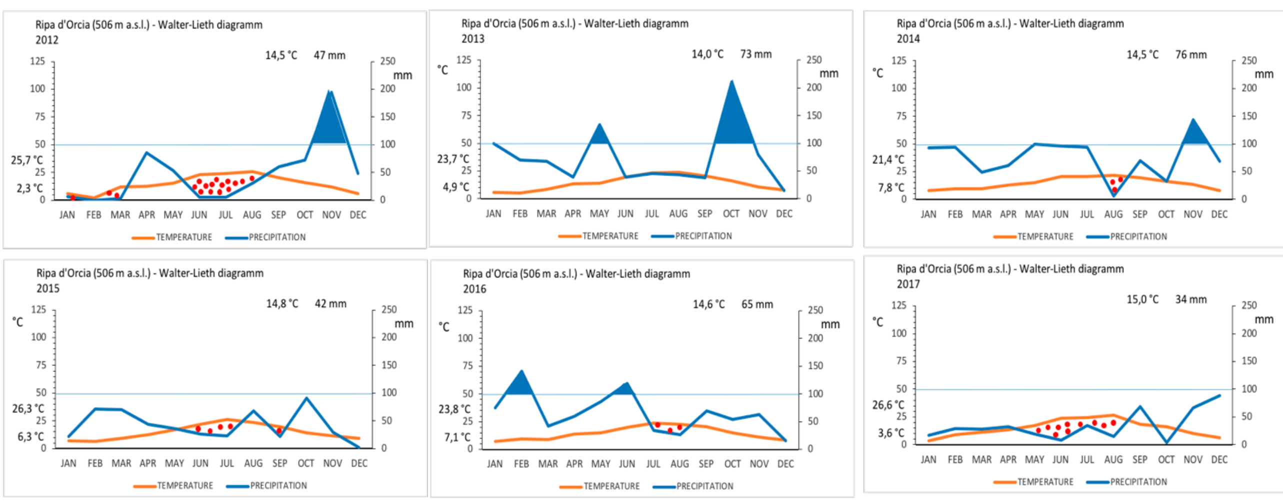

Fig. 3. Walter and Lieth climate diagram of Ripa d'Orcia meteorological station (station 2) for the period 2012-2017.
Fig. 3. Diagramma annuale di Walter e Lieth della stazione di Ripa d'Orcia (statione 2) per il periodo 2012-2017.

So, ultimately, the Val d'Orcia climate is typical of the Mediterranean area, characterized by the presence of mainly hot-dry summers and relatively cold winters.

The olive phenological response is insensitive to photoperiod (Osborne *et al.*, 2000) but strictly dependent on the monthly temperature regime (Bonofiglio *et al.*, 2009), knowing its trend may help to adopt management strategies in a timely manner and in yield forecasting. The Val d'Orcia monthly thermal regime during the period 2009-2017 is shown in Table 2. Monthly maximum air temperature (TX), minimum air temperature (TN) and average air temperature (TG) were

Tab. 2. Val d'Orcia monthly thermal regime. Monthly maximum air temperature (TX), minimum air temperature (TN) and average air temperature (TG) for each year and for the whole study period (2009-2017).
Tab. 2. Regime termico mensile della Val d'Orcia. Temperatura mensile massima (TX), temperatura mensile minima (TN), temperatura mensile media (TG) per ogni anno dello studio e media per tutto il periodo (2009-2017).

Month	2009	2010	2011	2012	2013	2014	2015	2016	2017	2009-2017
TX (°C)										
JAN	7.9	6.8	8.5	8.4	7.9	9.5	8.9	9.1	6.9	8.2
FEB	9.0	8.9	10.2	4.5	7.5	12.4	9.0	11.7	12.7	9.6
MAR	13.2	11.2	11.3	15.8	10.8	12.5	11.7	11.4	15.9	12.6
APR	17.2	16.2	16.8	15.7	17.1	16.2	16.1	17.8	18.5	16.9
MAY	23.9	18.8	20.6	19.0	17.2	18.7	20.8	18.8	22.5	20.0
JUN	24.5	24.5	24.0	27.8	23.7	24.9	26.2	24.0	29.6	25.5
JUL	29.4	29.9	25.3	29.6	27.6	24.4	31.3	28.6	30.6	28.5
AUG	31.2	27.1	28.7	30.8	28.2	25.5	28.3	27.0	32.7	28.8
SEP	24.9	20.7	25.5	23.7	24.6	22.5	23.4	24.1	23.6	23.7
OCT	18.1	16.3	17.8	18.6	18.9	19.2	16.7	17.3	20.7	18.2
NOV	14.4	13.1	14.2	14.1	12.5	15.5	13.7	13.9	13.6	13.9
DEC	9.6	8.7	10.7	8.2	9.9	9.4	10.7	10.7	9.1	9.7
TN (°C)										
JAN	1.1	1.3	3.1	3.2	2.9	5.3	3.9	4.5	-0.5	2.8
FEB	1.3	3.0	2.9	-0.9	1.2	6.3	2.8	6.0	4.6	3.0
MAR	4.4	4.3	4.0	7.4	4.8	5.9	5.5	4.9	5.7	5.2
APR	8.5	7.3	9.3	7.9	9.3	8.6	8.1	9.6	7.3	8.4
MAY	12.3	10.7	12.2	10.4	10.0	10.5	12.4	10.8	11.1	11.2
JUN	14.4	14.4	15.5	17.2	14.3	15.9	16.9	15.2	16.6	15.6
JUL	17.1	18.7	16.2	18.4	18.4	16.1	20.8	18.4	17.3	17.9
AUG	18.9	16.9	18.9	20.1	18.5	16.7	18.5	17.2	19.2	18.3
SEP	14.9	8.9	16.6	15.6	15.6	15.1	15.3	15.8	12.6	14.5
OCT	9.1	9.2	10.3	12.0	12.8	12.5	10.9	10.9	9.9	10.8
NOV	7.1	7.2	6.5	8.8	7.3	10.7	8.5	7.7	5.4	7.7
DEC	3.2	2.9	4.5	3.2	5.3	5.3	6.6	5.3	2.2	4.3
TG (°C)										
JAN	4.5	4.1	5.8	5.8	5.4	7.4	6.4	6.8	3.2	5.5
FEB	5.2	6.0	6.6	1.8	4.4	9.4	5.9	8.8	8.7	6.3
MAR	8.8	7.8	7.7	11.6	7.8	9.2	8.6	8.1	10.8	8.9
APR	12.9	11.7	13.1	11.7	13.2	12.4	12.1	13.7	12.9	12.6
MAY	18.1	14.8	16.4	14.7	13.6	14.6	16.6	14.8	16.8	15.6
JUN	19.5	19.5	19.8	22.5	19.0	20.4	21.5	19.6	23.1	20.5
JUL	23.3	24.3	20.8	24.0	23.0	20.2	26.0	23.5	24.0	23.2
AUG	25.0	22.0	23.8	25.4	23.4	21.1	23.4	22.1	25.9	23.6
SEP	19.9	14.8	21.1	19.7	20.1	18.8	19.4	20.0	18.1	19.1
OCT	13.6	12.7	14.0	15.3	15.8	15.9	13.8	14.1	15.3	14.5
NOV	10.7	10.1	10.4	11.5	9.9	13.1	11.1	10.8	9.5	10.8
DEC	6.4	5.8	7.6	5.7	7.6	7.3	8.6	8.0	5.6	7.0

calculated for each year and for the whole study period (2009-2017). The hottest months resulted to be July and August, with very similar TX, TN and TG values; while the coldest month was January, with a TG of 5.8 °C. The interannual thermal variability during the whole study period showed that February was the month with the highest variability: 7.9 °C in TX, 7.2 °C in TN and 7.6 °C in TG. On the contrary, April resulted to be the month with lower interannual thermal variability, with 2.8 °C in TX, 1.7 °C in TN and 2 °C in TG.

Flowering date seemed to be influenced in a decisive way from the trend of average air temperature. (Bonofiglio *et al.*, 2009), in a 26 years study (1982-2007) conducted in Central Italy, registered an anticipation of the flowering period, which was due mostly to an increase of the average temperature during the months of March, April, May and June, especially from May (start flowering) to June (full flowering). In our study period we observed the following average air temperature trend (Tab. 2): in March it ranged between 7.8 °C (2010 and 2013) and 11.6 °C (2012), in April between 11.7 °C (2010 and 2012) and 13.7 °C (2016), in May between 13.6 °C (2013) and 18,1 °C (2009) and in June between 19.0 °C (2013) and 23.1 °C (2017).

An annual average of 23 FD were recorded in the Val d'Orcia olive orchards area: 33, 15, and 22 FD in station 1, 2, and 3 respectively (Tab. 3). FD were recorded during the winter, in early spring and in late autumn. As expected, the months with a maximum number of FD were the winter ones (on average 7.9, 6.6 and 6.2 respectively in January, February and December), following by November with an average of 1.2 FD and March with an average of 1.8 FD.

The annual maximum number of FD (47) was recorded in 2017 by station 1 which (positioned at the lowest altitude). While, an FD value of 31 was recorded by station 3 evidencing the occurrence of a strong thermal inversion that is characteristic of the study area. The annual minimum number of FD (4) was recorded in 2016 in station 1 and in 2014 in station 2 (data not shown).

The olive tree is moderately resistant to below zero temperatures but suffers frost injury when specific thermal thresholds are exceeded: -16 °C for xilema and twig cambium, -12 °C for buds and leaves, and -6 °C for roots (Larcher, 1970). However, persistent temperatures below –7 °C can damage aerial parts and seriously reduce the productivity (Palliotti and Bongi, 1996). The most characteristic symptoms of frost damage include tip burn of shoots tips and nearby leaf tips, leaf chlorosis, defoliation, bark split on branches and also damages to buds and fruits (Barranco *et al.*, 2005).

During the study period the minimum average temperature values never dropped below -6 °C. The maximum minimum temperature (-8.2 °C) was reached only for a few consecutive hours in February 2012, in December 2016 and in January 2017 in station 3, such as not to damage olive trees, (data not shown).

An annual average of 91.3 RRs were recorded in the monitored area: 91.5, 88.0, and 94.3 RRs in station 1, 2, and 3 respectively. The maximum average number of RRs (116) were recorded in 2013 and 2014, while the lowest average number of RRs was recorded in 2017 (66) (Tab. 4).

RRs were continuously distributed throughout the year; no months without RRs were recorded during the observation period. On average, the largest number of RRs was recorded in spring (26,4 RRs), than in winter and autumn (25,1 RRs) and finally in summer (14,7 RRs). The month with the maximum average number of RRs was November (10,6 RRs) while the month with the minimum number was August (3,3 RRs) (Tab. 5).

Phenology can be considered a bio-indicator for climate change as a proxy for temperatures (Menzel, 2002). Heat accumulation, quantified by GDD, is the major factor for the determination of bud development, budburst, flower blooming and other phenological phases (Hänninen, 1990). During our study period, an average of 2434 GDD_{VP} was achieved in the whole Val d'Orcia. GDD_{VP} decreased as the altitude increased. Considering the annual average of the three stations, the hottest years were 2012 and 2017 when 2565.7 GDD_{VP} and

Tab. 3. Monthly and annual average Frost Days (FD) collected in Val d'Orcia during the study period (2009-2017) in the three stations: station 1: Buonconvento (altitude 188 m asl); station 2: Ripa d'Orcia (altitude 506 m asl); station 3: Castiglione d'Orcia (altitude 672 m asl).
Tab. 3. Valori medi mensili ed annuali dei Giorni di Gelo (Frost Days - FD) osservati in Val d'Orcia durante il periodo di studio (2009-2017) nelle tre diverse stazioni: stazione 1: Buonconvento (altitudine 188 m slm); stazione 2: Ripa d'Orcia (altitudine 506 m slm); stazione 3: Castiglione d'Orcia (altitudine 672 m slm).

2009-2017	G	F	M	A	M	G	L	A	S	O	N	D	TOT
Station 1	10.9	8.4	2.3	0	0	0	0	0	0	0	2.1	9.9	33.6
Station 2	5.9	4.7	1.1	0	0	0	0	0	0	0	0.4	3.2	15.3
Station 3	7.1	6.7	2.1	0	0	0	0	0	0	0	1.1	5.4	22.4
Average	7.9	6.6	1.8	0	0	0	0	0	0	0	1.2	6.2	23.7

Tab. 4. Annual and total amount of rainy days (RR) collected in Val d'Orcia during the study period (2012-2017) in the three stations: station 1: Buonconvento (altitude 188 m asl); station 2: Ripa d'Orcia (altitude 506 m asl); station 3: Castiglione d'Orcia (altitude 672 m asl).
Tab. 4. Numero di giorni piovosi (RR) annuale e totale per il periodo di osservazione (2012-2017) nelle tre stazioni: stazione 1: Buonconvento (altitude 188 m asl); station 2: Ripa d'Orcia (altitude 506 m asl); station 3: Castiglione d'Orcia (altitude 672 m asl).

RR	2012	2013	2014	2015	2016	2017	Tot.
Station 1	84	106	118	75	105	61	91.5
Station 2	75	117	115	69	93	59	88.0
Station 3	76	125	115	78	94	78	94.3
Average	78.3	116.0	116.0	74.0	97.3	66.0	91.3

2613.0 GDD_{VP} were achieved respectively. The coldest year was 2014 with 2196.3 GDD_{VP}. Considering the seasonal average values after summer (1383.1 GDD_{JJA}) the hottest season was autumn (565.4 GDD_{SO}). Only in 2017 spring was warmer (546.0 GDD_{MAM}) than autumn (533.3 GDD_{SO}) resulting to be the hottest in the period under review (Tab. 6). This result is consistent with the global warming trend: a progressive European warming might promote elongation of the summer period into the autumn (Fischer and Schär, 2009). However no trend in GDD was observed in our study, probably because of the limited number of years analyzed.

During the warmest years, values of 2748 GDDVP (2011) and 2735 GDDVP (2017) were achieved in station 1, whereas in the coldest one (2014), the GDDVP value was 2317. In spring, GDD varied between 430 (2013) and 622 (2011), in summer between 1250 (2014) and 1573 (2017), in autumn between 551 (2015) and 657 (2011).

In station 2, in the warmest years GDDVP values ranged about 2650 (2012) and 2732 (2017) in the warmest years, whereas in the coldest one (2014) GDDVP value was about 2281. The hottest season resulted to be always the summer, followed by autumn. In spring, GDD varied between 420 (2013) and 585 (2017), in summer between 1217 (2017) and 1585 (2017), in autumn between 554 (2015) and 632 (2013). The 2017 was the year characterized by the hottest summer and spring.

In station 3, the warmest years were 2012 and 2017 when 2378 GDDVP and 2372 GDDVP were achieved, respectively. The coldest year was 2014 reaching 2191 GDDvp. The hottest season resulted to be the summer followed by autumn and spring.

Contrary to what has been observed in other stations in 2017 spring was colder (458 GDD_{MAM}) than autumn (471 GDD_{SO}), although it was the warmest spring in the period under review. The autumn of 2017 was the coldest (471 GDD_{SO}) of the period. The GDD ranged between 320 in 2013 and 466 in 2011 during spring, between 1104 in 2014 and 1443 in 2017 during summer, and between 471 in 2017 and 568 in 2013 during autumn. 2013 was confirmed the year with the coldest spring and hottest autumn.

Finally, Table 8 shows yearly EVO yield (Y)

Tab. 5. Monthly amount of rainy days (RR) collected in Val d'Orcia during the study period (2012-2017) in the three stations: station 1: Buonconvento (altitude 188 m asl); station 2: Ripa d'Orcia (altitude 506 m asl); station 3: Castiglione d'Orcia (altitude 672 m asl).
Tab. 5. Numero mensile di giorni piovosi (RR) registrati durante il peiriodo di studio (2012-2017) nelle tre stazioni della Val d'Orcia: stazione 1: Buonconvento (altitude 188 m asl); station 2: Ripa d'Orcia (altitude 506 m asl); station 3: Castiglione d'Orcia (altitude 672 m asl).

RR 2012-2017	Jan	Feb	Mar	Apr	May	Jun	Jul	Aug	Sep	Oct	Nov	Dec
Station 1	8.0	11.2	8.2	8.5	9.5	5.8	3.3	3.0	6.5	8.0	11.2	8.3
Station 2	7.7	9.5	8.3	7.5	9.8	6.7	4.5	3.3	7.5	6.7	10.7	5.8
Station 3	7.7	10.2	8.7	8.5	10.2	7.8	5.8	3.7	7.7	7.3	10.0	6.8
Average	7.8	10.3	8.4	8.2	9.8	6.8	4.6	3.3	7.2	7.3	10.6	7.0

Tab. 6. Mean growing degree days (GDD) of the Val d'Orcia olive orchards area in the period 2009-2017 for the whole olive vegetative period (GDD_{VP}) and separately for each season (GDD_{MAM}, GDD_{JJA}, GDD_{SO}).
Tab. 6. Media dei gradi giorno (GDD) per il periodo di osservazione per l'area degli oliveti della Val d'Orcia per il periodo 2009-2017 relativi a tutto il periodo vegetativo (GDD_{VP}) e per ogni singola stagione: primavera (GDD_{MAM}) estate (GDD_{JJA}) e autunno (GDD_{SO}).

	2009	2010	2011	2012	2013	2014	2015	2016	2017	Ave 2009 - 2017
GDD_{MAM}	546.0	532.0	534.3	477.7	390.0	429.7	475.0	450.7	546.0	486.8
GDD_{JJA}	1390.3	1355.0	1346.0	1502.3	1303.0	1190.3	1471.3	1297.7	1533.7	1376.6
GDD_{SO}	562.3	571.7	608.3	585.7	613.0	576.3	527.7	556.3	533.3	570.5
GDD_{VP}	2498.7	2458.7	2488.7	2565.7	2306.0	2196.3	2474.0	2304.7	2613.0	2434.0

Tab. 7. Mean growing degree days (GDD) of the three SIR meteorological stations in Val d'Orcia olive orchards area in the period 2009-2017 for the whole olive vegetative period (GDD_{VP}) and separately for each season (GDD_{MAM}, GDD_{JJA}, GDD_{SO})
Tab. 7. Gradi giorno (GDD) medi relativi a tutto il periodo vegetativo (GDD_{VP}) e per ogni singola stagione: primavera (GDD_{MAM}) estate (GDD_{JJA}) e autunno (GDD_{SO}) nelle tre stazioni della Val d'Orcia per tutto il periodo di osservazione (2009-2017): stazione 1: Buonconvento (altitudine 188 m slm); stazione 2: Ripa d'Orcia (altitudine 506 m slm); stazione 3: Castiglione d'Orcia (altitudine 672 m slm).

Station 1	2009	2010	2011	2012	2013	2014	2015	2016	2017	Ave. 2009 - 2017
GDD_{MAM}	597	595	622	515	430	470	511	487	595	535.8
GDD_{JJA}	1414	1412	1469	1546	1358	1250	1523	1348	1573	1432.6
GDD_{SO}	588	596	657	608	639	597	551	568	567	596.8
GDD_{VP}	2599	2603	2748	2669	2427	2317	2585	2403	2735	2565.1
Station 2	2009	2010	2011	2012	2013	2014	2015	2016	2017	Ave. 2009 - 2017
GDD_{MAM}	575	564	549	511	420	460	498	473	585	515.0
GDD_{JJA}	1430	1395	1340	1529	1335	1217	1500	1329	1585	1406.7
GDD_{SO}	596	597	606	610	632	604	554	599	562	595.6
GDD_{VP}	2601	2556	2495	2650	2387	2281	2552	2401	2732	2517.2
Station 3	2009	2010	2011	2012	2013	2014	2015	2016	2017	Ave. 2009 - 2017
GDD_{MAM}	466	437	432	407	320	359	416	392	458	409.7
GDD_{JJA}	1327	1258	1229	1432	1216	1104	1391	1216	1443	1290.7
GDD_{SO}	503	522	562	539	568	528	478	502	471	519.2
GDD_{VP}	2296	2217	2223	2378	2104	1991	2285	2110	2372	2219.6

Tab. 8. Yearly EVO yield (Y) expressed in percentage (%) in the Val d'Orcia area in the period 2009-2017. Data provided by the Val d'Orcia Oil Mill, located in Castiglione d'Orcia (SI).
Tab. 8. Resa annuale e totale del periodo 2009-2017 delle olive (Y) espressa in percentuale (%) nell'area della Val d'Orcia. Dati forniti dalla Società Agricola Frantoio della Val d'Orcia con sede in Castiglione d'Orcia (SI).

	2009	2010	2011	2012	2013	2014	2015	2016	2017	Ave.
Y (%)	17.2	18.3	17.6	18.5	14.4	13.9	17.6	13.9	18.7	16.7

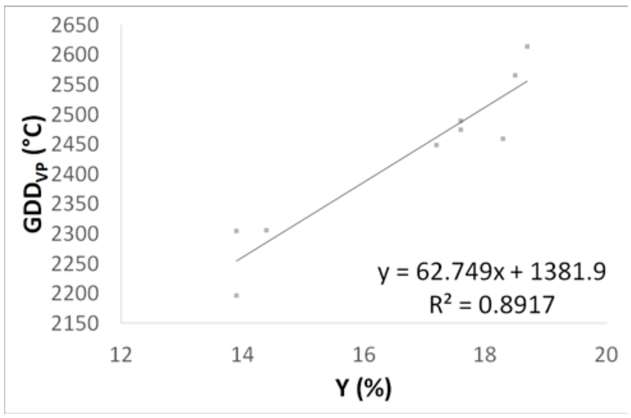

Fig. 4. linear regression between EVO yield (Y) and Growing degree days of the vegetative period (GDDVP) for the period 2009-2017.
Fig. 4. regressione lineare tra resa annuale di olio extra vergine di oliva (Y) e gradi giorno durante la stagione vegetativa dell'olivo (GDD_{VP}) nel periodo 2009-2017.

expressed in percentage (%). During the study period, Y was approximately of 16.7%, with maximum values in 2012 and 2017 with 18.5% and 18.7 % respectively, and minimum values in 2014 and 2016 with 13.9%.

In order to investigate if EVO yield was linked to thermo-pluviometric and GDD variables, a linear regression was made between Y and each index previously described. A positive trend was observed between Y, TX and TG, while a negative one was observed between Y and TN. No trend was found between T and RR and FD. On the contrary, a strong relationship was found between Y and GDD: in particular, a strong relationship was between Y and GDD_{JJA} (R^2 = 0.715) and with GDD_{VP} (R^2 = 0.819), while only a positive trend was observed with GDD_{MAM} and a negative one with GDD_{SO} (Figure 4).

The strong relationship observed between Y and GDD_{VP} and GDD_{JJA} confirmed how heat accumulation period (expressed ad GDD) can influence EVO yield and suggesting that GDD during the summer season (GDD_{J-JA}) can be a predictor of olive yield.

CONCLUSIONS

This is a preliminary analysis of thermo-pluviometric variability of Val d'Orcia olive orchards area (Tuscany, Italy), a not well investigated area despite of its agro-economic relevance.

The knowledge of the trend and the interseasonal and interannual behaviour and variability of air temperature in olive orchards area is essential to forecast some phenological phase that play an important role in olive production, i.e. flowering stage, helping to prevent agronomic problem such as biotic and abiotic diseases, i.e. olive fly, olive peacock spot, etc.

The variability observed in precipitation in areas very close together shows the strong influence of topography and atmospheric circulation on local precipitation distribution. This outcome could be linked to an ongoing change in the Mediterranean weather circulation which increasingly determines heavy precipitation events but extremely localized. The strong relationship observed between EVO yield and heat accumulation period during the summer season (GDD_{JJA}) suggests that this index can be a good predictor of olive yield.

The results of this study help to increase the knowledge of agro-climatic variability of Val d'Orcia olive orchards area. Moreover, they could be useful for implementing precision farming techniques in this area, such as the optimization of some olive management practices, and the application of models for evaluating the development of plants and plant pathogens.

DATA AVAILABILITY

Thermo pluviometrioc data used in this paper can be requested to the Regional Hydrological Sector of Tuscany (SIR) following the instructions on the website www.sir.toscana.it/

FUNDING STATEMENT

Research funded by: Progetto AppAGO – Applicazioni agronomiche innovative per la gestione dell'olivicoltura collinare. Misura 16.2 – PSR 2014-2020 Regione Toscana

REFERENCES

Barranco D., Ruiz N., Gómez-del Campo M., 2005. Frost tolerance of eight olive cultivars. HortScience, 40(3): 558-560.

Bartolini G., Morabito M., Crisci A., Grifoni D., Torrigiani T., Petralli M., Maracchi G., Orlandini S., 2008. Recent trends in Tuscany (Italy) summer temperature and indices of extremes. International Journal of Climatology, 26: 1751-1760.

Bartolini G., Messeri A., Grifoni D., Mannini D., Orlandini S., 2014. Recent trends in seasonal and annual precipitation indices in Tuscany (Italy).Theoretical and Applied Climatology, 118: 147.

Beniston M., Stephenson D.B., 2004. Extreme climatic events and their evolution under changing climatic conditions. Global and Planetary Change, 44:1-9.

Bonofiglio T., Orlandi F., Sgromo C., Romano B., Fornaciari M., 2008. Influence of temperature and rainfall on timing of olive (Olea europaea) flowering in southern Italy. New Zealand Journal of Crop and Horticultural Science, 36(1): 59-69.

Bonofiglio T., Orlandi F., Sgromo C., Romano B., Fornaciari M., 2009. Evidences of olive pollination date variations in relation to spring temperature trends. Aerobiologia, 25(4): 227.

Brunetti M., Maugeri M., Nanni T., 2001. Changes in total precipitation rainy days and extreme events in north-eastern Italy. International Journal of Climatology, 21: 861-871.

Fischer E.M., Schär C., 2009. Future changes in daily summer temperature variability: driving processes and role for temperature extremes. Climate Dynamics, 33: 917-935.

Galán C., García-Mozo H., Cariñanos P., Alcázar P., Domínguez-Vilches E., 2001. The role of temperature in the onset of the Olea europaea L. pollen season in southwestern Spain. International Journal of Biometeorology, 45(1): 8-12.

Hänninen H., 1990. Modelling bud dormancy release in trees from cool and temperate regions. Acta Forestalia Fennica, 213: 1-47.

Köppen W., 1936. Das Geographische System der Klimate Handbuch der Klimatologie, 46.

Larcher W., 1970. Kalteresistenz und uberwinterungsvermogen mediterraner Holzpflanzen. Oecol Plant.

Loumou A., Giourga C., 2003. Olive groves:``The life and identity of the Mediterranean". Agriculture and Human Values, 20(1): 87-95.

Manton M.J., Della-Marta P. M., Haylock M.R., Hennessy K.J., Nicholls N., Chambers L.E., Inape K., 2001. Trends in extreme daily rainfall and temperature in Southeast Asia and the South Pacific: 1961-1998. International Journal of Climatology, 21(3): 269-284.

Massetti L., Petralli M., Orlandini S., 2015. The effect of urban morphology on Tilia x Europaea flowering. Urban Forestry and Urban Greening, 14(1): 187-193

Menzel A., 2002. Phenology: Its Importance to the Global Change Community. Climatic Change, 54: 379.

Milanesi C., Sorbi A., Paolucci E., Antonucci F., Menesatti P., Costa C., Pallottino F., Vignani R., Cimato A., Ciacci A., Cresti M., 2011. Pomology observations, morphometric analysis, ultrastructural study and allelic profiles of "olivastra Seggianese" endocarps from ancient olive trees (Olea europaea L.). Comptes Rendus Biologies, 334(1): 39-49.

Murray M.G., Galán C., 2016. Effect of the meteorological parameters on the Olea europaea L. pollen season in Bahía Blanca (Argentina). Aerobiologia, 32(3): 541-553.

Orlandi F., Ruga L., Romano B., Fornaciari M., 2005. Olive flowering as an indicator of local climatic changes. Theoretical and Applied Climatology, 81(3-4): 169-176.

Osborne C.P., Chuine I., Viner D., Woodward F.I., 2000. Olive phenology as a sensitive indicator of future climatic warming in the Mediterranean. Plant, Cell & Environment, 23(7): 701-710.

Palliotti A., G. Bongi., 1996. Freezing injury in the olive leaf and effects of mefluidide treatment. Journal of Horticultural Science, 71(1): 57-63.

Peterson T.C., Folland C., Gruza G., Hogg W., Mokssit A., Plummer N., 2001. Report of the activities of the working group on climate change detection and related rapporteurs. World Meteorological Organization Technical Document No 1071. World Meteorological Organization, Geneva, p. 146.

Recio M., Cabezudo B., Trigo M.M., Toro F.J., 1996. Olea europaea pollen in the atmosphere of Málaga (S. Spain) and its relationship with meteorological parameters. Grana, 35(5): 308-313.

Rosenzweig C., Iglesias A., Yang X.B., Epstein P.R., Chivian E., 2001. Climate change and extreme weather events; implications for food production, plant diseases, and pests. Global Change and Human Health, 2(2): 90-104.

Sofo A., Manfreda S., Fiorentino M., Dichio B., Xiloyannis C., 2008. The olive tree: a paradigm for drought tolerance in Mediterranean climates. Hydrology and Earth System Sciences Discussions,12(1): 293-301.

Walter H. and Lieth H., 1960. Klimadiagramm Weltatlas.

Yan Z., Jones P.D., Davies T.D., Moberg A., Bergström H., Camuffo D., Cocheo C., Maugeri M., Demarée G.R., Verhoeve T., Thoen E., Barriendos M., Rodríguez R., Martín-Vide J., Yang C., 2002: Trends of extreme temperatures in Europe and China based on daily observations. Climatic Change, 53: 355-392.

Italian Journal of Agrometeorology
Rivista Italiana di Agrometeorologia

Firenze University Press
www.fupress.com/ijam

OPEN ACCESS

Citation: B Latrech, H. Ghazouani, A. Lasram, B. Douh M'hamdi, M. Mansour, A. Boujelben (2019) Assessment of different methods for simulating actual evapotranspiration in a semi-arid environment. *Italian Journal of Agrometeorology* (2): 21-34. doi: 10.13128/ijam-650

Received: September 14, 2018

Accepted: April 18, 2019

Published: October 29, 2019

Data Availability Statement: All relevant data are within the paper and its Supporting Information files.

Competing Interests: The Author(s) declare(s) no conflict of interest.

Assessment of different methods for simulating actual evapotranspiration in a semi-arid environment

Valutazione di diversi metodi per simulare l'evapotraspirazione reale in un ambiente semi arido

Basma Latrech[1,*], Hiba Ghazouani[1,2], Asma Lasram[1], Boutheina Douh M'hamdi[1], Mohsen Mansour[3], Abdelhamid Boujelben[1]

[1] *Superior Institute of Agronomy - Chott Mariem, Université de Sousse, Tunisia*
[2] *Department of Agricultural and Forest Sciences (SAF), Università degli Studi di Palermo, Palermo, Italy*
[3] *Regional Research center on Horticulture and Organic Agriculture (CRRHAB)*
*Corresponding author e-mail: basma.latrech@gmail.com

Abstract. Field experiment was carried out to examine the effects of full and deficit irrigation treatments on yield and irrigation water productivity of potato crop conducted under semi-arid conditions of Tunisia. In addition, the accuracy of different models for computing daily ET_0 have been assessed against the standardized FAO 56-Penman Monteith estimations. An application of the FAO-56 dual approach to calculate actual evapotranspiration (ETa) is reported, implemented by means of the FAO-56 model. The obtained daily values of ET_0, were used as input in the FAO-56 model, in order to assess their impact on simulated actual evapotranspiration of potato crop. The obtained results indicate that potato yield decrease significantly with decreasing irrigation amount. However, no significant difference was obtained in term of WP_{irrig}. Comparison between the different ET_0 methods against the FAO-56 PM, revealed that the Makkink and Priestley-Taylor models might be considered as efficient alternatives for estimating ET_0. Furthermore, the simulated actual evapotranspiration are compared with their corresponding obtained by the water balance method. The statistical results of comparison highlighted that the best performances are accorded to the FAO-56 PM. More detailed analysis, evidenced also that the Hargreaves-Samani, Pristley-Taylor and Makkink approaches can be used as valid alternatives for estimating ETa.

Keywords. Reference evapotranspiration, FAO-56 model, deficit irrigation, irrigation water productivity, potato.

Abstract. L'esperimento è stato condotto per esaminare gli effetti sia di trattamenti di piena irrigazione che di irrigazione di soccorso sulla resa delle patate e la produttività di queste legata all'acqua di irrigazione in un ambiente semi arido in Tunisia. In aggiunta, è stata sperimentata l'accuratezza di diversi modelli per calcolare l'ET_0 giornaliera in confronto con le stime standardizzate della FAO 56-Penman Monteith. Nello studio è riportato l'uso del doppio sistema FAO 56 per calcolare l'evapotraspirazione potenziale (ETa). I dati giornalieri di ET_0 ottenuti sono stati usati come input nel modello FAO 56, per valutare la loro influenza sull'evapotraspirazione reale simulata sulle patate. I risultati ottenuti indicano che la resa delle patate diminuisce significativamente con la diminuzione dell'irrigazione. Comunque, non è stata osservata differenza significativa in termini di WP_{irrig}. Un confronto tra i diversi metodi ET_0 con il FAO 56 PM, ha rivelato che i modelli Makking e Priestley – Taylor potrebbero essere considerati delle alternative efficienti per stimare l'ET_0. Inoltre, le-evapotraspirazioni reali simulate sono state confrontate con le loro corrispondenti ottenute dal metodo del bilancio idrico. I risultati del confronto hanno evidenziato che le migliori performance si sono verificate nel metodo FAO-56 PM. Analisi aggiuntive più dettagliate, hanno anche evidenziato che gli approcci Hargreaves-Samani, Pristley-Taylor e Makkink possono essere usati come valide alternative.

Parole chiave. Evapotraspirazione di riferimento, modello FAO-56, irrigazione di soccorso, produttività legata all'acqua di irrigazione, patata.

1. INTRODUCTION

In the Mediterranean regions, characterized by arid and semi-arid climate, water availability is being severely scare (Rinaldi *et al.*, 2011; Provenzano *et al.*, 2013) as consequence of climate change (Rijsberman, 2006) and the increasing competition between municipal, industrial and environmental water users (McCann *et al.*, 2007; Yavuz *et al.*, 2015). In these regions, irrigation consumes more than 85% of the total available water (Er-Raki *et al.*, 2008). In particular, in Tunisia, irrigation water availability is characterized by frequent cutting events which results in social conflict over irrigated area. Therefore, to ensure the sustainability and integrity of the water resources, a substantial improvement in agriculture water use efficiency is required (Shahnazari *et al.*, 2007; Katerji *et al.*, 2013). In this context, irrigation scheduling techniques as full and deficit irrigation applied through regulated drip irrigation systems were widely used (Nagaz *et al.*, 2016). Moreover, Actual evapotranspiration reflects the crop water requirement as it is reflecting water losses from plant transpiration and soil evaporation (Alberto *et al.*, 2014). Thus, accurate estimation of actual evapotranspiration is a key factor for a sustainable water resource management and an effective irrigation scheduling (Rana and Katerji, 2000; Liu and Luo, 2010; Qiu *et al.*, 2015; Odi-Lara *et al.*, 2016).

A wide range of methods (direct and indirect) have been adopted to quantify actual crop evapotranspiration (Djaman *et al.*, 2016). Among the direct methods, it has been reported the weighting lysimeters (Kahyap and Panda, 2003; Xu and Chen, 2005; Liu and Luo, 2010; Schrader *et al.*, 2013) and the Eddy Covariance technique (Er-Raki *et al.*, 2008; Sun *et al.*, 2008; Alberto *et al.*, 2014; Zitouna-Chebbi *et al.*, 2018). Regarding indirect methods, different approaches were described in literature such as the Sap flow measurement method (Wilson *et al.*, 2001; Charfi Masmoudi *et al.*, 2011; Rallo *et al.*, 2014; Qiu *et al.*, 2015) and remote sensing data (Er-Raki *et al.*, 2008; Sánchez *et al.*, 2010; Maeda *et al.*, 2011). However, costs of the above mentioned methods remain quite high and demanding in terms of skilled user and the availability of the instruments are limited especially in the developing countries as Tunisia. Hence, the water balance model can be considered practical for an indirect method of actual evapotranspiration estimation (Katerji *et al.*, 2013; Qiu *et al.*, 2015; Tari, 2016; Tong *et al.*, 2016) since it doesn't require costly equipment and well trained personal.

Although the advanced techniques and methods that have been carried out for crop evapotranspiration determination, the Food and Agriculture Organization (FAO)-crop coefficient approach still to be the most common and simpler method (Allen *et al.*, 2005; Charfi Masmoudi *et al.*, 2011; Odi-Lara *et al.*, 2016; Wang *et al.*, 2018). This method consist on multiplying the reference evapotranspiration by a pre-determined crop specific coefficient (Qiu *et al.*, 2015). According to Allen *et al.* (1998), ET0 is defined as "the rate of evapotranspiration from a hypothetical reference crop, characterized by height of 0.12 m, surface resistance of 70 s m^{-1} and albedo of 0.23, closely resembling the evapotranspiration from an extensive surface of green grass of uniform height, actively growing, well-watered, and completely shading the ground" and Kc, defined as ETc/ET0. Commonly, the FAO-56 Penman Monteith model has been adopted and recommended as a standard method to estimate ET0 (Allen *et al.*, 1998). However, this method is not always evident to apply since it requires several meteorological data such as air temperature, relative humidity, solar radiation and wind speed at 2 m height, which are often incomplete or not available in most of developing and poor countries (Sahli and Jabloun, 2008; Djaman *et al.*, 2016). Thus, several alternative estimations considering limited weather data sets have been proposed and calibrated under different climate conditions (Tabari, 2009). They can be classified into one of the following four categories (1) temperature-based (e.g., Hargreaves and Samani, 1985); (2) radiation based (e.g., Makkink, 1957); (3) mass-based (e.g., Mahring, 1970) or (4) methods combining energy and mass balance (e.g., Penman, 1948).

In addition, simulation models, after calibration and validation related to a specific context, can be a suitable tool for water management and irrigation scheduling. Rallo *et al.* (2010) considered Agro-hydrological models as one of the most efficient models for these purposes. Despite their reliability, physically based and stochastic agro-hydrological models, cannot always be applied because of the high number of input data that require (Rallo *et al.*, 2010; Rallo *et al.*, 2014). Therefore, the simplified agro-hydrological model, such FAO-56 model (Allen *et al.*, 1998), which consider a simple water bucket approach, represent a balance between robustness and simplicity to be useful for irrigation scheduling decisions for a wide range of users background and skills level (McCann *et al.*, 2007). Accurate estimation of the seasonal ET is a basic component for calculating the water use efficiency (Katerji *et al.*, 2013). Thus, if a model is conceived to be used for irrigation water scheduling, it is necessary to verify, under water stress conditions, that the daily ET is also correctly simulated by the model during the crop cycle (Stewart *et al.*, 1977).

The main objectives of this research were firstly to investigate the effect of two irrigation levels on yield and irrigation water productivity of potato crop conducted under semi-arid conditions of Tunisia. Secondly to assess, in the same climatic context, the performance of different simpler daily reference evapotranspiration methods by comparing their values against those obtained by the standardized FAO-56 Penman Monteith model using different statistical parameters. Finally, to study the impact of different ET_0 methods, forced as input in the calibrated FAO-56 model on actual evapotranspiration of potato crop conducted under full and deficit irrigation treatments.

2. MATERIAL AND METHODS

2.1 Description of the experimental site and irrigation treatments

Field experiments were conducted at the experimental field of the High Agronomic Institute of Chott Mariem, Sousse, Tunisia (Long. 10.5632° N; Lat. 35.9191° N, Altitude 19 m above sea level). As evidenced by the data registered by the Regional Research center on Horticulture and Organic Agriculture weather station from 1983 to 2014 nearby the experimental site, climate is semi-arid with mild rainy winters and dry hot summers. Minimum and maximum monthly air temperature range from 7 to 21°C and from 17 to 32°C, respectively. The average annual rainfall is about 230 mm (Ghazouani *et al.,* 2016) and is almost concentrated in autumn and winter. Annual reference evapotranspiration, estimated using FAO-56 PM method, is about 1200 mm.

The experiments took place from February 25th, 2017 to Juin 4th, 2017 on a drip irrigation system of 572 m^2 cultivated with Potato crop '*Solanum Tubersum* L.', cultivar *Spunta*. Plants were spaced 40 cm along the rows, and 80 cm between the rows. The drippers were inline type and were set 40 cm apart and had a flow rate of 4 l/h at 1.0 atm pressure.

Data related to the soil properties of the experimental site are summarized in Tab. 1. In addition, the vertical soil profile revealed the presence of calcareous layer at about 1 m deep. Daily climate variables relative to minimum and maximum temperature, relative humidity, wind speed and solar radiation in order to estimate daily reference evapotranspiration were collected from a weather station located adjacent to the High Agronomic Institute of Chott Mariem.

Deficit and full irrigation treatments replicated three times (6 sub-plots) were set according to a split plot design with a subplot size of about 63 m^2 (2.4 m×26 m). The experimental plots were irrigated on the same day. For full irrigation treatment, the irrigation amount per time was equal to the actual evapotranspiration of the previous days as estimated using the FAO crop coefficient approach. However, for deficit treatment, 50% of

Tab. 1. Physical characteristics of the experimental field soil.
Tab. 1. Caratteristiche fisiche del suolo del campo sperimentale.

Soil layer (cm)	Texture	Bulk density (g/cm^3)	Field capacity (%)	Permanent wilting point (%)	Hydraulic conductivity (cm/min)
0- 35	Sandy loam	1.56	21.85	8.13	0.256
35-55	Sandy loam	1.68	25.15	9.74	0.213
55-90	Sandy loam	1.61	21.9	10.3	0.209

full irrigation was imposed along the entire crop season. The first period of the growth cycle was characterized by relatively low atmospheric demand associated to small plants with limited roots which result in a little crop evapotranspiration. Thus, during that period, plants were irrigated once time per week, while, thereafter, irrigation frequency was running twice per week. Each plot was connected by the flowmeter to deliver the desired amount of water.

2.2 Determination of actual evapotranspiration

Actual ET was determined through two-fold approaches, involving the measured water balance model and estimated according to the FAO-56 model.

2.2.1 Soil Water balance model

Actual evapotranspiration was indirectly computed using the simplified water balance method from the change in soil water content. During the investigation period, soil water content was measured gravimetrically, at depths of 0 - 0.25 and 0.26 - 0.45 m from the soil surface. For both treatments, soil water content was recorded before plantation, at approximately every 7 days intervals, and at harvesting. Since maximum depth does not exceed 0.35 m and maximum roots density were in the first layer, the change in soil storage was calculated only for the first soil layer. In addition, runoff and capillary rise can be neglected because of the flat ground and the presence of calcareous layer at 1 m deep that prevents the water stored in the deeper soil layer from moving up to the soil surface (Katerji *et al.*, 2013). Deep percolation was assumed to be zero since irrigations were performed through drip irrigation (Tari, 2016), and that precipitation, over the growing season, was characterized by very low rainfall events with a total precipitations of 10 mm. Thus, actual evapotranspiration can be estimated, at weekly time step, with the following equation

$$ET_a = I + P - \Delta S \quad (1)$$

where ETa actual evapotranspiration (mm); I, irrigation (mm); P, precipitation (mm); ΔS, change in soil water storage (mm).

2.2.2 FAO-56 model

The FAO-56 model estimates actual evapotranspiration from the reference evapotranspiration and the basal and evaporation coefficients. For this purpose, daily ET_0 values, computed by different methods, were forced as input in the model in order to evaluate their corresponding effects on actual ET estimated for potato crop.

2.2.2.1. ET_0 models description

FAO-56 Penman Monteith model (FAO 56-PM)

The FAO 56-Penman Monteith equation for the grass reference crop described by Allen *et al.* (1998) can be estimated as:

$$ET_0 = \frac{0.408\Delta(Rn - G) + \gamma\left(\frac{900}{T_{avg} + 273}\right)u_2(e_s - e_a)}{\Delta + \gamma(1 + 0.34u_2)} \quad (2)$$

where: ET_0: Reference evapotranspiration (mm day^{-1}), R_n: net radiation at the crop surface (MJ m^{-2} day^{-1}, G: soil heat flux density (MJ m^{-2} day^{-1}), T_{avg}: mean daily air temperature at 2 m height (°C), u_2: wind speed at 2 m height (m s^{-1}), e_s: saturation vapour pressure (kPa), e_a: actual vapour pressure (kPa), e_s-e_a: the saturation vapour pressure deficit (kPa), Δ: slope of the vapour pressure curve (kPa°C^{-1}), γ: psychrometric constant (kPa°C^{-1}).

Hargreaves-Samani model (HgS)

When solar radiation, relative humidity, and wind speed variables are missing, Hargreaves and Samani (1985) proposed the following simplified ET_0 model:

$$ET_0 = 0{,}0135\frac{Ra}{\lambda}\left(T_{avg} + 17{,}8\right) K_{rs}\sqrt{(T_{max} - T_{min})} \quad (3)$$

where Ra: the extraterrestrial radiation MJ m^{-2} day^{-1}, Tmax, Tmin: maximum and minimum daily air temperatures (°C), Tavg: mean daily air temperature (°C), K_{rs}: radiation adjustment coefficient (°$C^{-0.5}$); λ: latent heat of vaporization (MJ m^{-2} mm^{-1}).

Priestley Taylor model (PT)

Priestley and Taylor (1972) model is a shorten version of the original Penman model. It is defined as:

$$ET_0 = \alpha\frac{\Delta}{(\Delta + \gamma)}\frac{(R_n - G)}{\lambda} \quad (4)$$

α: the Priestley-Taylor parameter is equal to 1.26. However, it can vary from 1.08 to more than 1.6 (Minacapilli *et al.*, 2015).

Turc model (Turc)

Under humid conditions, Turc equation provides the most accurate estimation of ET0 when climatic data are insufficient (Trajkovic and Kolakovic, 2009)

$$ET_0 = 0.31\,C\,(Rs - 2.094)\frac{T_{avg}}{(T_{avg}+15)} \quad (5)$$

where Rs is the daily solar radiation MJ m^{-2} day^{-1}. If average relative humidity is greater than 50%, then

$$C = 1 \quad (5a).$$

If not, then it can be calculated by

$$C = 1 + \frac{50 + RHavg}{70} \quad (5b)$$

Irmak model (IK)

Irmak *et al.* (2003) developed an empirical models using a minimum number of input data. The model showed reasonable results in wet, arid, coastal, and inland sites under humid climates. According to these authors, ET0 can be estimated as:

$$ET_0 = 0.149Rs + 0.079T_{avg} - 0.611 \quad (6)$$

Makkink model (Mak)

The Mak model (Makkink, 1957), was presented in Netherlands as a modification of the Penman model as:

$$ET_0 = 0.61\frac{\Delta}{\Delta+\gamma}\frac{Rs}{\lambda} - 0.12 \quad (7)$$

Hansen model (Hsn)

The Hsn model (Hasen, 1984), was presented as a modification of the Makkink model. It is defined as:

$$ET_0 = 0.7\frac{\Delta}{\Delta+\gamma}\frac{Rs}{\lambda} \quad (8)$$

2.3 Model calibration

The FAO-56 model evaluates actual crop evapotranspiration (ETa) based on the dual crop coefficient method that separates evaporation from transpiration as:

$$ETa = E + T = (K_s K_{cb} + K_e)ET_0 \quad (9)$$

where ET_0 is the reference evapotranspiration (mm d^{-1}), Kcb is the basal crop coefficient; Ke is the soil evaporation coefficient. Ke is a function of the evaporation reduction coefficient (Kr), the maximum and basal crop coefficient, and the exposed and wetted soil fraction; Ks is dimensionless water stress coefficient, variable between 0 and 1 (Allen *et al.*, 1998).

Firstly, measured data collected during the experiment, related to plant (root depth, plant height), soil (soil fraction cover, initial depletion, available water) and weather data (Midseason average wind speed, Midseason relative humidity) were used as input in the model. The average values of basal crop coefficient were considered as the same values proposed by Allen *et al.* (1998). The readily evaporable water (REW) was considered as the same value referred by Qui *et al.,* (2015). The used value of REW is also inside the range of variability, for Sandy-loam soil, proposed by Allen *et al.* (1998). Thereafter, the FAO-56 model calibration procedure consisted of adjusting two parameters related to soil (depletion coefficient, p; and Effective depth of evaporable layer, Ze). Thus, estimation of the two considered parameters through iterative approximations was carried out and ceased only when the simulated values of potato actual evapotranspiration become similar to measured values. The daily values of ET0 used for the calibration procedure were estimated according the FAO-56 Penman Monteith method. Based on soil water content observations, the initial depletion for root zone was 20% of TAW (Tab. 2).

2.4 Plant measurements

Field observations included root depth, plant height, fraction of soil covered by crop canopy (fc), and leaf area were measured on different plants collected at different crop stages, from randomly chosen locations of each subplot. Every two weeks, after removing the plants from the soil and washing the roots carefully, the root depths were measured directly using a graduated ruler. Measurements of fc were performed every week. The fraction of the ground covered with the leaves was estimated using a 120 cm*80 cm area divided into 96 squares with equal dimensions, held over the central row. The covered fraction, which ranged from 0,01 to 1 (Allen *et al.*, 1998), was calculated as the number of cells at least half-filled of green leaf divided by the total number of cells (96) (Boyed *et al.*, 2002). However, measurement of leaves area was performed every two weeks with help of planimetric instrument. At harvesting, the crop yield was determined by weighting, per treatment and replicate, the total production obtained in 10 plants.

Tab. 2. Values of input variables used for simulations in the FAO-56 model.
Tab. 2. Valori delle variabili di input usate per le simulazioni nel modello FAO – 56.

Parameter	Value	Source
Soil water content at field capacity (m^3m^{-3})	0.22	m
Soil water content at wilting point (m^3m^{-3})	0.08	m
Available water (mm/m)	140	m
Depletion coefficient during initial stage (%)	20	e
Depletion coefficient after initial stage (%)	10	e
Total evaporable water, TEW (mm)	22	e
Readily evaporable water, REW (mm)	8	b[1],b[2]
Effective depth of evaporable layer, Ze (m)	0.12	e,b[1]
Lengh of initial stage (day)	20	e,b[1]
Lengh of development stage (day)	30	e,b[1]
Lengh of midseason stage (day)	35	e,b[1]
Lengh of late stage (day)	30	e,b[1]
Basal crop coefficient at initial season, $K_{cb\ ini}$	0.15	b[1]
Basal crop coefficient at mid-season, $K_{cb\ mid}$	1.10	b[1]
Basal crop coefficient at late season, $K_{cb\ end}$	0.65	b[1]
Maximuim crop height (m)	0.6	m
Minimuim rooting depth (m)	0.07	m
Maximuim rooting depth (m)	0.35	m
Midseason average wind speed (m s^{-1})	1.3	m
Midseason relative humidity (%)	60	m

m: measured data; e: estimated from field data; b; obtained from bibliography; 1: Allen *et al.* (1998), 2: Qui *et al.*, (2015).

2.5 Irrigation Water productivity (WP_{irrig})

The WP_{irrig} is expressed as the ratio of actual harvestable yield (Ya) and irrigation water (I) received from planting to harvest (Leogrande *et al.*, 2016; Nagaz *et al.*, 2016).

$$WP_{irrig}\left(\text{kg m}^{-3}\right) = \frac{Y_a}{I} \quad (10)$$

where: Ya actual harvestable yield (Kg ha^{-1}) and I is the irrigation water (m^3 ha^{-1}).

2.6 Statistical analysis

The normality of data (yield, irrigation water productivity) was tested by Shapiro-Wilk test, following which the data was subjected to one-way ANOVA (irrigation level) conducted by MINITAB.14 software. Tukey's test was used for comparing means estimated at $p<0.05$ probability level.

Evaluation of the accuracy and goodness of fit of model predictions were carried out by simple linear regression forced through the origin. Then, the performance of the models was evaluated using different statistical indices: coefficient of determination (R^2), Root Mean Square Error (RMSE), Mean Bias Error (MBE), Mean Absolut Error (MAE) and Efficiency coefficient (E).

$$RMSE = \sqrt{\frac{\sum_{i=1}^{N}\left(ET_{ref} - ET_{est}\right)^2}{N}} \quad (11)$$

$$MBE = \frac{\sum_{i=1}^{N}(ET_{ref} - ET_{est})}{N} \quad (12)$$

$$MAE = \frac{\sum_{i=1}^{N}\left|ET_{ref} - ETa_{est}\right|}{N} \quad (13)$$

$$E = 1 - \frac{\sum_{i=1}^{N}\left(ET_{est} - ET_{ref}\right)^2}{\sum_{i=1}^{N}\left(ET_{ref} - \overline{ET_{ref}}\right)^2} \quad (14)$$

RMSE allow to determine the error with the same units of the original variable (Sabziparvar *et al.*, 2016). MAE quantify the average absolute errors between reference and simulated data, whereas, MBE measure the average tendency of over or underestimation. Finally, E, is used to evaluate the predictive power of the model (Autovino *et al.,* 2016).

Values of RMSE and MAE can range from 0 to infinity (Alexandaris *et al.,* 2008). However, the lower the values of RMSE and MAE, the better the agreement.

There is no higher or lower bound of MBE. Values equal to 0 indicate that the model does not deviate from reference data, considered as true values. Positive MBE value indicates a certain underestimation of the considered variables and negative value corresponds to an overestimation (Negm *et al.,* 2017).

E can vary between -∞ and 1. E=1 correspond to perfect fit between model and reference data (Rinaldi *et al.,* 2011). Values between 0 and 1 are generally considered as an acceptable level of performance, and values lower than 0 indicate that the mean reference value predicts better than the model, indicating its unacceptable performance (Maulé *et al.,* 2006; Marti *et al.,* 2015; Autovino *et al.,* 2016).

3. RESULTS

Fig. 1 shows the temporal dynamics of daily average air Temperature, Tavg, vapor pressure deficit, VPD, short radiation, Rs, and precipitation height. Initial analysis of the climatic variables showed that Tavg and VPD follow the same trend over time. During the experimental period, the Rs values increase progressively from 35 to 47 MJ m^{-2} d^{-1}. However, reductions in Rs values were occurred during rainy events and cloudy days.

The total irrigation volumes applied during the potato cropping cycle, final yield and the Irrigation water productivity for both treatments are reported in Tab. 3. Potato yield varied widely with irrigation amount. In fact, higher yield (28.94 t/ha) was observed under full irrigation treatment, while, reducing irrigation volume by around 50%, resulted in a significant yield decrease of about 36%. Regarding irrigation water productivity, no significant difference was observed between both treatments.

Dynamic of daily reference evapotranspiration estimated by different models are depicted in Fig. 2. At the begin of the experiment (begin of Mars), the values of ET_0 were not very high, varying from 2.5 to 5.5 mm d^{-1} respectively for Hargreaves-Samani and Hansen methods. From the second decade of April, an important increase in term of ET_0 were registered with all considered methods. The highest values were attributed to Hansen and Turc approaches. Excluding Hargreaves Samani model, the increase of ET_0 can be explained by

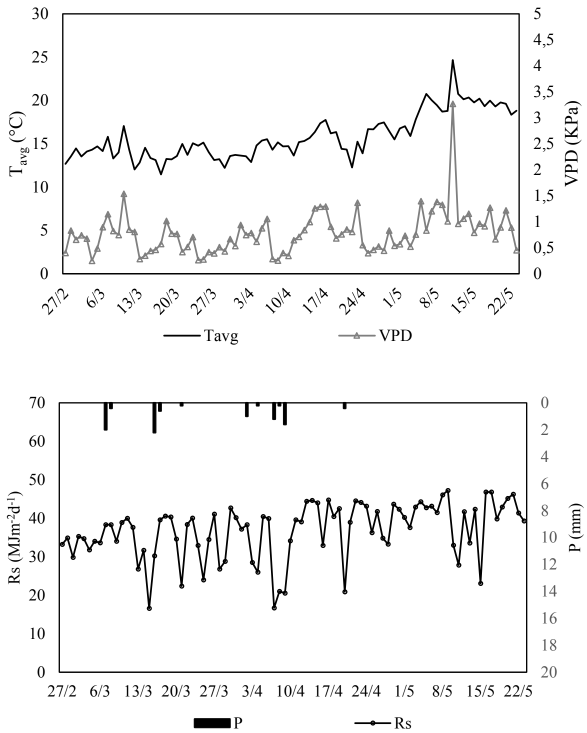

Fig. 1. a) average air Temperature, Tavg (left y-axis), and vapor pressure deficit, VPD (right y-axis); **b**) short radiation, Rs (left y-axis), Precipitation, P (right y-axis).

Fig. 1. a) Temperatura media dell'aria, Tavg (sinistra - asse y), deficit di pressione di vapore, VPD (destra – asse y); b) radiazione a onde corte, Rs (sinistra - asse y), Precipitazioni, P (destra - asse y).

Tab. 3. Potato total irrigations amount, yield and WP_{irrig}.
Tab. 3. Quantità totale di irrigazione, resa e WP_{irrig} nelle patate.

Treatment	Water supply (mm)	Yield (t/ha)	WP_{irrig} (kg/m^3)
Full irrigation	258.9 ± 8.8	28.94 ± 1.78	11.20 ± 1.03
Deficit irrigation	133.15 ± 5.6	18.44 ± 1.83	13.96 ± 1.92
Significance level		**	n.s

**= significant at the p≤ 0.01; n.s.= not significant.

the combining effect of hot temperature and solar radiation during all the investigation period.

Regarding its reliable estimations, the FAO-56 PM results were considered as the benchmark for comparison with the investigated daily ET_0 methods. The statistical results, based on the slope of the regression line, R^2, RMSE and MBE, are summarized in Tab. 4. With reference to the regression equations, the Makkink and Priestly-Taylor methods resulted in a slope values close to the unity (1.14 and 1.18 respectively) showing the best predicted values. Except for Hargreaves-Samani

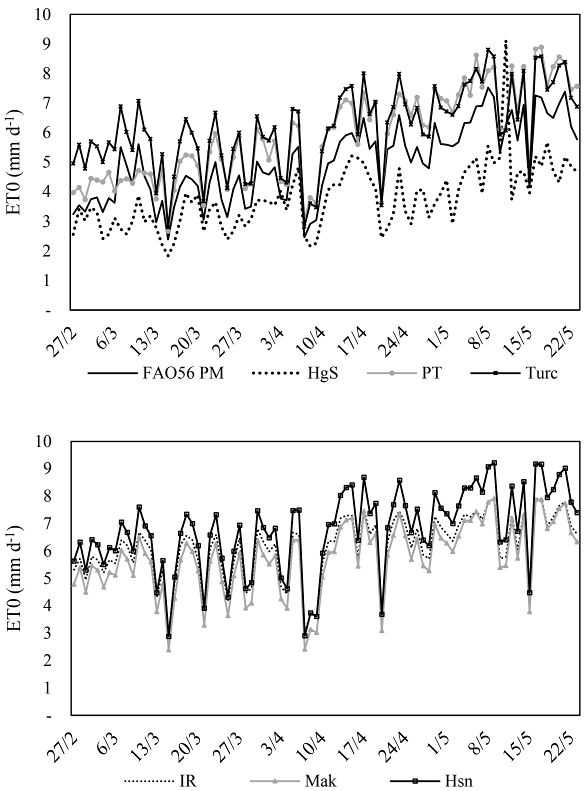

Fig. 2. Temporal patterns of daily reference evapotranspiration estimated by different models.

Fig. 2. Andamenti giornalieri della evapotraspirazione di riferimento stimata da diversi modelli.

Tab. 4. Statistical indicators computed by comparing daily reference evapotranspiration values estimated with the different methods against their corresponding standardized FAO-56 PM values.

Tab. 4. Indicatori statistici calcolati confrontando i valori di evapotraspirazione di riferimento giornalieri stimati con i diversi metodi con i corrispondenti valori standardizzati di FAO-56 PM.

Methods	HgS	PT	Turc	IK	Mak	Hsn
Slope (-)	0.75	1.18	1.23	1.20	1.14	1.33
R^2 (-)	0.54	0.89	0.87	0.60	0.80	0.79
RMSE (mm d^{-1})	1.49	1.04	1.27	1.26	0.93	1.86
MBE (mm d^{-1})	1.21	-0.89	-1.19	-1.13	-0.77	-1.76

and Irmak models, the used alternatives are strongly correlated with the FAO-56 PM method with R^2 values higher than 0.79. The RMSE values ranged between 0.93 and 1.86 mm d^{-1} respectively for Makkink and Hansen methods. Statistically, the RMSE associated to Makkink and Priestly-Taylor models were the most satisfactory and equal to 0.93 and 1.04 mm d^{-1}, indicating that these models yielded the lowest mean deviation from ET0 values computed with FAO-56 PM method. On average, all ET_0 methods show negative MBE indicating an overestimation of ET0 values during the springer season. The greatest overestimation (MBE= -1.76 mm d^{-1}) was obtained with Hansen method, giving the worst estimates among all the considered methods. Makkink and Pristley-Taylor models produced the lowest overestimations (MBE= -0.77 and -0.89 mm d^{-1} respectively) showing the best estimates among all the considered methods. However, an unsatisfactory underestimation was obtained for daily ET_0 computed by HgS method with an MBE value equal to 1.21 mm d^{-1}. Considering the statistical results and the linear regressions achieved in this study, it is concluded, in decreasing order, that Makkink, Pristley Taylor, and Turc alternatives are the most promising equations that could be used to estimate ET_0 when climatic data are limited.

The used and calibrated parameters of the FAO-56 model are given in Tab. 2.

The daily values of ET_0 computed by different methods were finally used as input in the calibrated FAO-56 model in order to assess their impact on actual evapotranspiration for a potato crop. The comparisons among actual evapotranspiration values simulated by the FAO-56 model by considering separately each investigated ET_0 method against their corresponding obtained by the simplified water balance model are shown in Fig. 3. As can be noticed from the graphs, the estimated values were in line with the corresponding measurements, with the slope of the regression line forced through the origin varying from 1 to 1.06 respectively for Hansen and Hargreaves-Samani model.

Despite a certain difference between measured and estimated ETa values, the performance of the considered ET_0 methods to estimate actual evapotranspiration were assessed through statistical descriptors (Tab. 5). In fact, all investigated methods are fairly well correlated with the simplified water balance model measurements with an R^2 values greater than 0.7. Except for Hansen model, all methods have a negative mean bias errors indicating that the FAO-56 model tend to overestimate ETa. As can be noticed from Tab. 5, the FAO-56 PM approach shows the best performance with an R^2 and efficiency coefficient (E) values of 0.82 and 0.79 and an RMSE and MAE values of 0.49 and 0.36 mm d^{-1} respectively. However, a further and more detailed analysis evidenced that, Hargreaves-Samani, Priestly-Taylor and Makkink approaches can be used, in such conditions and studies, when climatic data are missing. These methods provide also satisfactory results with an RMSE values varying from 0.55 to 0.61 and MBE values ranging between 0.40 and 0.44 mm d^{-1}.

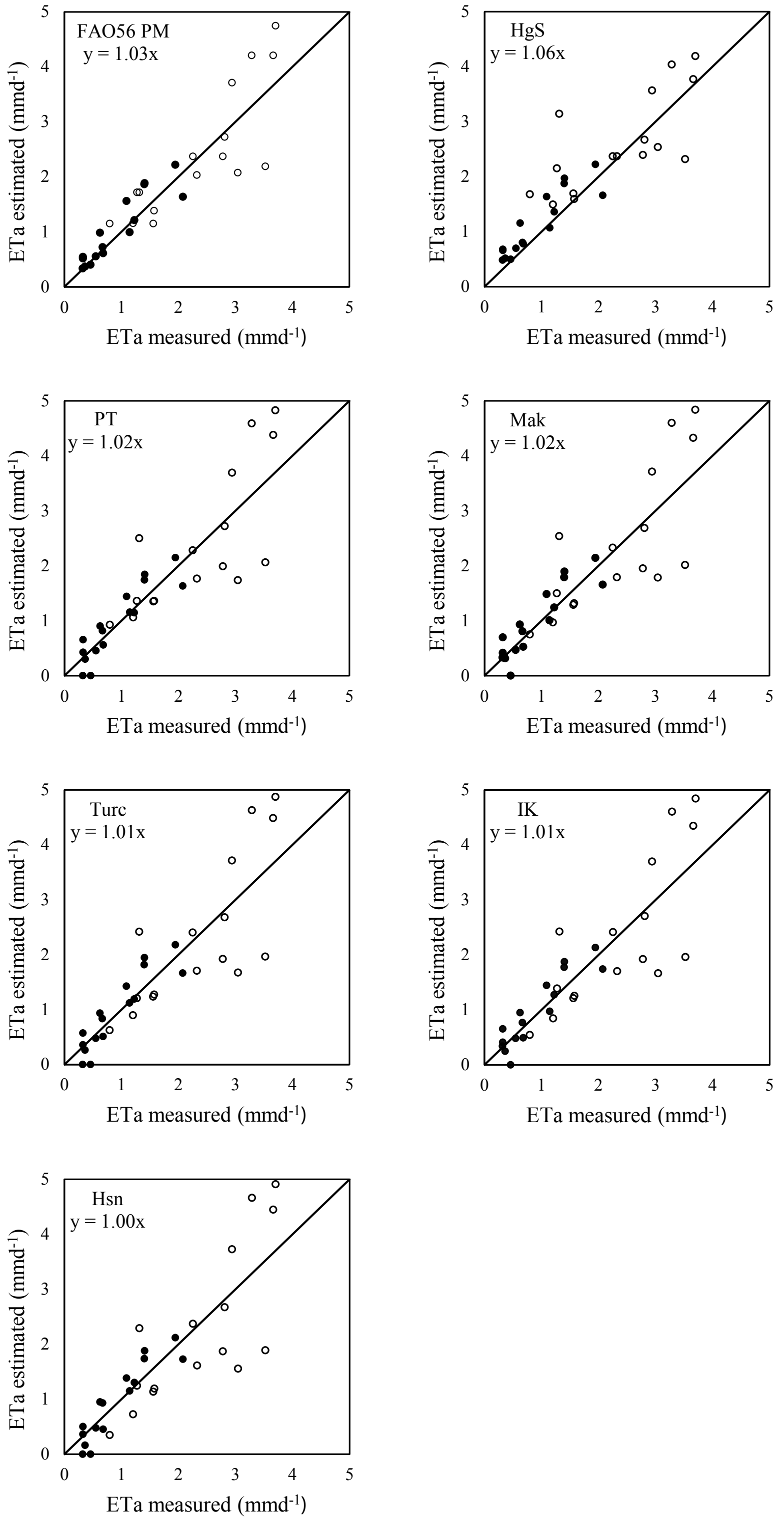

Fig. 3. Scatterplots of comparison between measured and estimated daily actual evapotranspiration under full (open circle) and deficit (filled circle) irrigation treatments.

Fig. 3. Confronto tra l'evapotraspirazione reale giornaliera misurata e quella stimata nei trattamenti di piena irrigazione (tondo aperto) e irrigazione di soccorso (tondo chiuso).

Tab. 5. Statistical indicators computed by comparing daily measured and estimated actual evapotranspiration.
Tab. 5. Indicatori statistici calcolati confrontando l'evapotraspirazione effettiva misurata quotidianamente e stimata.

Method	R^2 (-)	MBE (mm d^{-1})	RMSE (mm d^{-1})	MAE (mm d^{-1})	E (-)
FAO56 PM	0.82	-0.08	0.49	0.36	0.79
HgS	0.73	-0.23	0.55	0.40	0.73
PT	0.76	-0.04	0.60	0.43	0.68
Turc	0.75	-0.01	0.63	0.47	0.65
Ik	0.75	-0.01	0.62	0.46	0.66
Mak	0.75	-0.04	0.61	0.44	0.67
Hsn	0.74	0.03	0.66	0.49	0.62

4. DISCUSSION

A yield reduction of 36%, under deficit irrigation, suggests that potato crop is moderately tolerant to the considered water stress level. As it is known, yield decrease depends on degree, duration and timing of the imposed water stress (Tari, 2016). Therefore, deficit irrigation may be adopted, especially under circumstances of restricted water resources. However, reduction in yield can be avoided by regulating the applied water amount during the most sensitive stage of crop growth to water deficiencies.

Under full irrigation treatment, the obtained water productivity value (11.2 kg/m^3) falls within the range of variability of irrigation water productivity, for potato crop, proposed by Steduto *et al.* (2012). In our case, even it is not statistically different, the higher WP_{irrig} value is associated with the lower yield (18.44 t/ha). Meanwhile, the high WP_{irrig} are of little interest if they are not associated with high or acceptable yield (Ali *et al.,* 2007).

In fact, the FAO-56 PM ET_0 method has been proven to accurately estimate reference evapotranspiration under different climatic conditions (Allen *et al*., 1998; Er-Raki *et al*., 2010; Minacapilli *et al*., 2015). As described by Fisher *et al*., (2005), the accuracy of FAO-56 PM to estimate ET_0 is related to the fact that this method simulate well the aerodynamic component, while it is not the case for the other models. All the investigated ET_0 alternatives resulted in relatively similar simulations due to the common theoretical basis of their equations. Except for Hargreaves Samani model, all the considered methods required solar radiation data as input to accurately estimate ET0. Thus, they are classified as radiation based methods. Considering the results achieved in this study, it is concluded that, Makkink, Pristley Taylor, and Turc approaches can be used as efficient alternatives to estimate ET_0 while Hargreaves Samani model is not well appropriate in such conditions. The accuracy of both Makkink and Priestley-Taylor methods may be related to the fact that these two methods are established based on a modification of the original Penman equation. These results are consistent with those previously published by Minacapilli *et al.* (2015) who, evaluated in Southern Italy, the performance of seven ET_0 methods against ET_0 measurements acquired with a laser scintillometer. The authors found relatively the same rank of models suitability when the FAO-56 formulations are excluded. In the same context, results obtained by Er-Raki *et al.* (2010), for assessment of ET_0 estimation methods using climatic data generated from ALADIN model, showed that the reliability of Priestley-Taylor and Makkink models is much higher under humid conditions. Therefore, the accuracy of these approaches, in our conditions, may accorded to the closest position of the study area to the sea where relative humidity are relatively high.

The mentioned suggestion is confirmed by the accuracy estimations accorded to Turc approach and the lowest performance achieved by HgS model. In fact, Tabari (2009); Trajkovic and Kolakovic, (2009), found that Turc model is suitable to provide satisfactory estimates of ET_0 in humid conditions. Our findings are in good agreement with those obtained by Kashypa and Panda, (2001), who revealed that Hargreaves model is not to be recommended under sub-humid climatic regions. Moreover, the performances of HgS model achieved in our study, are considered below level when compared with results previously published, in semi-arid conditions, by Jabloun and Sahli, (2008) and Gavilàn *et al.* (2006). The authors found high correlation in the comparison between HgS and FAO-56 PM methods applied in different regions in Tunisia and Southern Spain respectively. It is worth mentioning that their results were also achieved using on ground climatic data. Hence, as recommended by Raziei *et al.* (2013), a local calibration of Hargreaves coefficient (K_{rs}) is required to improve its accuracy. Nevertheless, the suitability of Hargreaves-Samani approach may vary according to the season.

In the previous sections, the suitability of the FAO-56 model to predict actual evapotranspiration was verified according to water balance measurements during the investigation period. However, a little overestimation of ET by about 3.5% was shown with the model results. This mismatch may be the result of measurement errors of rooting depth, Zr, generated by the used method that doesn't reflect the architectural distribution of roots in soil profile. Meanwhile, the bucket models are very sensitive to this parameter (Er-Raki *et al*., 2008). In fact, higher Zr values causes an increase of TAW within the root zone and consequentially an increments of Ks values (Rallo *et al.*, 2014). Additionally, Er-Raki *et al.* (2008), showed that not only the rooting depth can affect the outputs of FAO-56 model, but also inappropriate depletion factor leads to an overestimation of Ks values.

The results of simulations revealed that the FAO-56 PM method provides the best performance, compared to measured actual evapotranspiration values, followed by Hargreaves-Samani, Priestley Taylor, Makkink and Turc results. These results are relatively consistent with those recently published by Minacapilli *et al.* (2015), who assessed the performance of different ET_0 methods forced as input in the FAO-56 model, on estimating actual evapotranspiration for an olive grove in Southern Italy. They showed that, the considered methodologies provide satisfactory estimated values when compared to FAO56-PM results with according the best performance to Priestly Taylor method so far as daily ET_0 estimation is concerned. Er-Raki *et al.* (2011), evaluated the suitability of four different reference evapotranspiration model to estimate actual evapotranspiration of winter wheat crop, conducted in semi-arid region in Morocco, using the simple Kc approach. The authors found that the Hargreaves-Samani method is the most appropriate model to estimate actual evapotranspiration when compared to results obtained by either FAO-Penman Monteith method or Eddy Covariance measurements. Moreover, the suitability of Priestly-Taylor and Makkink model were proven under different climatic conditions and time scales. In this way, Xu and Chen (2005) assessed the performance of different evapotranspiration models in water balance studies against lysimeter measurement in Germany. They inferred that, for the calculation of actual evapotranspiration at monthly and seasonal scale, the Makkink model perform better than the other methods. However, at yearly scale, the Priestly Taylor can be also used as an efficient alternative with a mean annual error less than 5%. They reported that performances of the investigated methods can be improved by a local calibration of the parameter values used for each model.

Despite its limited accuracy to estimate ET_0, the HgS method provides reliable estimations of actual evapotranspiration when it is used as input in the FAO-56 model. In fact, the obtained results could be due to the over-predictions generated by the FAO-56 model associated to the decrease of the soil water content through the investigated season. Thus a more precise parameterization of the FAO 56 dual approach model in order to improve both the estimation of the evaporation and transpiration rates is recommended.

5. CONCLUSION

Results of this study suggest that deficit irrigation, allows about 50% of water saving, can be considered an appropriate strategy under limited water circumstances. In addition, several reference evapotranspiration models were assessed through comparison with the FAO-56 PM results. This kind of studies is interesting, when climatic data required for computing PM ET0 are lacking. Thus, evaluating the suitability of different simplified methods characterized by limited input data is required. Based on RMSE, MAE, and linear regression analysis, the Makkink, Priestly-Taylor and Turc methods showed the best performances, for this particular study area, so far as daily ET0 estimation is concerned. However, the performances of these methods can be improved by a local coefficients calibration. Furthermore, the FAO-56 model was calibrated and used to simulate actual evapotranspiration of potato crop. The model simulations agreed well with their corresponding measurements based on water balance method.

This paper also evaluates the performance of the different alternatives of estimating ET0, forced as input in the calibrated FAO-56 model, on predicting actual evapotranspiration of potato crop under full and limited water conditions. Exploring the results of the model and the water balance measurements, it can be concluded that the FAO-56 model slightly over-predict actual evapotranspiration. Despite its over-predictions, the highest accuracy of the model is achieved when ET0 values computed by the FAO-56 PM method are forced as input in the model. Although the lowest accuracy of HgS model to estimate ET0, this model provides satisfactory results in term of actual evapotranspiration. Additionally, the performances of Priestly Taylor, Makkink and Turc approaches to estimate reference and actual evapotranspiration have been emphasized. Therefore, it is feasible to affirm that these methods are considered most appropriate for applying in such study area conditions. Nevertheless, in order to obtain more suitable results, an improvement of the FAO-56 model functions is recommended.

AKNOWLEDGMENTS

A special thanks is directed to Pr. Provenzano Giuseppe, associate Professor of Irrigation Plants at the Agricultural Faculty (Università degli Studi di Palermo_ Italy, UNIPA) for his help and encouragement.

REFERENCES

Alberto M. C. R., Quilty J. R., Buresh R. J., Wassmanna R., Haidar S., Correa Jr T.Q., Sandro J.M., 2014. Actual evapotranspiration and dual crop coefficients for dry-seeded rice and hybrid maize grown with overhead sprinkler irrigation. Agricultural Water Management, 136: 1-12.

Alexandaris S., Stricevic R., Petkovic S., 2008. Comparative analysis of reference evapotranspiration from the surface of rainfed grass in central Serbia calculated by six empirical methods against the Penman-Monteith formula. European Water 21/22: 17-28.

Ali M.H., Hoque M.R., Hassan A.A., Khair A., 2007. Effects of deficit irrigation on yield, water productivity and economic returns of wheat. Agricultural Water Management, 92: 151-161.

Allen R.G., Pereira S.L., Raes D., Smith M., 1998. Crop evapotranspiration. Guidelines for computing crop water requirements. FAO Irrigation and Drainage Paper 56. Rome, 300 pp.

Allen R.G., Pereira S.L., Smith M., Raes D., Wright J.L., 2005. FAO-56 dual crop coefficient method for estimating evaporation from soil and application extensions. Irrigation and drainage engineering, 131 (1): 2-13.

Autovino D., Minacapilli M., Provenzano G., 2016. Modelling bulk surface resistance by MODIS data and assessment of MOD16A2 evapotranspiration product in an irrigation district of Southern Italy. Agricultural Water Management, 167: 86-94.

Ayas S., 2013. The effects of different regimes on potato (Solanum tuberosum L. Hermes) yield and quality characteristics under unheated greenhouse conditions. Bulg. J. Agric. Sci., 19: 87-95

Bao-Zhong Y., Soichi N., Yaohu K., 2003. Effects of different irrigation regimes on the growth and yield of drip-irrigated potato. Agricultural Water Management, 63: 153-167.

Beyazgul M., Kayam Y., Engelsman F., 2000. Estimation methods for crop water requirements in the Gediz Basin of western Turkey. Journal of Hydrology, 229: 19-26.

Boyd N.S., Gordon R., Martin R.C., 2002. Relationship between leaf area index and ground cover in potato under different management conditions. Potato Research, 45: 117-129.

Carli C., Yuldashev F., Khalikov D., Condori B., Mares V., Monneveux P., 2014. Effect of different irrigation regimes on yield, water use efficiency and quality of potato (Solanum tuberosum L.) in the low lands of Tashkent, Uzbekistan: A field and modeling perspective. Field Crops Research journal, 163: 90-99.

Charfi Masmoudi Ch., Masmoudi M., Abid-Karray J., Ben Mechlia N., 2011. Sap flow measurements in young olive trees (Olea europaea L.) cv. Chétoui under Tunisian conditions. Scientia Horticulturae, 129: 520-527.

Chuanyan Z., Zhongren N., 2007. Estimating water needs of maize (Zea mays L.) using the dual crop coefficient method in the arid region of northwestern China. African Journal of Agricultural Research, 2: 325-333.

Djaman K., Tabari H., Balde A.B., Diop L., Futakuchi K., Irmak S., 2016. Analyses, calibration and validation of evapotranspiration models to predict grass-reference evapotranspiration in the Senegal river delta. Journal of Hydrology: Regional Studies, 8: 82-94.

Er-Raki S., Chehbouni A., Hoedjes J., Ezzahar J., Duchemin B., Jacob F., 2008. Improvement of FAO-56 method for olive orchards through sequential assimilation of thermal infrared-based estimates of ET. Agricultural Water Management, 95: 309-321.

Er-Raki S., Chehbouni A., Khabba S., Simonneaux V., Jarlan L., Ouldbba A., Rodriguez J.C., Allen, R., 2010. Assessment of reference evapotranspiration methods in semi-arid regions: Canweather forecast data be used as alternate of ground meteorological parameters?. Journal of Arid Environments, 74:1587-1596.

Er-Raki S., Chehbouni A., Ezzahar J., Khabba S., Lakhal E.K., Duchemin B., 2011. Derived Crop Coefficients for Winter Wheat Using Different Reference Evpotranspiration Estimates Methods. J. Agr. Sci. Tech., 13: 209-221.

Fisher J.B., DeBiase T.A., Qi Y., Xu M., Goldstein A.H., 2005. Evapotranspiration models compared on a Sierra Nevada forest ecosystem. Environmental Modelling & Software, 20: 783-796.

Gavilán P., Lorite I.J., Tornero S., Berengena J., 2006. Regional calibration of Hargreaves equation for estimating reference ET in a semi-arid environment. Agricultural water management, 81: 257-281.

Ghazouani H., Autovino D., Rallo G., Douh B., Provenzano G., 2016. Using HYDRUS-2D model to assess the optimal drip lateral depth for Eggplant crop in a sandy loam soil of central Tunisia. Italian Journal of Agrometeorology, DOI:10.19199/2016.1.2038-5625.047, 1:47-58.

Hansen S., 1984. Estimation of potential and actual evapotranspiration. Nord. Hydrol., 15: 205-212.

Hargreaves G.H., Samani Z.A., 1985. Reference crop evapotranspiration from temperature: Applied Engineering in Agriculture, 1: 96-99.

Irmak S., Irmak A., Allen R.G., Jones J.W., 2003. Solar and net radiation based equations to estimate refer-

ence evapotranspiration in humid climates. Journal of irrigation and drainage engineering, 129: 336-347.
Jabloun M., Sahli A., 2008. Evaluation of FAO-56 methodology for estimating reference evapotranspiration using limited climatic data Application to Tunisia. Agricultural water management, 95: 707-715.
Katerji N., Campi P., Mastrorilli M., 2013. Productivity, evapotranspiration, and water use efficiency of corn and tomato crops simulated by AquaCrop under contrasting water stress conditions in the Mediterranean region. Agricultural Water Management, 130: 14-26.
Kifle M., Gebretsadikan T.G., 2016. Yield and water use efficiency of furrow irrigated potato under regulated deficit irrigation, Atsibi-Wemberta, North Ethiopia. Agricultural Water Management, 170: 133-139.
Leogrande R., Vitti C., Lopedota O., Ventrella D., Montemurro F., 2016. Effects of irrigation volume and saline water on maize yield and soil in Southern Italy. Irrigation and drainage, DOI: 10.1002/ird.1964.
Liu Y., Luo Y., 2010. Consolidated evaluation of the FAO-56 dual crop coefficient approach using the lysimeter data in the North China Plain. Agricultural Water Management, 97: 31-40.
Maeda E.E., Wiberg D.A., Pellikka, P.K.E., 2011. Estimating reference evapotranspiration using remote sensing and empirical models in a region with limited ground data availability in Kenya. Applied Geography, 31: 251-258.
Mahring W., 1970. Verdunstungsstudien am neusiedler See. Theor. Appl. Clim., 18: 1-20.
Makkink G.F., 1957. Testing the Penman formula by means of lysimeters. J. Inst. Water Eng., 11: 277-288.
Marti P., Gonzàlez-Altozano P., Lopez-Urrea R., Mancha L.A., Shiri J., 2015. Modeling reference evapotranspiration with calculated targets. Assessment and implications. Agricultural Water Management, 149: 81-90.
Maulé C., Helgalson W., McGinn S., Cutforth H., 2006. Estimation of standardized reference evapotranspiration on the Canadian Prairies using simple models with limited weather data. Canadian Biosystems Engineering, 48: 1-11.
McCann I.R., Bruggeman A., Oweis T. Y., Pala M., 2007. Modification of the FAO-56 spreadsheet program for scheduling supplemental irrigation of winter crops in a Mediterranean climate. Applied Engineering in Agriculture, 24: 203-214.
Minacapilli M., Cammalleri C., Ciraolo G, Rallo G., Provenzano G., 2015. Using scintillometry to assess reference evapotranspiration methods and their impact on the water balance of olive groves. Agriculture water management, 170: 49-60.
Nagaz K., EL Mokh F., Alva A.K., Masmoudi M.M., Ben Mechlia N., 2016. Potato response to different irrigation regimes using saline water. Irrigation and drainage, 65: 654-663.
Negm A., Jabro J., Provenzano G., 2017. Assessing the suitability of American National Aeronautics and Space Administration (NASA) agro-climatology archive to predict daily meteorological variables and reference evapotranspiration in Sicily, Italy. Agricultural and Forest Meteorology, 244-245: 111-121.
Odi-Lara M., Campos I., Neale Ch. M. U., Ortega-Farías S., Poblete-Echeverría C., Balbontín, C., Calera A., 2016. Estimating Evapotranspiration of an Apple Orchard Using a Remote Sensing-Based Soil Water Balance. Remote Sensing, 8: 1-20.
Penman H.L., 1948. Natural evaporation from open water, bare soil and grass. Proc. R. Soc. Lond. A, 193: 120-145.
Priestley C.H.B., Taylor R.J. 1972. On the assessment of surface heat flux and evaporation using large-scale parameter. Mon. Weather Rev., 100: 81-92.
Provenzano G., Tarquis A. M., Rodriguez-Sinobas L., 2013. Soil and irrigation sustainability practices. Agricultural water management, 120: 1-4.
Qiu R., Du T., Kang S., Chen R., Wu L., 2015. Assessing the SIMDual Kc model for estimating evapotranspiration of hot pepper grown in a solar greenhouse in Northwest China. Agricultural Systems, 138: 1-9
Rallo G., Agnese C., Blanda F., Minacapilli M., Provenzano G., 2010. Agro-Hydrological models to schedule irrigation of Mediterranean tree crops. Italian journal of agrometeorology, 1: 11-21.
Rallo G., Baiamonte G., Manzano Juàrez J., Povenzano G., 2014. Improvement of FAO-56 Model to Estimate Transpiration Flux of Drought Tolerent Crops under Soil Water Deficit: Application for Olive Groves. Irrigation and drainage Engineering, ASCE, A4014001: 1-8.
Rana G., Katerji N., 2000. Measurement and estimation of actual evapotranspiration in the field under Mediterranean climate: a review. European Journal of Agronomy, 13: 125-153.
Raziei T., Pereira L.S., 2013. Estimation of ETo with Hargreaves-Samani and FAO-PM temperature methods for a wide range of climates in Iran. Agricultural water management 121: 1-18.
Rijsberman F.R., 2006. Water scarcity: fact or fiction? Agricultural Water Management, 80 (1), 5-22.
Rinaldi M., Garofalo P., Rubino P., Steduto P., 2011. Processing tomatoes under different irrigation regimes in Southern Italy: agronomic and economic assessments in a simulation case study. Italian Journal of Agrometeorology, 3: 39-56.

Sabziparvar A.A., Mirgaloybayat R., Marofi S., Zare-Abyaneh H., Khodamorad Pour M., 2016. Evaluation of Some Net Radiation Models for Improving Daily Reference Evapotranspiration Estimation in Iran. Journal of irrigation and drainage engineering, ASCE, 0401605:1-8.

Sánchez N., Martínez-Fernández J., Calera A., Torres E., Pérez-Gutiérrez C., 2010. Combining remote sensing and in situ soil moisture data for the application and validation of a distributed water balance model (HIDROMORE). Agricultural Water Management, 98: 69-78.

Schrader F., Durner W., Fankb J., Gebler S., Pützc T., Hannesd M., Wollschläger U., 2013. Estimating precipitation and actual evapotranspiration from precision lysimeter measurements. Proc. Environ. Sci., 19: 543-552.

Shahnazari A., Liu F., Andersen M.N., Jacobsen S.E., Jensen Ch. R., 2007. Effects of partial root-zone drying on yield, tuber size and water use efficiency in potato under field conditions. Field Crops Research, 100: 117-124.

Steduto P., Hsio Th.C., Fereres E., Raes D., 2012. Crop yield response to water. FAO Irrigation and Drainage Paper 56. Rome, 500 pp.

Sun Z.G., Wang Q.X., Matsushita B., Fukushima T., Ouyang Z., Waternabe M., 2008. A new method to define the VI-Ts diagram using subpixel information: a case study over a semiarid agricultural region in the North China Plain. Sensors, 8: 6260-6279.

Tabari H., 2009. Evaluation of Reference Crop Evapotranspiration Equations in Various Climates. Water Resources Management, 24: 2311-2337.

Tari A.F., 2016. The effects of different deficit irrigation strategies on yield, quality, and water-use efficiencies of wheat under semi-arid conditions. Agricultural Water Management, 167: 1-10.

Tong G. D., Liu H. L., Li F. H., 2016. Evaluation of dual crop coefficient approach on evapotranspiration calculation of cherry trees. Int. J. Agric. & Biol. Eng., 9 (3): 29-39.

Trajkovic S., Kolakovic S., 2009. Evaluation of reference evapotranspiration equations under humid conditions. Water Resources Management, 23: 3057-3067.

Wilson K.B., Hanson P.J., Mulholland P.J., Baldocchi D.D., Wullschleger S.D., 2001. A comparison of methods for determining forest evapotranspiration and its components: sap-flow, soil water budget, eddy covariance and catchment water balance. Agricultural and Forest Meteorology, 106: 153-168.

Xu C.Y., Chen D., 2005. Comparison of seven models for estimation of evapotranspiration and groundwater recharge using lysimeter measurement data in Germany. Hydrological processes, 19: 3717-3734.

Yavuz D., Yavuz N., Seymen M., Türkmen Ö., 2015. Evapotranspiration, crop coefficient and seed yield of drip irrigated pumpkin under semi-arid conditions. Scientia Horticulturae, 197: 33-40.

Zitouna-Chebbi R., Prévot L., Chakhar A., Marniche-Ben Abdallah M., Jacob F., 2018. Observing Actual Evapotranspiration from Flux Tower Eddy Covariance Measurements within a Hilly Watershed: Case Study of the Kamech Site, Cap Bon Peninsula, Tunisia. Atmosphere, 9, 68:1-1.

Italian Journal of
Agrometeorology
Rivista Italiana di Agrometeorologia

Firenze University Press
www.fupress.com/ijam

OPEN ACCESS

Citation: D. Kociper, K. Vintar Mally, L. Kajfež Bogataj (2019) Climate vulnerability of agriculture in statistical regions of Slovenia. *Italian Journal of Agrometeorology* (2): 35-48. doi: 10.13128/ijam-651

Received: March 30, 2019

Accepted: August 16, 2019

Published: October 29, 2019

Data Availability Statement: All relevant data are within the paper and its Supporting Information files.

Competing Interests: The Author(s) declare(s) no conflict of interest.

Climate vulnerability of agriculture in statistical regions of Slovenia

Vulnerabilità climatica dell'agricoltura nelle regioni statistiche della Slovenia

Doroteja Kociper[1,*], Katja Vintar Mally[2], Lučka Kajfež Bogataj[3]

[1]Gregorčičeva 32 a, 2000 Maribor, Slovenia
[2] PhD; University of Ljubljana; Faculty of Arts, Department of Geography, Aškerčeva cesta 2, 1000 Ljubljana, Slovenia
[3] PhD; University of Ljubljana, Biotechnical Faculty, Department of Agronomy, Jamnikarjeva 101, 1000 Ljubljana, Slovenia
*Corresponding author e-mail: doroteja.kociper@gmail.com

Abstract. Climate variability and extreme weather events, especially droughts, floods, hailstorms, low temperatures with frost and heat waves have significant negative effects on agriculture in Slovenia and increase its vulnerability. This study took into account the concept of vulnerability of the International Panel on Climate Change. The index of climate vulnerability of agriculture was developed on the basis of three indicators: exposure (climate variability and extreme weather events), sensitivity (threats due to natural conditions, changes in agriculture, vitality of the population) and adaptive capacity (income, sustainable management and natural resources). Climate vulnerability of agriculture was quantitatively analyzed with vulnerability indicators through the statistical regions of the Republic of Slovenia, and thus contributed to the regionally oriented approaches that seek to answer the challenges of climate vulnerability of agriculture in Slovenia. The results show higher climate vulnerability of agriculture in the western and central Slovenia and lower vulnerability in the eastern and northeastern part of the country.

Keywords. Climate change, vulnerability index, exposure, sensitivity, adaptive capacity.

Abstract. La variabilità climatica e gli eventi meteorologici estremi, specialmente la siccità, le alluvioni, le tempeste, l'abbassamento di temperature per le gelate e le ondate di calore, hanno effetti signifcativamente negativi per l'agricoltura in Slovenia ed aumentano la sua vulnerabilità. Questo studio ha preso in considerazione il concetto di vulnerabilità proposto dal IPCC. L'indice di vulnerabilità climatica dell'agricoltura è stato sviluppato sulla base di 3 indicatori: esposizione (variabilità climatica ed eventi meteo estemi), sensibilità (minaccia dovuta a condizioni naturali, cambiamenti in agricoltura, vitalità della popolazione) e capacità di adattamento (reddito, conduzione sostenibile e risorse naturali). La vulnerabilità climatica dell'agricoltura è stata analizzata quantitativamente con indicatori nelle regioni della Slovenia, e così ha contribuito agli approcci orientati regionalmente che cercano di rispondere alle sfide della vulnerabilità climatica dell'agricoltura in Slovenia. I risultati mostrano una più alta vulnerabilità climatica dell'agricoltura nell'ovest e centro della Slovenia e una minore nella parte est e nordest del paese.

Parole chiave. Cambiamento climatico, indice di vulnerabilità, esposizione, sensibilità, capacità di adattamento.

1. INTRODUCTION

Climate change has been scientifically confirmed and represents a challenge for the professional and general public to reflect on what can be expected in the future (Sušnik, 2014). Agricultural production is highly dependent on weather and consequently highly vulnerable in terms of climate change, mostly due to extreme weather, including droughts, floods, hailstorms and also low temperatures with frosts and heat waves (Antle, 1996). Slovenia is extremely diverse in terms of climate, it is located at the juncture of Alpine, continental and Mediterranean climate, and it is therefore necessary to interpret the trend of climate change with the complexity of the climate in each region (de Luis *et al*., 2014). Climate change will affect agriculture in many ways; the physiology of cultivated crops and animals, and the phenology and adaptability of organisms will be changed. Climate change will affect livestock production directly and indirectly, mainly through changes in pastures and grazing and through health and nutrition of livestock (Kajfež Bogataj 2005). Among the rare, seemingly positive influences, the increase in air temperature will result in spatial changes in agricultural production: upward shift of vegetation belts, change in the extent of cultivated land - the improvement in thermal characteristics of previously cold areas, deterioration of characteristics of already flooded areas, movement of arable land to higher positions etc. (Olesen and Bindi, 2002).

The climate scenarios for the two upcoming 30-year periods: the near future (2011-2040) and mid-century (2041-2070) ones show that continued warming is expected in Slovenia in the future. In the next thirty years, the annual mean air temperature is expected to increase by 1 °C, and an additional degree in the following period. For precipitation, climate scenarios show greater uncertainty, but signals with a shift to the future are increasing. At the annual level, the changes are only visible in the second 30-year period (2041-2070) when the amount of precipitation should increase in the eastern half of Slovenia. At the seasonal level, the changes are already reflected in the first 30-year period. In winter period, the amount of precipitation is expected to increase, and it will decrease in the summer. In the second 30-year period, this signal is intensifying. Changes in potential evapotranspiration in the first 30-year period should not be significant. In the next thirty years, there is an increase in potential evapotranspiration, especially in the summer and autumn (EEA, 2017). Slovenia is already facing extreme weather events that are causing devastation in agriculture, and with further changes these events will be even more frequent and more pronounced, and the climate vulnerability in agriculture will increase. Climate changes are also represented by trends of meteorological variables (i.e. mean temperature), not only by extreme events. These will affect the population, especially at local and regional levels. Due to these events it is important to plan adaptations of potential scenarios of change at regional and local level (El Gafy and Grigg, 2016). The present study aims at supporting the planning of adaptation by developing indicators of climate vulnerability of Slovenian agriculture. The assessment of climate vulnerability of agriculture is presented through all 12 statistical regions of Slovenia (i.e. regions at NUTS 3 level) which are Mura, Drava, Carinthia, Savinja, Central Sava, Lower Sava, Southeast Slovenia, Littoral–Inner Carniola, Central Slovenia, Upper Carniola, Gorizia and Coastal–Karst region.

A wide spectrum of different scientific fields uses the term vulnerability (such as economics, anthropology, sociology and philosophy), it is also commonly used term in the field of climate change. The International Panel on Climate Change (hereinafter: IPCC) interprets vulnerability as a link, function of exposure, sensitivity, and adaptive capacity (McCarthy *et al*., 2001). In a broader sense (Adger, 1999), the term vulnerability of a system, community or individual is related to the ability to cope with the problem. Sociologists and climatologists understand very different phenomena under the term vulnerability. Sociological vulnerability is a set of socio-economic factors that determine the ability of people to cope with stress or change (Allen, 2003). Most often, vulnerability is interpreted as an integrated concept linking the social and biophysical dimensions of environmental change (Turner *et al*., 2003). Fellmann (2012) defines vulnerability as a function of some variable, intensity, extent of climate change and the degree of system's (eg. region's) exposure, the sensitivity of the system and its adaptive capacity. Various definitions of climate vulnerability derive from various interpretations of climate change (O'Brian *et al.*, 2013) and various political responses to them (Demerritt, 2001; Forsyth, 2003). The vulnerability is not affected only by the change in the natural and social environment, but also by changes in social, economic, technological and other structures and processes so-called contextual state according to O'Brien *et al.* (2013). Vulnerability is interpreted as a negative state of a unit that is exposed to the consequences of climate change, and this situation can be quantified and improved. Vulnerability cannot be quantitatively measured as it is influenced by a wide range of factors and conditions. According to definitions of many authors dealing with the topic of vulnerability and climate change, the main parameters of vulnerability are: stress, which the system is exposed to, the sensitivity of the system and adaptive capacity of the system (e.g. regions, agriculture) to climate change (Adger, 2006).

The assessment of climate vulnerability represents an important basis for the development of guidelines for adaptation to climate factors in agriculture and for the development of appropriate policies for each statistical region and Slovenia as a whole. The assessment of vulnerability is complex and involves social, environmental and economic factors and is a prerequisite for the development of sustainable, low emission plans and strategies (Jun *et al.*, 2013). It also becomes an important assessment of vulnerability at local levels due to natural geographical and socio-economic differences between regions (Jun *et al.*, 2013). The adaptation of agriculture to extreme weather events is related not only with the decisions and measures of a particular farmer, but also with agricultural policy, market mechanisms and development and technological research (Kajfež Bogataj, 2005).

2. MATERIALS AND METHODS

2.1 Selection of conceptual framework of vulnerability

Individual vulnerability definitions describe individual vulnerability components, while the conceptual framework gives meaning to definitions so that they can be analysed according to the analytical context. Our approach is based on the definition of the IPCC (Parry *et al.*, 2007), according to which vulnerability to climate change is the degree to which geophysical, biological and socio-economic systems are susceptible to the negative impacts of climate change and can not cope with them. The system that is being dealt with is agriculture in the region. This means that the system is vulnerable if it is exposed and sensitive to the effects of climate change, but at the same time it has only limited adaptive capacity. Contrary to this, the system is less vulnerable when being less exposed, less sensitive, or has a strong adaptive capacity. Exposure refers to the nature and extent to which the system is exposed to significant climate change (McCarthy *et al.*, 2001). Exposure is represented by the climatic conditions and stimuli to which the system responds, and any changes in these conditions. Sensitivity means the degree of responsiveness of the system to climate change. The response to climate change can be as useful as it is also harmful to climate variability (O'Brian *et al.*, 2004). The effect may be direct (a change in crop in response to a change in average temperature, range or temperature variability) or indirect (damage caused by an increase in the frequency of floods) (Parry *et al.*, 2007). Sensitivity reflects the system's responsiveness to climate impacts and the extent to which climate change could be affected in its current form. Thus, the sensitive system is highly responsive to the climate and severely affected by moderate degree of climate change. Adaptive capacity is defined as the ability (or potential) of the system to successfully adapt to climate change (including climate and extreme variability), reducing potential damage, exploiting opportunities and/or managing the consequences (Füssel and Klein, 2006). Adaptive capacity involves the adaptation of both behavior and resources (Adger *et al.*, 2007) and can be thoroughly managed by human action's, which affects the biophysical and social elements of the system (Edenhofer *et al.*, 2014).

2.2 Research area

The index and indicators of climate vulnerability of agriculture are shown at the level of spatial units of Slovenia (regions). Statistical regions of Slovenia represent units of the research area for which climate vulnerability of agriculture and its indicators were presented (exposure, sensitivity and adaptive capacity), which were compared and evaluated. In addition to cohesion regions and municipalities, the statistical regions of Slovenia are one of the territorial levels for which the Statistical Office of the Republic of Slovenia collects and presents statistical data. In 2016, Eastern Slovenia consisted of 8 statistical regions (Mura, Drava, Carinthia, Savinja, Central Sava, Lower Sava, Southeastern Slovenia and Littoral–Inner Carniola). The Cohesion Region of Eastern Slovenia has an area of 12.212 km^2 and represents 60.2% of the territory of the Republic of Slovenia. In 2016, it had 1.091.570 inhabitants, representing 53% of the total population of Slovenia. Western Slovenia consists of 4 statistical regions (Central Slovenia, Upper Carniola, Gorizia and Coastal–Karst) with a total area of 8,061 km^2, representing 39.8% of the territory of the Republic of Slovenia. Population of western Slovenia represents 47% of Slovenia's total population (2016, 972.671 inhabitants). Western Slovenia covers the most economically developed areas in the country. Gross domestic product per capita amounted to 119.5% of the Slovenian average. The services contributed 75% of gross added value. In the cohesion region of Eastern Slovenia, the gross domestic product per capita was 82.7% of the Slovenian average. It is characterized by agricultural activity as it includes more than 70% of agricultural holdings and the majority of agricultural land (Regije v številkah ..., 2016).

2.3 Selection and design of variables and indicators that build Climate vulnerability index of agriculture

Later on, indicators and sub-indicators were developed and selected variables were chosen. In the selection of variables, derivation was made from the specific characteristics of agriculture in Slovenia, taking into account the availability of data by statistical regions of Slovenia from various data sources, which are also presented in Table 1. When selecting and designing variables and indicators, the following fundamental questions were followed: What is vulnerable (system)? Agriculture in the region. What is agriculture exposed to (exposure indicator)? To climate variability and extreme weather events. Why is agriculture sensitive (sensitivity indicator)? Because of the threats due to natural conditions, changes in agriculture, the vitality of the population. How can the vulnerability of agriculture (adaptive capacity indicator)be reduced? With income, sustainable management and natural resources.

The entire set of data was limited to those that can be displayed at the level of statistical regions. Since the statistical regions of Slovenia are not equally large, nor the agricultural activity is evenly distributed, the variables were dealt with in relation to agriculture - if the variable does not specifically refer to the agricultural activity, for example, air temperature, the temperature was treated only on agricultural surfaces or at meteorological stations below 1000 m of altitude. When defining the timing of the variables, the most uniform period and the latest available data were sought. Since this cannot always be achieved, some deviations also exist in the period 1961-2016 that was under consideration. For climatic variables, longer time period (30-50 years) was used. For variables that show greater fluctuations within individual years, the interest was also focused on a multiannual (e.g. 10-year) average or change. For variables that do not indicate significant fluctuations during years, particular interest was shown in the last situation, in our case this was 2016 and, exceptionally, also 2017. For each variable, it was necessary to find an appropriate method of calculation and display by statistical regions. The source of data and preliminary methodological treatment and, consequently, data quality were also important in this part. For example, in the case of climate variables, better quality data being those from meteorological stations of homogenized time series. Since these are limited to the last year of 2012, certain meteorological variables are not processed in the later period. A different treatment methodology was also encountered, for example, of agricultural land - once it was limited with an altitude of 1000 m, the next time they were treated in the graphic display of actual use of agricultural and forest land (RABA) and then as agricultural land in use from register of agricultural holdings (RKG).

When variables based on the available data were selected and developed, functional relationships between variables, indicators and vulnerability were determined, based on which the indicators and vulnerability across the statistical regions of Slovenia were evaluated (Table 1).

The selection and design of variables, the definition of mutual functional relationships between variables, indicators and vulnerability are important steps in the research, which are partially subjective. The choice itself also depends on the availability and quality of the data on which no influence was possible. Vintar Mally (2006) explains that, regardless of the scope of objective efforts, the choice of indicators (variables) is always at least partly subjective, since their choice is based on the subjective belief of an individual or group that they are important for measuring a certain amount of sustainability, in our case vulnerability. Therefore, it is necessary to realize that the ideal indicators do not exist and the indicators used are only better or worse substitutes for those who should completely capture certain phenomena, states and processes at all stages of the research.

2.4 Methods for combining variables for forming a composite index (aggregation)

In international literature, several different approaches are used to create a composite index based on different indicators and their variables. Many authors are concerned with comparing different methods of forming a composite vulnerability index that includes different approaches of standardization, weighting and aggregation in order to show similarities and differences between them (Monterroso, 2012; Tonmoy *et al.*, 2014; Yoon 2012; Žurovec *et al.*, 2017). All authors note that the final results of the vulnerability assessment depend on the choice of methods.

Tab. 1. Functional relationships of variables to vulnerability.
Tab. 1. Relazioni funzionali tra le variabili e la vulnerabilità.

Indicator	Sub-indicator	Variable	*Functional relationship	*Source
Exposure	Climate varaiability	Linear trend of average height of summer precipitation (%/decade), 1961–2011	-	ARSO
		Linear trend of average summer air temperature (°C/decade), 1961–2011	+	ARSO
		Linear trend of average summer potential evapotranspiration (%/decade), 1971–2012	+	ARSO
		Standard deviation of average summer precipitation on agricultural land (mm), 1981–2010	+	ARSO, MKGP
	Extreme weather events	75th percentile of summer meteorological water balance on agricultural land (mm), 1981–2010	-	ARSO, MKGP
		Average annual number of hot days, 1987–2016	+	ARSO
		Average annual amount of maximum daily precipitation (mm), 1987–2016	+	ARSO
		Average annual number of days with precipitation above 20 mm, 1987–2016	+	ARSO
		Average annual number of days with storms, 1987–2016	+	ARSO
		Weighted average of project wind speed on agricultural land (m/s), 1961–2006	+	ARSO, MKGP
		Average number of cold days in the spring, 1987–2016	+	ARSO
		Average number of frigid days in the spring, 1987–2016	+	ARSO
Sensitivity	Threats due to natural conditions	Share of flood threatened agricultural land (%), 2017	+	MKGP
		Weighted average of plants of accessible water for 50 cm deep soil on agricultural land (mm), 1999–2017	-	TIS/ICPVO, MKGP
		Share of utilised agricultural area in less-favored areas for agricultural activity (%), 2016	+	MKGP
		Share of average annual damage due to weather-related natural hazards in average gross domestic product (%), 2009–2016	+	SURS
	Changes in agriculture	Index of growth in the number of employees in agricultural activity, 2016/2007	-	SURS
		Growth index of utilized agricultural area, 2016/2007	-	SURS
	Vitality of population	Average age of the manager of the agricultural holding (in years), 2016	+	MKGP
		Average age of members of the agricultural holdings (in years), 2016	+	MKGP
Adaptive capacity	Income	Share of gross value added of agricultural activity in total gross value added (%), 2016	-	SURS
		Ratio between the standard income and the annual work unit of the agricultural (1000 EUR), 2016	-	SURS
		Share of agricultural holdings with supplementary farm activities (%), 2016	-	MKGP
		Ratio between average payments of agricultural policy measures and the average utilised agricultural area (1000 EUR/ha), 2007–2016	-	MKGP
	Sustainable management	Share of average annual investments for environmental protection in the average annual gross domestic product (%), 2007–2016	-	SURS
		Share of agricultural holdings with organic farming or in the state of conversion (%), 2016	-	MKGP
	Natural resources	Share of agricultural land with irrigation systems (%), 2017	-	MKGP, DRSV
		Ratio between the forest area and the number of inhabitants (ha/inh.), 2016	-	SURS

*Functional relationship:
In the functional relationship between vulnerability and variable higher and positive values of the variable in the + label mean higher vulnerability and in the – label lower vulnerability.
*Sources:
SEA – Slovenian Environmental Agency (ARSO – Agencija Republike Slovenije za okolje in proctor)
SIS/ICPEP – Soil Information System/Infrastructure Centre for Pedology and Environment Protection (Talni informacijski sistem/Infrastrukturni center za pedologijo in varstvo okolja)
MAFF – Ministry of Agriculture, Forestry and Food (MKGP – Ministrstvo za kmetijstvo, gozdarstvo in prehrano)
SWA – Slovenian water agency (DRSV – Direkcija Republike Slovenije za vode)
SORS – Statistical Office of Republic of Slovenia (SURS – Statistični urad Republike Slovenije)

2.4.1 Standardization of variables

The variables that build a common index and indicators in our research derive from different areas (social, economic and environmental), and therefore have different units and scales. Data normalization is a very important step when it comes to the variables of different units and scales. To ensure data comparability, the same measuring scale had to be used, in the interval between 0 and 1. Among the higher number of standardization methods, standardization proposed by UNDP for the calculation of the Human Development Index was selected. This methodology was also applied in the Balanced Development Index (Vintar Mally, 2011). In this respect, the methodology used to calculate the HDI before 2010 was followed. In 2010, unlike this method, it was calculated with an arithmetic mean, a geometric mean for the calculation of HDI, which is still used today (UNDP, 2018).

The variables were standardized according to the following equation:

$$Index = \frac{x - xmin}{xmax - xmin}$$

and for inverse ratios:

$$Index = 1 - \left(\frac{x - xmin}{xmax - xmin} \right)$$

Meaning: x - the value of the variable in the region, xmin - the minimum value of the variable (state or development in the country), xmax - the maximum value of the variable (state or development in the country).

In the next step, maximum and minimum values were set. According to Seljak (2001b), several solutions are possible for determining the lower and the upper limits of variables or limit referential values. When comparing the regions at a given time (state), the lowest value that appears in the observed row at the lower limit, and the highest value for the upper one can be observed, but this causes a problem in the interim comparison. When comparing changes in time (development), it is best to set the lower and upper limits as permanent. In our contribution, values of each variable were always calculated for all statistical regions of Slovenia, meaning that for each variable, the maximum value is always the highest value of the variable among all the values of the considered variable, and the same applies to the minimum value.

2.4.2 Assigning weights to variables and indicators

In the design of composed index, problems arise with selection of appropriate weights to determine the comparative power of individual variables. The simplest approach is where all variables have the same weight (Seljak, 2001a). Thus, in this research, the same weight was assigned to each indicator and also to the variables that build the individual indicator. A simple unweighted average (arithmetic mean) of normalized variables was used for creating indicators and a simple average (arithmetic mean) of indicators that form a composed vulnerability index. The most common method of assigning equal weights to variables was chosen according to international comparisons in the area of the composite index of vulnerability (Aubrecht and Özceylan, 2013; Chow *et al.*, 2012; Hahn *et al.*, 2009; Heltberg and Bonch-Osmolovskiy, 2010; Khajuria and Ravindranath, 2012; Krishnamurthy *et al.*, 2014; Tomlinson *et al.*, 2011; Yusuf and Francisco, 2009).

$$Average\ indicator = \frac{(Variable\ 1 + \ldots + Variable\ y)}{y}$$

Y is the number of variables in an indicator.

$$CVA = \frac{1}{3}(EAC + SAC + AACi)$$

The Climate vulnerability index of agriculture (CVA) is therefore 1/3 the exposure indicator of agriculture to the climate (EAC) + the sensitivity indicator of agriculture to the climate (SAC) + the adaptive capacity indicator of agriculture to the climate inverse (AACi).

The average indicator represents the arithmetic mean of all variables that build the indicator. Vulnerability is the arithmetic mean of all three indicators - exposure, sensitivity and adaptive capacity. Finally, in the same way that variables and indicators were normalized on a scale of 0 - 1, the same was done for final vulnerability index based on the average indices of individual indicators (exposure, sensitivity and adaptive capacity). Several international studies use the same normalizing method and display the final vulnerability index on a scale of 0-1 or 0-100 (Ahsan and Warner, 2014; Khajuria and Ravindranath, 2012; Krishnamurthy *et al.*, 2014; Sugiarto *et al.*, 2017; Yusuf and Francisco, 2009). In our survey, the lowest degree of vulnerability is represented by the value 0 and the highest with 1.

2.5 Methods for calculating the variables for presentation by statistical regions

Data for the calculations of variables were obtained from various databases and sources in various forms. The types of data vary greatly, and they also receive different treatment. For example, SORS data require fewer calculations since they are basically tabulated and already processed and sorted by region. On the other hand, raw data from the archives of the meteorological data of the SEA require much more caution and processing to reach final results - a presentation by statistical regions of Slovenia. Likewise, more processing requires data and graphic layers that have to be addressed with the ESRI ArcGIS software (hereinafter: ArcGIS). In addition to the ArcGIS software, MS Excel 2016 (hereinafter: MS Excel) was used for calculations.

In most cases, an arithmetic mean is used for the average value. The variables are also shown in proportions, ratios, indices, and the summer meteorological water balance as 75th percentile. In two cases, for plant-accessible water and project wind speed, a weighted average was used when the individual values have a different significance. The standard deviation is calculated for average precipitation using ArcGIS. The linear trend for each measuring station over a 10-year time period for precipitation variables, air temperature and potential evapotranspiration was calculated using the LINEST function within the MS Excel program with the least squares method.

3. RESULTS

3.1 Climate vulnerability of agriculture by statistical regions of Slovenia

The results of climate vulnerability of agriculture are at the level of statistical regions of Slovenia. Figure 1 shows the sum of all three indicators that build the vulnerability of each statistical region. The higher the sum of indices, the higher the climate vulnerability of agriculture. In this case, adaptive capacity is inverse, since the individual indices of the indicators are added and adaptive capacity has an inverse (positive) value at the index value of 1.00. Figure 1 shows the impact of each indicator on vulnerability. Mura region, for example, has a higher sensitivity than the Upper Carniola and the Central Slovenia regions, but the total vulnerability of the Mura region is still lower, as it has the lowest exposure. Each indicator contributes significantly to the overall vulnerability.

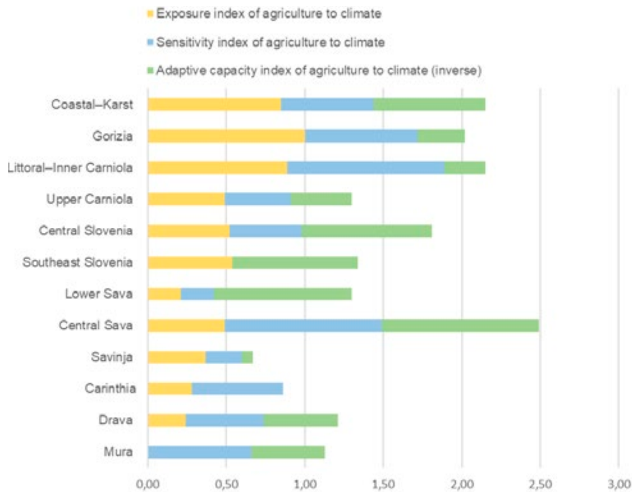

Fig. 1. Climate vulnerability of agriculture as a function of all three indicators: exposure, sensitivity and adaptive capacity (inverse).
Fig. 1. Vulnerabilità climatica dell'agricoltura in funzione di 3 indicatori: esposizione, sensibilità e capacità di adattamento (opposto).

Table 2 shows the final values of indices of individual indicators and vulnerability of the statistical regions in Slovenia. It was found that high exposure does not necessarily mean high sensitivity (Coastal–Karst region) or low adaptive capacity (Littoral–Inner Carniola region). The indicators are therefore independent of each other. The exposure of agriculture to the climate can be the highest and, at the same, time adaptive capacity can also be high (Gorizia region). Exposure may also be the lowest and there is still high sensitivity (Mura region). However, increasing vulnerability is exacerbated by increasing exposure and sensitivity and reducing adaptive capacity. The Central Sava region has the highest sensitivity (I = 1.00) and the lowest adaptive capacity (I = 0.00; I inverse = 1.00); therefore, the vulnerability is the highest (I = 1.00). The Savinja region does not have any extreme values. Since both exposure and sensitivity are low and adaptive capacity is very high which resulting in the lowest vulnerability (I = 0.00).

Figures 2-5 show the values of the indices of exposure, sensitivity, adaptive capacity and vulnerability according to the statistical regions of Slovenia. Index value 1.00 (green) means less exposure, less sensitivity, higher adaptive capacity and less vulnerability. Index value 0.00 (red) means the opposite.

Exposure index of agriculture to climate is concerned with climate variability and extreme weather events and declines in west-east direction. From the Mura region, where it attains the lowest value (I = 0.00) to Gorizia region with the highest value (I = 1.00) (Figure 2). The exposure of agriculture to climate is low in

Tab. 2. Values of indices of exposure, sensitivity, adaptive capacity and vulnerability by statistical regions of Slovenia.
Tab. 2. Valori degli indici di esposizione, sensibilità, capacità di adattamento e vulnerabilità nelle regioni della Slovenia.

Statistical region	Exposure index of agriculture to climate	Sensitivity index of agriculture to climate	Adaptive capacity index of agriculture to climate	Adaptive capacity index of agriculture to climate (inverse)	Climate vulnerability index of agriculture
Mura	0.00	0.66	0.53	0.47	0.25
Drava	0.24	0.50	0.53	0.47	0.30
Carinthia	0.28	0.58	1.00	0.00	0.10
Savinja	0.37	0.23	0.93	0.07	0.00
Central Sava	0.49	1.00	0.00	1.00	1.00
Lower Sava	0.21	0.21	0.12	0.88	0.35
Southeast Slovenia	0.54	0.00	0.20	0.80	0.37
Central Slovenia	0.52	0.46	0.17	0.83	0.63
Upper Carniola	0.49	0.42	0.61	0.39	0.35
Littoral–Inner Carniola	0.89	1.00	0.74	0.26	0.81
Gorizia	1.00	0.72	0.70	0.30	0.74
Coastal–Karst	0.85	0.59	0.29	0.71	0.81

the eastern part of Slovenia, which covers the Drava, Savinja, Carinthia in Lower Sava regions. In the central part of Slovenia (Upper Carniola, Central Sava, Central Slovenia in Southeast Slovenia), the exposure of agriculture to the climate is medium. The western part of Slovenia has the highest exposure of agriculture to climate in the Coastal–Karst, Littoral–Inner Carniola and Gorizia regions. The latter has the highest value (I = 1.00).

The climate variability was determined by the following variables: linear trend of average height of summer precipitation (%/decade) in the period 1961-2011, linear trend of average summer air temperature (°C/decade) in the period 1961-2011, linear trend of average summer potential evapotranspiration (%/decade) in the period 1971-2012 and the standard deviation of the average spring and summer precipitation on agricultural land (mm) in the period 1981-2010. It was found that the linear trend of average height of summer precipitation is negative at the vast majority of the measuring stations, which means that the summer precipitation will decrease. This leads to a lack of water in the growing season and a greater climatic vulnerability of agriculture. The decline in the precipitation rate in west-east direction is noticeable. Average values by statistical regions of Slovenia in the period 1961-2011 range from -0.1 %/10 years in the Carinthian region up to -4.9 %/10 years in the Coastal–Karst region. On the other hand, the linear trend of average summer air temperature increases at all measuring stations, which also affects the increased dryness. The eastern and south-eastern part of Slovenia is particularly exposed to the warming of the atmosphere. The average values by statistical regions in the period 1961-2011 ranged from 0.4 °C/10 years in the Upper Carniola, Gorizia to 0.5 °C/10 years Coastal–Karst regions. Linear trend of average summer potential evapotranspiration is also positive. So, evaporation is increasing which additionally affects the deficit of water. The southwestern part of Slovenia has the highest evaporation rate. The average values by regions in the period 1971-2012 ranged from 3.7 % in the Upper Carniola region to 5.1 % in the Gorizia region. The highest variability of precipitation, which is shown with the standard deviation of average spring and summer precipitation on agricultural land, is represented in the northwestern part of Slovenia, that is, in the area with the highest average precipitation values. The deviation values range from 3.8 mm in the Central Sava region to 37.1 mm in the Gorizia region.

Extreme weather events have been identified with various variables that are related to a particular event. Drought is shown with two variables; these are the 75th percentile of the summer meteorological water balance on agricultural land (mm) in the period 1981-2016, and the average annual number of hot days in the period 1987-2016. The average number of hot days varies from 5.3 in the Upper Carniola region to 36.8 days in the Gorizia region. Hot days when the temperature reaches or exceeds 30 °C has negative effects on the growth and development of crop plants. The 75th percentile of summer meteorological water balance on agricultural land has a positive value in only three regions; in the Upper Carniola region, where the highest value reaches 60.3 mm, and Carinthia and Gorizia, mainly because of higher precipitation. In all other regions, 75th percentile of summer meteorological water balance is negative. The highest negative value is in the Coastal–Karst region with -166.9 mm, which means high exposure to drought and thus higher vulnerability of agriculture. The flood as the second extreme weather event is defined by the average annual amount of the maximum daily precipitation (mm) in the period 1987-2016 and the average annual number of days with precipitation above 20 mm during the same period 1987-2016. Like a drought with water scarcity, it has a negative impact on agriculture as well, surplus water that causes damage to both crops and agricultural equipment. Both variables reach the highest values in the northwestern, the mountainous part of Slovenia. The average annual height of maximum daily precipitation varies from 49.6 mm in Mura to 123.0 mm in the Gorizia region. The average annual number of days with precipitation above 20 mm has the same pattern and range in the Mura region for at least 10.0 days, while in Gorizia it is a maximum of 34.1 days. Storms also have negative consequences in agriculture and increase climate vulnerability. It is shown with the average annual number of days with a storm in the period 1987-2016 and the weighted average of annual project wind speed on agricultural land (m/s) in the period 1961-2006. Storm occurrence can also be transferred to the hail. In the area where storms are more frequent, it is assumed that there is a greater likelihood of the occurrence of a hail, often accompanied by storms in Slovenia and destroying agricultural crops. Storms are typical for the whole area of Slovenia, with the most frequent occurrences in the Carinthian region an average of 28.2 storm days per year, and the least frequent in the Posavje region with 18.3 days per year. Project wind speed is an extreme value, and that is why most of Slovenia achieves the same weighted average annual project wind speed on agricultural land, 20 m/s with a return period of 50 years at a height of 10 m. The southwestern part of Slovenia is the most exposed to strong winds, where the Coastal–Karst region attains the highest average speed of 29.2 m/s. Spring frost is particularly problematic in fruit cultivation and wine growing when temperatures drop below -2°C. This was associated with the average number of cold days and average number of frigid days with frost in spring in the period 1987-2016. The average number of frigid days in the spring, when the air temperature reaches or drops below -10°C, is the lowest in the Gorizia region, where frigid days are rarely recorded, and the highest in the Littoral–Inner Carniola region with 0.6 days. The average number of cold days in the spring, when the air temperature drops below 0°C, varies from 2.1 days in the Coastal–Karst region to 9.1 days in the Upper Carniola region.

Sensitivity index of agriculture to climate concerned with threat due to natural conditions, changes in agriculture and the vitality of the population. Compared to exposure, the sensitivity pattern is somewhat different, and different index categories are distributed throughout Slovenia (Figure 3). The sensitivity index of agriculture to climate is the highest in the two regions, Central Sava and Littoral–Inner Carniola (I = 1.00), where agriculture is the most sensitive to the climate. Among the more sensitive (high sensitivity) are the Gorizia and Mura regions. The majority of statistical regions has medium sensitivity: the Coastal–Karst, Central Slovenia, Upper Carniola, Carinthia and Drava. The low sensitivity of agriculture to climate is in the Savinja and Lower Sava regions. The lowest sensitivity has Southeast Slovenia (I = 0.00).

The adaptive capacity index of agriculture to climate is concerned with income, sustainable management and natural resources. A certain pattern of allocation of categories of the index of adaptive capacity across Slovenia was detected (Figure 4). In the central and south-eastern part of Slovenia, agriculture has the least adaptive capacity to the climate. The Central Sava (I = 0.00), Lower Sava, Central Slovenia and Southeast Slovenia, have very low adaptive capacity, and only Coastal–Karst region has low adaptive capacity. The Mura and Drava regions in the north-eastern part of the country have medium adaptive capacity, while the western part of Slovenia with the Upper Carniola, Gorizia and Littoral–Inner Carniola regions has a high adaptive capacity. Agriculture is most capable of adapting to climate in the Savinja and Carinthia regions. The latter has the highest adaptive capacity (I = 1.00).

Climate vulnerability index of agriculture by statistical regions of Slovenia (Figure 5) reflects the indicators of exposure, sensitivity and adaptive capacity of agriculture to the climate. The demarcation between the more vulnerable western and central part of Slovenia and the less vulnerable eastern and northeastern part is evident. Each indicator has its own influence on the final vulnerability of the region (Figure 1). In the most vulnerable western and central part of Slovenia, Central Sava region (I = 1.00) has the highest vulnerability with the highest sensitivity (I = 1.00) and the lowest adaptive capacity (I = 0.00). The Coastal–Karst and Littoral–Inner Carniola regions, both with the same index value (I = 0.81), are also highly vulnerable (Table 2). The result in the Littoral–Inner Carniola region is mainly due to the highest sensitivity (I = 1.00) and very high exposure, while in the Coastal–Karst region there are very high exposure and low adaptive capacity. Highly vulnerable regions are the Gorizia and Central Slovenia regions; Gorizia achieves the highest exposure (I = 1,00) and high sensitivity, while the Central Slovenia has a very low adaptive

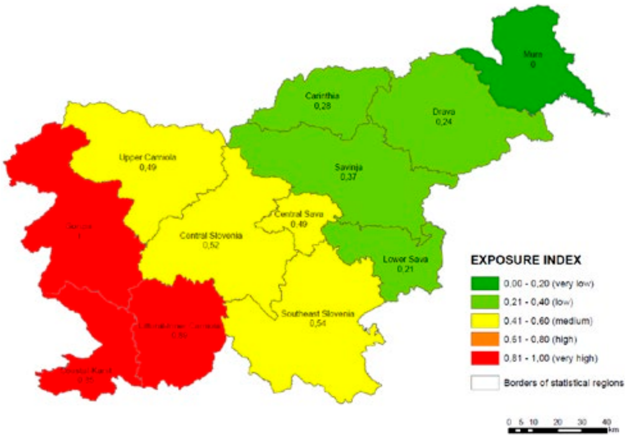

Fig. 2. Exposure index of agriculture to climate by statistical regions of Slovenia.
Fig. 2. Indice di esposizione dell'agricoltura al clima nelle regioni della Slovenia.

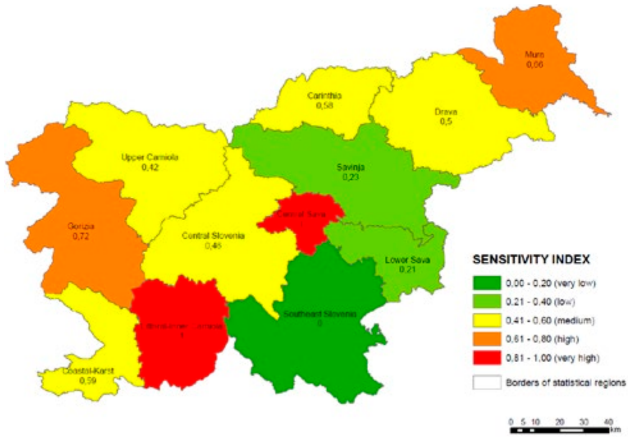

Fig. 3. Sensitivity index of agriculture to climate by statistical regions of Slovenia.
Fig. 3. Indice di sensibilità dell'agricoltura al clima nelle regioni della Slovenia.

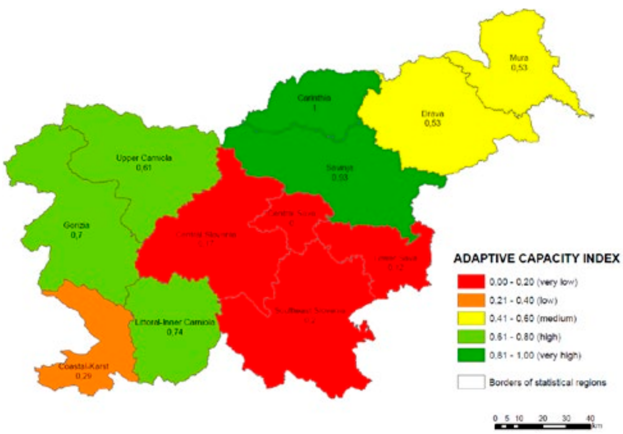

Fig. 4. Adaptive capacity index of agriculture to climate by statistical regions of Slovenia.
Fig. 4. Indice di capacità di adattabilità dell'agricoltura al clima nelle regioni della Slovenia.

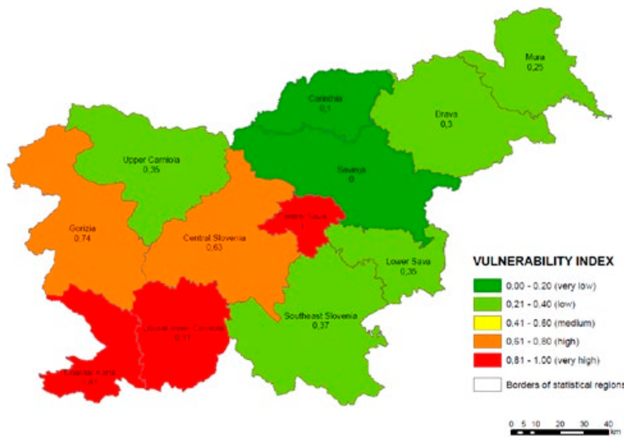

Fig. 5. Climate vulnerability index of agriculture by statistical regions of Slovenia.
Fig. 5. Indice di vulnerabilità climatica dell'agricoltura regioni della Slovenia.

capacity. Medium vulnerability was not detected. The western part of Slovenia with the Upper Carniola region is less vulnerable. The lowest vulnerability is recorded in the Savinja and Carinthia regions. The Savinja region has the lowest index value (I = 0.00) mainly due to the very high adaptive capacity and low exposure and sensitivity. Carinthia has very low vulnerability due to the highest adaptive capacity (I = 1.00) and low exposure. Most - five regions - are in the low vulnerability category: Mura, Drava, Lower Sava, Southeast Slovenia and the Upper Carniola. The Mura region has the lowest (I = 0.00), while the Drava and Lower Sava regions have very low exposure of agriculture to the climate. South-eastern Slovenia has the lowest sensitivity (I = 0.00), while the Upper Carniola region has the medium values in all three indicators (Figure 5).

4. DISCUSSION

Agriculture in Slovenia has an important role in economy and urgently needs a proper policy, since more than half of the population lives in rural areas, and agricultural land occupies one third of all areas. For agricultural policy, the greatest challenge is to find the right balance between adjustment of agricultural production and ensuring sufficient quantities of food and energy resources while reducing greenhouse gas emissions. Agriculture is heavily affected by climate change. Natural disasters are becoming more frequent and thus increase the production and income risks of agriculture. The agro-meteorological profession can help in dealing with problems and challenges in agriculture through its monitoring. It is necessary to improve knowledge on climate and weather, to draw up plans to identify and manage risk in agriculture. However, proper adaptation is a long-term process. In future, production processes in agriculture will need to be explicitly linked to weather and climate informations (Kajfež Bogataj *et al.*, 2003). Climate vulnerability assessments are carried out with the aim of helping policy makers to identify "hot spots" for allocating resources for adjustments, improving public awareness of climate risks, monitoring the effects of adaptation measures and improving understanding of weaknesses in the socio-ecological system, leading to vulnerability (Tonmoy *et al.*, 2014).

The Climate vulnerability index of agriculture in Slovenia was developed and was used to quantitatively evaluate the climate vulnerability of agriculture in all 12 statistical regions of Slovenia. It is a composite index from three indicators: exposure, sensitivity and adaptive capapcity, 11 sub-indicators and 28 variables, taking into account the social, economic and environmental factors that interact with the climate vulnerability of agriculture in Slovenia. The results show that the climate vulnerability of agriculture is the highest in the western and central part of Slovenia. The most vulnerable are the Central Sava region (I = 1.00) and the southwestern part of the country with the Littoral–Inner Carniola and Coastal–Karst region. Gorizia and Central Slovenia region are also highly vulnerable. In the northwestern part of Slovenia, with the Upper Carniola region, agriculture is less vulnerable to climate. Savinja (I = 0.00) and Carinthia regions are the least vulnerable. The low climate vulnerability of agriculture is present in most regions: Southeastern Slovenia, Upper Carniola, Posavina, Drava and Mura regions. It can be assumed that vulnerability, with the increasing frequency of extreme weather events and climate variability, will continue to increase, and most likely to impact the most vulnerable regions.

The work included dealing with issues of selecting the concept of vulnerability, methods of work, selection of the area and variables that build indicators and vulnerability. The literature on vulnerability assessments of socio-ecological systems is very diverse due to numerous quantitative and qualitative approaches. The vulnerability assessment based on indicators, which was used in this research, is one of the most common methods of assessment (Tonmoy *et al.*, 2014). The study follows a deductive approach using theories, models and frameworks on climate vulnerability. Regardless of the approach, standardization, aggregation and weighting of indicators are an inevitable subjective process (Vincent, 2004). In the development of the composite vulnerability index, one of the fundamental problems is the choice of the aggregation method (Adger *et al.*, 2004). Should the average value be used for the variables, or should the weights be assigned to the variables? If weights are used, how to determine them - by quantitative methods or by expert judgment? If weights are used, how can be taken into account the fact that the relative importance of vulnerability indicators varies by space and time? Experts' opinions are different, Eakin and Bojorquez-Tapia (2008) point out that the use of the same weights implies an implicit assessment of each variable and suggests the equal weighting of variables as the simplest but at the same time acceptable process that is available to us. However, determining weights based on expert judgment, in which this was subjectively decided on the basis of our knowledge of the problem, this may cause disagreements within the profession. Quantitative methods for determining weights are based on data variability which can represent an indicator with factor analysis and analysis of the main components. However, such approaches may be inadequate because they do not disclose the impact of each indicator on vulnerability (Hinkel, 2011). In this study, simple, unweighted averages of normalized variables were used, from which three main indicators were formulated (exposure, sensitivity and adaptive capacity) and the vulnerability index from these indicators. As Tonmoy *et al.* (2014) found, the equal weights is the method most commonly used in similar research. Planners, researchers and other actors must take into account that the degree of uncertainty is incorporated into the methods of work that were used. The results can vary significantly with the use of different methods.

5. CONCLUSION

The development of Climate vulnerability index of agriculture attempts to fill an important research gap, since for Slovenia such index has not been constructed yet. The main goal of the present research was the assessment of the climate vulnerability of agriculture to inform policy makers, farmers and researchers that it is necessary to reduce the risks associated with climate change. The assessment of the climate vulnerability of Slovenian agriculture was made in order to increase understanding of climate-vulnerable systems such as agriculture, as the purpose is to encourage policy and research institutions to prioritize the regions where climate vulnerability is highest, and to develop strategies that reduce vulnerability. It is important to raise awareness and encourage the agricultural holdings to implement agricultural practices that reduce vulnerability, but further research and analyzes of the climate vulnerability of Slovenian agriculture is needed: monitoring climate and impacts on agriculture and planning measures at regional and national levels.

The results which show the assessment of the climate vulnerability of Slovenian agriculture are primarily intended for farmers and agricultural policy. Since this is a global problem, public awareness and participation of both national and international policies, better results in reducing climate vulnerability of agriculture can not be expected without further investment in climate change research.

In order to better understand why agriculture is vulnerable to climate, further research, planning and engagement in practice is needed. Comparative research on the climate vulnerability of agriculture in Slovenia should be prepared and the new ways of assessing the climate vulnerability of agriculture should be sought. It is important to upgrade existing indicators in line with new developments in science. Further research and analysis of the agriculture climate vulnerability are encouraged: climate monitoring and impacts on agriculture and planning measures at regional and national level. Development of climate and socio-economic models, data for forecasting the future should also be included in the assessment of vulnerability. It is necessary to establish a comprehensive and effective publicly accessible geographic information system for monitoring the impact of climate change and the present/future climate vulnerability of agriculture. In order to achieve these goals, better availability and quality of publicly available environmental, social and economic data at the level of municipalities, regions and the state is essential. Geographic visualization can also be used for more transparent evaluation meaning more relevant information for understanding where and how vulnerability occurs.

6. REFERENCES

Adger W.M., Brooks N., Bentham G., Agnew M., Eriksen S. 2004. New indicators of vulnerability and adaptive capacity: Tyndal project It.1.11, July 2001 to June 2003: Final project report. Norwich, Tyndall Centre for Climate Change Research, University of East Anglia, School of Environmental Sciences: 128 p.

Adger W.N. 2006. Vulnerability. Global Environmental Change, 16: 268–281.

Adger W. N., Agrawala S., Mirza M.M.Q, Conde C., O'Brien K., Pulhin J., Pulwarty R., Smit B., Takahashi K. 2007. Assessment of adaptation practices, options, constraints and capacity. V: Climate change 2007, impacts, adaptation and vulnerability: Contribution of Working Group II to the Fourth Assessment Report of the Intergovernmental Panel on Climate Change. Cambridge, UK, Cambridge University Press, 17: 719–743.

Adger W.M. 1999. Social Vulnerability to Climate Change and Extremes in Coastal Vietnam. World Development, University of East Anglia, Norwich, UK, 27, 2: 249–269.

Ahsan M. N., Warner J. 2014. The socioeconomic vulnerability index: A pragmatic approach for assessing climate change led risks–A case study in the southwestern coastal Bangladesh. International Journal of Disaster Risk Reduction, 8: 32–49.

Allen K. 2003. Vulnerability reduction and the community-based approach: a Philippines study. V: Natural Disasters and Development in a Globalizing World. M. Pelling (ur.). New York, Routledge: 170–184.

Antle J. 1996. Methodological issues in assessing potential impacts of climate change on agriculture. Agricultural and Forest Meteorology, 80, 1: 67–85.

Aubrecht C., Özceylan D. 2013. Identification of heat risk patterns in the U.S. National Capital Region by integrating heat stress and related vulnerability. Environment International, 56: 65–77.

Chow W. T. L., Chuang W.C., Gober P. 2012. Vulnerability to Extreme Heat in Metropolitan Phoenix: Spatial, Temporal, and Demographic Dimensions. The Professional Geographer, 64(2): 286–302.

de Luis M., Čufar K., Saz M.A., Longares L.A., Ceglar A., Kajfež Bogataj L. 2014. Linearni trend s in seasonal precipitation and temperature in Slovenia during 1951–2007. Regional Environmental Change, 14: 1801–1810.

Demeritt D. 2001. The construction of global warming and the politics of science. Annals of the Association of American Geographers, 91, 2: 307–337.

Eakin H., Bojórquez Tapia L.A. 2008. Insights into the composition of household vulnerability from multi-criteria decision analysis. Glob Environ Change, 18:112–127.

Edenhofer O., Pichs-Madruga R., Sokona E., Farahani E., Kadner S., Seyboth K., Adler A., Baum I., Brunner S., Eickemeier P., Kriemann B., Savolainen J., Schlömer S., von Stechow C., Zwickel T., Minx J.C. (ur.) 2014.

Climate Change. Mitigation of Climate Change. Contribution of Working Group III to the Fifth Assessment Report of the Intergovernmental Panel on Climate Change, Cambridge University Press, Cambridge, UK and New York, NY.

EEA,. 2017. Climate change, impacts and vulnerability in Europe 2016: an indicator- based report 2017. European Environment Agency: 419 p.

El Gafy I., Grigg N. 2016. Climate change vulnerbility index and multi-criteria ranking approach for assessing the vulnerability to climate change: case study Egypt. Journal of American Science, 12,8: 29–40.

Fellmann T. 2012. The assessment of climatechange-related vulnerability in the agricultural sector: reviewing conceptual frameworks. V: Building resilience for adaptation to climate change in the agriculture sector. Food and Agriculture Organization of the United Nations (FAO) and the Organization for Economic Co-operation and Development (OECD).

Forsyth T. 2003. Critical Political Ecology: the Politics of Environmental Science. London, Routledge.

Füssel H. M., Klein R. J. T. 2006. Climate change vulnerability assessments: an evolution of conceptual thinking. Climate Change, 75: 301–329.

Heltberg R., Bonch-Osmolovskiy M. 2010. Mapping vulnerability to climate change. Washington, The World Bank: 19 p.

Hinkel J. 2011. Indicators of vulnerability and adaptive capacity: Towards a clarification of the science–policy interface. Global Environmental Change, 21(1): 198–208.

Kajfež Bogataj L., Sušnik A., Črepinšek Z., Bergant K., Matajc I., Rogelj D., Cegnar T., Žust A., Dolinar M., Pečenko A., Gregorič G., Reškar J. 2003. Ranljivost slovenskega kmetijstva in gozdarstva na podnebno spremenljivost in ocena predvidenega vpliva. Ljubljana, Ministrstvo za okolje, prostor in energijo, ARSO: 124–127 .

Kajfež Bogataj L. 2005. Podnebne spremembe in ranljivost kmetijstva. Acta agriculturae Slovenica, 85,1: 25–40.

Khajuria A, Ravindranath N.H. 2012. Climate Change Vulnerability Assessment: Approaches DPSIR Framework and Vulnerability Index. Earth Sci. Climat. Change, 3 (1): 1–6.

Krishnamurthy P. K., Lewis K., Choularton R. J. 2014. A methodological framework for rapidly assessing the impacts of climate risk on national-level food security through a vulnerability index. Global Environmental Change, 25: 121–132.

McCarthy J., Canziani O., Leary N., Dokken D., White K. 2001. Impacts, Adaptation, and Vulnerability. Contribution of Working Group II to the Third Assessment Report of the Intergovernmental Panel on Climate Change. Cambridge, UK, and New York, NY, USA, Cambridge University Press: 1032 p.

Monterroso A., Conde C., Gay C., Gómez D., López, J. 2012. Two methods to assess vulnerability to climate change in the Mexican agricultural sector. Mitigation and Adaptation Strategies for Global Change, 19(4): 445–461.

Nicholls R.J., Hoozemans F.M.J. 2000. Global Vulnerability Analysis. V: Encyclopedia of Coastal Science. Schwartz M. (ur.). Kluwer Academic Publishers: 116 p.

O'Brian K, Leichenko R., Kelkar U., Venema H., Aandahl G., Tompkins H., Javed A., Bhadwal S., Barg S., Nygaard L., West J. 2004. Mapping vulnerability to multiple stressors: climate change and globalization in India. Global Environmental Change, 14: 303–313.

O'Brian K., Eriksen S., Nygaard L.P., Schjolden A. 2013. Why different interpretations of vulnerability matter in climate change discourses. Climate Policy, 7,1: 73–88.

Olesen J. E., Bindi M. 2002. Consequences of climate change for European agricultural productivity, land use and policy. European Journal of Agronomy, 16: 239–262.

Parry M. L., Canziani O. F., Palutikof J. P., Van der Linden P. J., hanson C.E. 2007. Climate Change 2007: Impacts, Adaptation and Vulnerability: Contribution of Working Group II to the Fourth Assessment Report of the Intergovernmental Panel on Climate Change. Cambridge, Cambridge University Press: 976 p.

Regije v številkah. Statistični portret slovenskih regij 2016. 2016. Ljubljana, SURS https://www.stat.si/dokument/8941/regije-v-stevilkah.pdf 2016 (4. 5. 2017).

Seljak J. 2001a. Kazalec uravnoteženega razvoja (Sustainable Development Indicators). (Zbirka analize, raziskave in razvoj). Ljubljana, Urad za makroekonomske analize in razvoj: 195 p.

Seljak J. 2001b. Nove mere razvoja – kazalec uravnoteženega razvoja (KURA). IB revija, 35, 4: 27–37.

Spremembe podnebja v Sloveniji do sredine 21. stoletja. Ljubljana, ARSO http://meteo.arso.gov.si/uploads/probase/www/climate/PSS/scenariji/letak_RCP45_2070.pdf (16. 8. 2017).

Sugiarto Y., Perdinan, Atmaja T., Wibowo A. 2017. Developing Vulnerability Analysis Method for Climate Change Adaptation on Agropolitan Region in Malang District. IOP Conference Series: Earth and Environmental Science, 58: 1–9.

Sušnik A. 2014. Zasnove kazalcev spremljanja suše na kmetijskih površinah: doktorska disertacija. (Univ. v Ljubljani, Biotehniška fakulteta). Ljubljana, samozal.: 225 p.

Tomlinson C. J., Chapman L., Thornes J. E., Baker C. J. 2011. Including the urban heat island in spatial heat health risk assessment strategies: a case study for Birmingham, UK. International Journal of Health Geographics, 10(42): 1–14.

Tonmoy F. N., El-Zein A., Hinkel J. 2014. Assessment of vulnerability to climate change using indicators: a meta-analysis of the literature. Wiley Interdisciplinary Reviews: Climate Change, 5(6): 775–792.

Turner B.L., Kasperson R.E., Matson P.A., McCarthy J.J., Corell R.W., Christensen L., Eckley N., Kasperson J.X., Luers A., Martello M.L., Polsky C., Pulsipher A., Schiller A. 2003. A framework for vulnerability analysis insustainability science. Proceedings of the National Academy of Sciences of the USA, 100: 8074–8079.

UNDP (2018), "Human development indices and indicators: 2018 statistical update", in *Human Development Indices and Indicators 2018: Statistical update*, UN, New York, https://doi.org/10.18356/9a42b856-en (29. 12. 2018).

Vincent K. 2004. Creating an index of social vulnerability to climate change for Africa. (Research Working Paper, 56). Tyndall Centre for Climate Change: 50 p.

Vintar Mally K. 2006. Prednosti in omejitve uporabe kazalcev sonaravnega razvoja. Dela, 26: 34–59.

Vintar Mally K. 2011. Measuring Progress Towards Sustainability. The Geographer´ s view. Hrvatski geografski glasnik, 73, 2: 67–80.

Yoon D. K. 2012. Assessment of social vulnerability to natural disasters: a comparative study. Natural Hazards, 63(2): 823–843.

Jun K., Chung E., Kim YO., Kim Ye. 2013. A fuzzy multicriteria approach to flood risk vulnerability in South Korea by considering climate change impact. Expert systems with Applications, 40: 1003–1013.

Yusuf A.A., Francisco H. 2009. Climate Change Vulnerability Mapping for Southeast Asia. Economy and Environment Program for Southeast Asia (EEPSEA), Singapor: 10–15.

Žurovec, O., Čadro, S., Sitaula, B. (2017). Quantitative Assessment of Vulnerability to Climate Change in Rural Municipalities of Bosnia and Herzegovina. Sustainability, 9(7), 1208.

Italian Journal of Agrometeorology
Rivista Italiana di Agrometeorologia

Firenze University Press
www.fupress.com/ijam

Citation: S. Karayusufoğlu Uysal, L. Şaylan (2019) Assessment of Soil Heat Flux Equations for Different Crops under Semi Humid Conditions. *Italian Journal of Agrometeorology* (2): 49-61. doi: 10.13128/ijam-652

Received: June 25, 2019

Accepted: August 28, 2019

Published: October 29, 2019

Data Availability Statement: All relevant data are within the paper and its Supporting Information files.

Competing Interests: The Author(s) declare(s) no conflict of interest.

Assessment of Soil Heat Flux Equations for Different Crops under Semi Humid Conditions

Valutazione delle equazioni di flusso termico nel suolo per diverse colture in condizioni semi-umide

Sezel Karayusufoğlu Uysal[1,*], Levent Şaylan[2]

[1] *Turkish State Meteorological Service, Department of Weather Forecast, Remote Sensing Division, Ankara, Turkey*
[2] *Department of Meteorology, Faculty of Aeronautics and Astronautics, Istanbul Technical University, Istanbul, Turkey*
*Corresponding author email: skarayusufoglu@mgm.gov.tr

Abstract. Soil heat flux (G) is an important component of energy balance by constraining the available amount of latent heat and sensible heat. There are many methods and formulations in the literature to estimate G accurately. In this study, widely used G estimation models are chosen to test. The models are based on Spectral Vegetation Indices (SVIs) namely, Normalized Difference Vegetation Index (NDVI), and Soil Adjusted Vegetation Index (SAVI) together with leaf area index (LAI), and crop height. Two successive growing periods of winter wheat (Triticum Aestivum L.), sunflower (Helianthus annuus L.), and maize (Zea mays L.) fields, located in the northwest part of Turkey, are used. Midday values (average of 09:30- 13:30) of G and net radiation (R_n) used in order to capture the time period, when G is proven to be much dominant. According to the results, overall the best relation obtained with an exponential NDVI model with a determination coefficient value of 0.83 and a root mean square (RMS) error value of 20.28 Wm^{-2} for maize. For winter wheat, G is predicted the best with SAVI based model (r^2=0.74), and for sunflower, LAI based model worked best with 0.75 r^2 value. Crop height (CH) based nonlinear regression G model that suggested in this study worked better than linear models suggested in the literature with a better determination coefficient (r^2=0.70) and a lower RMS error value (10.8 Wm^{-2}).

Keywords. Surface energy fluxes, Spectral Vegetation Indices, Bowen Ratio Energy Balance, Net Radiation.

Abstract. Il flusso termico nel suolo (G) è una componente importante del bilancio di energia capace di limitare la quantità disponibile di calore latente e calore sensibile. Ci sono molti metodi e formule in letteratura per estimare accuratamente G. In questo studio, i modelli di stima di G più utilizzati sono stati confrontati. I modelli sono basati sugli Indici di Vegetazione Spettrali (SVIs) chiamati Normalized Difference Vegetation Index (NDVI) e Soil Adjusted Vegetation Index (SAVI) insieme all'indice di area fogliare (LAI) e l'altezza della coltura. Due successivi cicli vegetativi del frumento (Triticum Aestivum L.), girasole (Helianthus annuus L.) e mais (Zea mays L.), coltivati nella parte nordovest della Turchia, sono stati valutati. I valori presi a metà mattina (circa tra le ore 09:30-13:30) di G e radiazione netta (Rn) sono stati usati al fine di cogliere il momento in cui G raggiunge i valori più elevati. In accordo con i risultati, la migliore relazione complessiva ottenuta è con il modello di NDVI esponenziale con un coefficiente di determinazione di 0.83 e un valore quadratico medio (RMS) di 20.28 W m^{-2} per il mais. Per il frumento, G è stato predetto meglio con il modello SAVI (r2=0.74) e per il girasole, il modello basato sul LAI ha funzionato meglio con un valore di 0.75 r^2. Il modello G di regressione non lineare basato sull'altezza della coltura (CH) proposto in questo studio ha lavorato meglio che il modello lineare suggerito in letteratura con un migliore coefficiente di determinazione (r^2=0.70) e un più basso errore RMS (10.8 Wm^{-2}).

Parole chiave. Flussi di energia superficiale, Indici spettrali di vegetazione, Bowen Ratio Energy Balance, Radiazione netta.

1. INTRODUCTION

Soil (ground) heat flux (G), is known to be the smallest component of the earth's energy balance and widely assumed to be negligible. However, it has been proven that G is an essential component regarding land surface energy dynamics, especially during the daytime, almost for all ecosystems (Dugas *et al.*, 1996; Kustas *et al.*, 2000; Murray and Verhoef, 2007a). For a very well irrigated and fully covered vegetation surfaces, it is reported to be of the same order as sensible heat flux (H) (Kustas and Daughtry, 1990; Clothier *et al.*, 1986). For dry soil surfaces, G is as high as almost up to 50% (Idso *et al.*, 1975) and for forests, it is 30-50% of net radiation (Ogee *et al.*, 2001). In addition, for relatively sparse vegetation, G may grow into a meaningful component (Kustas *et al.*, 2000) and surpass others during the night (Murray and Verhoef, 2007a). Although occasionally neglected in daily evapotranspiration (ET) models, for much frequent ET estimations (e.g. 30 mins, hourly, etc.) and for sparse vegetation cover, G's contribution has been demonstrated to be significant (Kumar and Rao, 1984; Payero *et al.*, 2003, Payero *et al.*, 2005). Obtaining G, correctly, is crucial to understand the energy balance thoroughly.

Besides various measurement techniques, there are several methods to estimate G which depend on soil thermal properties and diurnal variation of soil surface temperature, weather data, and soil properties (e.g., Verhoef 2004; Murray and Verhoef 2007a and b; Núñez *et al.*, 2010; Verhoef *et al.*, 2012; Van der Tol 2012; Wang and Bras 1999; Hsieh *et al.* 2009). As an alternative, there are several empirical G estimation equations for different types of crops at different locations, in which remote sensing data involves (Choudhury *et al.*, 1987; Jackson *et al.*, 1985; Kustas and Daughtry, 1990; Kustas *et al.*, 1993; Boegh *et al.*, 2002, Tasumi, 2003).

Although it is not feasible to directly estimate G using satellite measurements, yet the ratio of G to another component in the energy budget can be estimated (Kustas and Daughtry, 1990). For that, Jackson *et al.* (1985) suggested net radiation, because of its calculation ease with a minimum amount of meteorological data requirement.

Clothier *et al.* (1986) estimated the midday ratio of soil heat flux to net radiation (G/R_n) as a linear function of a spectral vegetation index (near infrared to red ratio) over several regrowth cycles of alfalfa. Kustas and Daughtry (1990) demonstrated that multispectral data could provide a means of computing the G/R_n ratio for several cover types. Both studies showed that the G/R_n ratio linearly decreases with increasing vegetation cover and the multispectral vegetation indices.

G/R_n ratio can be estimated close to the noontime via empirical relations from the leaf area index (LAI), normalized difference vegetation index (NDVI), soil adjusted vegetation index (SAVI), albedo (α), land-surface temperature (LST) that are obtained by satellites (Choudhury *et al.*, 1987; Bastiaanssen, 1995; Tasumi, 2003; Boegh *et al.*, 2002; Allen *et al.*, 2011).

Availability of data necessary to understand and analyse crop growth at field scale with a good temporal and spatial resolution and precision is possible with costly in situ measurements (Stroppiana *et al.*, 2006). Therefore, although being an indirect estimation technique, remote sensing is emphasized to be beneficial and useful considering areal scale assessments (Allen *et al.*, 2011). Even though micrometeorological measurement techniques such as Eddy Covariance provide much precise quantification, their spatial coverage and costs make remote sensing much preferable. For a thorough understanding of G, different types of crop-soil combinations are necessary to be studied.According to Turkish Statistical Institute's (TUIK) recent data (2017), within total cereal and other crops sawn area (approximately 15.5 million ha), wheat has the greatest portion with about 8 million ha and around 21.5 million tonnes of total production. Maize is holding third place with about 640 000 ha cultivated area and almost 6 million tonnes of total production per year. Sunflower has the greatest portion off of the oilseeds with about 780 000 ha with a corresponding total production of around 195 000 tonnes per year. According to those mentioned information, wheat, sunflower, and maize are of great importance in terms of shaping the economy. Understanding and monitoring crops' growth by means of energy fluxes is almost an untouched topic for Turkey. Few studies are done and more needed to be carried out for better understanding.

Finally, the main purpose of this study is to to test, optimize, and compare SVIs, LAI, and crop height-based empirical equations for G estimation and determine the best method for winter wheat, sunflower and maize. Additional aim is to asses and evaluate the relationships between G/R_n and biophysical factors such as biomass, crop height, and LAI.

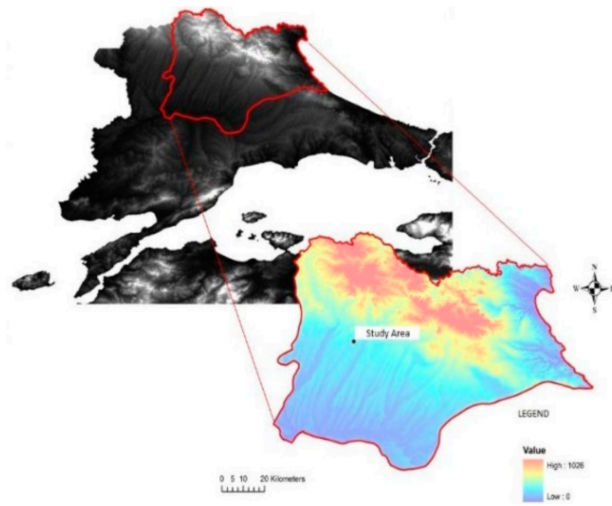

Fig. 2. Digital elevation map (DEM) of Kırklareli City (SRTM data).
Fig. 2. La mappa di elevazione digitale (DEM) della città di Kırklareli (SRTM dati).

2. MATERIALS AND METHOD

2.1 Study area

The study area is located in the Kırklareli city, in the north-western part of Turkey (41.69 N, 27.21 E). Experiments are conducted over winter wheat, sunflower and maize sown at Directorate of Atatürk Soil Water and Agricultural Meteorology Research Institute (AMRI) (Fig. 1).

Kırklareli city centre is 203 m above the mean sea level. On the north side of the city, Istranca Mountains lie in a northwest-southeast direction with the maximum elevation of approximately 1030 m at the southeast part (Fig. 2).

In a geographical information system (GIS) media, aspect and slope maps of the city generated from the digital elevation model (DEM). According to the results, the study area is oriented to the southeast with a 154° angle and ranked as a 0-2 class with 0.39-degree slope (Fig. 3).

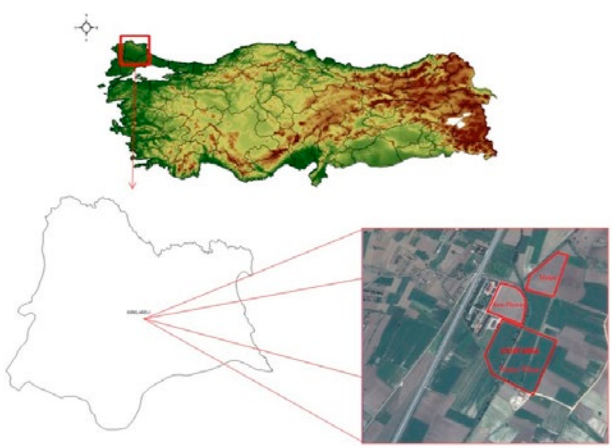

Fig. 1. Location of the study area.
Fig. 1. Posizione dell'area di studio.

2.2 Data used

2.2.1. Meteorological and Soil Data

According to the long term mean monthly rainfall accumulations obtained from the Turkish State Meteorological Service (TSMS) from 1950 to 2014, the minimum amount of precipitation was observed in August (21.1 mm), and the maximum amount of precipitation was observed in December (70.6 mm). Besides, the mean annual accumulated rainfall amount for the study region is 573.6 mm. According to long term monthly temperature means, July is the warmest with 24°C whereas the coolest month was January (2.9°C). Extremes were also recorded in July for summer (42.5 °C on 27 July 2000) and in January for winter (-15.8 °C on 14 January 1972). As reported by the study conducted by TSMS's Climatology Branch (2000), Kırklareli city's climate has semi-humid properties with cool winters and warm summers as a shared output of well-accepted climate classification methods (Aydeniz, Erinç, De Martonne, Trewartha and Thornthwaite).

Automated weather observation systems settled in the planted area measured wind speed and direction, air temperature, relative humidity, global and net radiation, photosynthetic active radiation, surface tem-

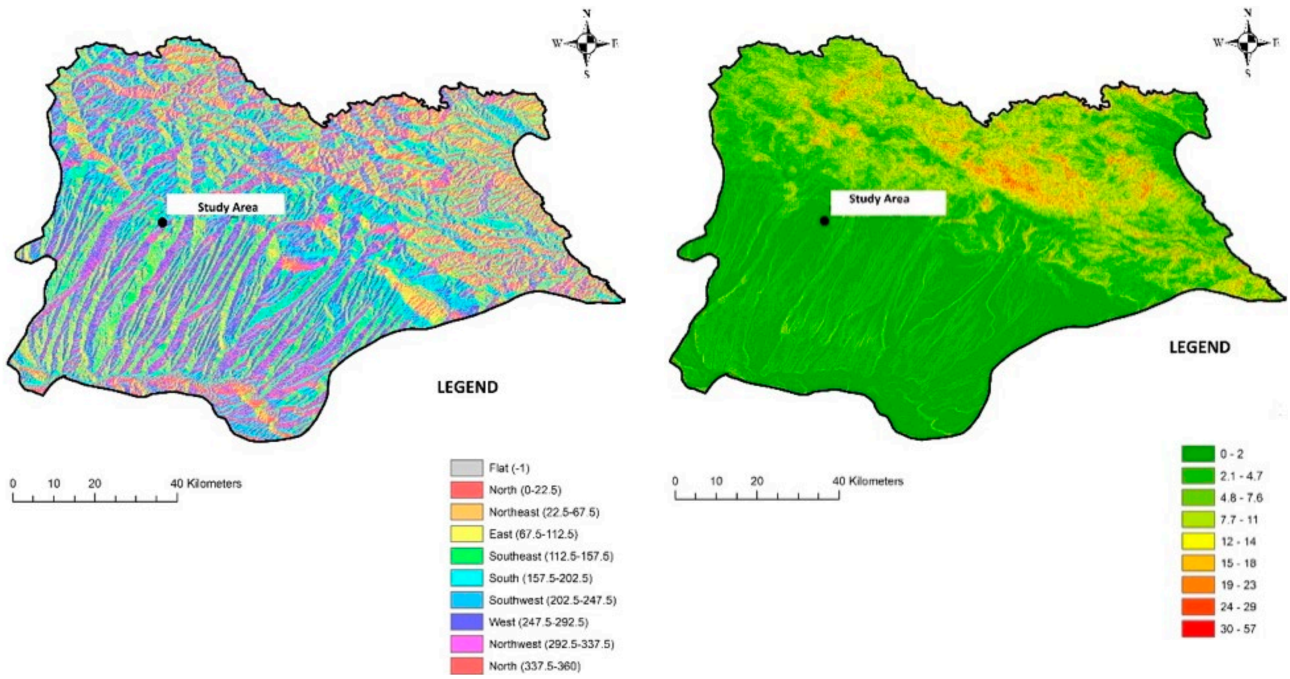

Fig. 3. Aspect and slope maps of Kırklareli City.
Fig. 3. Mappe di esposizione e pendenza della città di Kırklareli.

perature, heat fluxes, volumetric soil water content and rainfall amount during the growing periods (Şaylan et.al., 2010; Şaylan et.al 2018). Distribution of rainfall amount (mm), volumetric soil water content (%) for 0-30 and 30-60 cm of levels; soil temperature values at 2, 5 ,10 and 20 cm depths for sunflower first and second growing periods (Fig. 4); for winter wheat's first and second growing periods (Fig. 5); and finally for maize first and second growing periods (Fig. 6) were demonstrated below.

According to the field studies, soil texture of wheat for 0-90 cm depth was 59 % sand, 25 % silt, and 16 % clay; for sunflower, 57 % sand, 20.8 % silt, and 22.2 % clay and finally for maize, 52.8 % sand, 16.7 % silt and 30.6 % clay. Considering FAO soil classification criteria the soil type of wheat area was sandy loam soil and it was sandy-clay loam for sunflower and maize fields.

2.2.2 Phenological Data

Phenological stages of winter wheat, sunflower and, maize observed and recorded during two sequential growing periods, and demonstrated in Fig. 7-9. For winter wheat, because less rainfall observed during the beginning of the second growing period, planting was done later than the first one. As a result, all phenological stages observed a few days later than the first period.

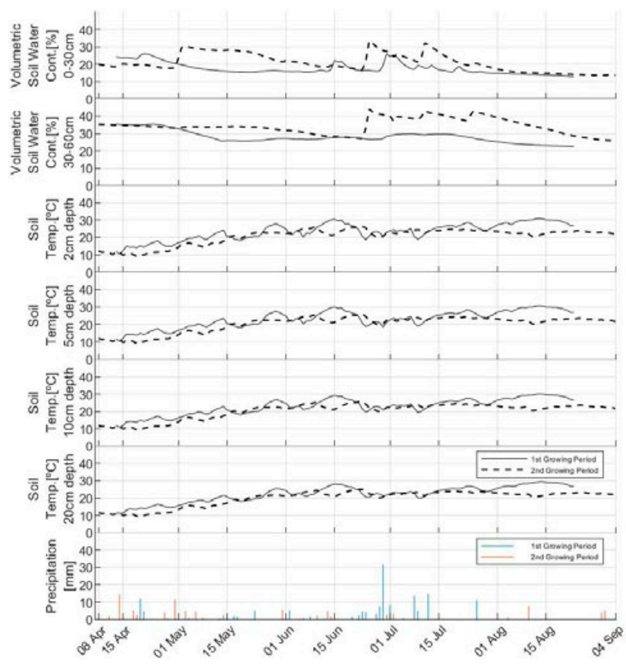

Fig. 4. Time series of volumetric soil water content, soil temperature, and precipitation, during both growing periods of sunflower.
Fig. 4. Serie temporale di umidità del suolo, temperatura del suolo e precipitazioni, durante entrambe le stagioni di crescita del girasole.

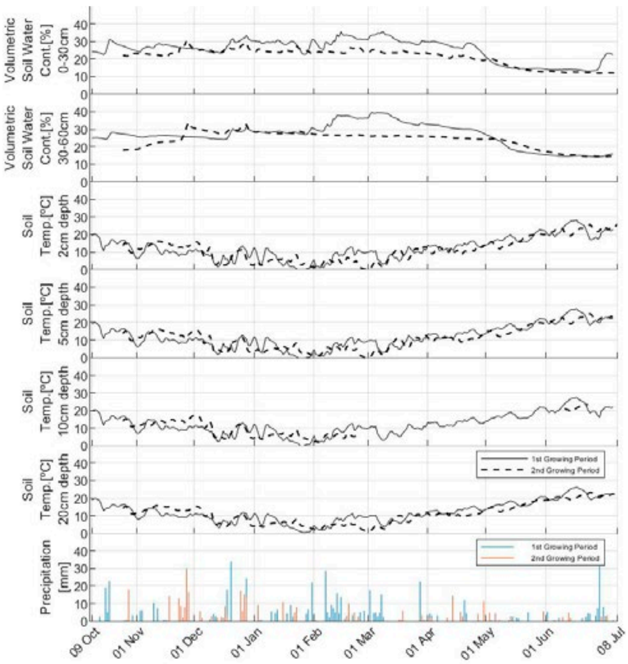

Fig. 5. Time series of volumetric soil water content, soil temperature, and precipitation, during both growing periods of winter wheat.
Fig. 5. Serie temporale di umidità del suolo, temperatura del suolo e precipitazioni, durante entrambe le stagioni di crescita del frumento.

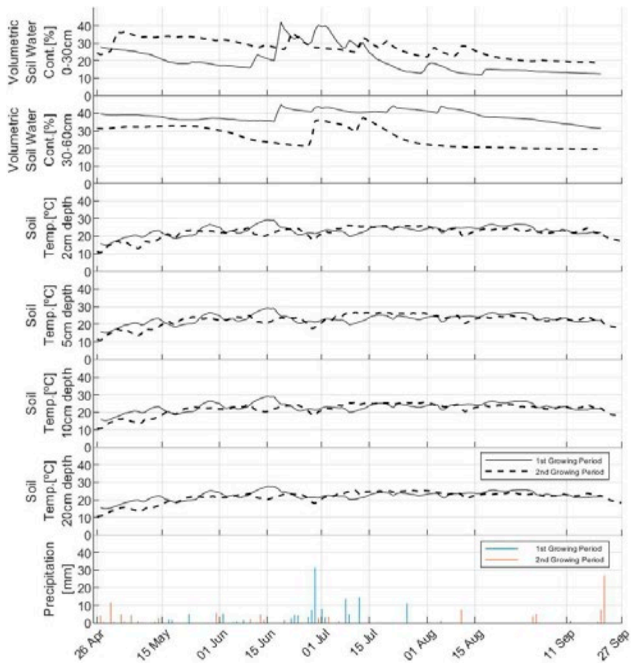

Fig. 6. Time series of volumetric soil water content, soil temperature, and precipitation, during both growing periods of maize.
Fig. 6. Serie temporale di umidità del suolo, temperatura del suolo e precipitazioni, durante entrambe le stagioni di crescita del mais.

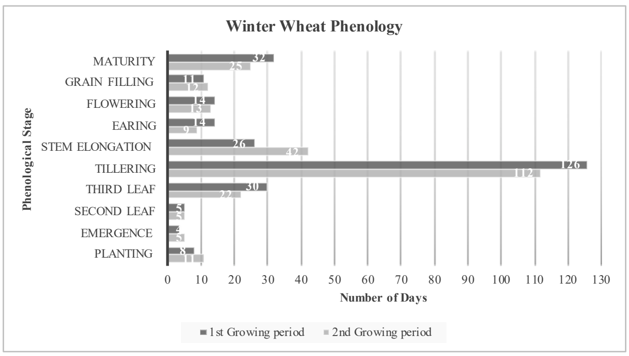

Fig. 7. Phenological stages of winter wheat for two growing periods.
Fig. 7. Stadi fenologici del grano durante i 2 periodi di crescita.

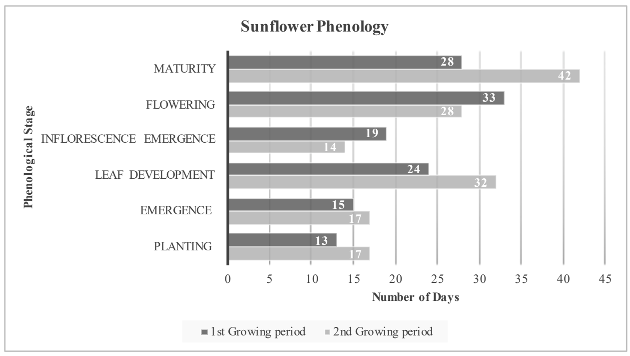

Fig. 8. Phenological stages of sunflower during two growing periods.
Fig. 8. Stadi fenologici del girasole durante i 2 periodi di crescita.

Each crop field was fertilized by N fertilizer. Additionally, herbicide and fungicide treatments applied. Sunflower and maize irrigated but for winter wheat both seasons were without irrigation.

2.2.3 Spectral Reflectance Measurements

Each object has its unique reflectance pattern along the electromagnetic (EM) spectrum which is called spectral signature (Parker and Wolff, 1965). Spectral signature has a key role in remote sensing in order to discriminate between objects. For instance, vegetation cover tends to absorb most of the incoming solar energy in visible (VIS) portion of the EM spectrum while it mainly reflects near-infrared (NIR) radiation incident upon it. Significant absorption in the VIS band is caused by the leaf pigments, namely because of the chlorophyll. Likewise, high reflection in the NIR band is a result of the cellular structure of the leaves (Basso *et al.*, 2001). Spectral vegetation indices (SVIs) have been

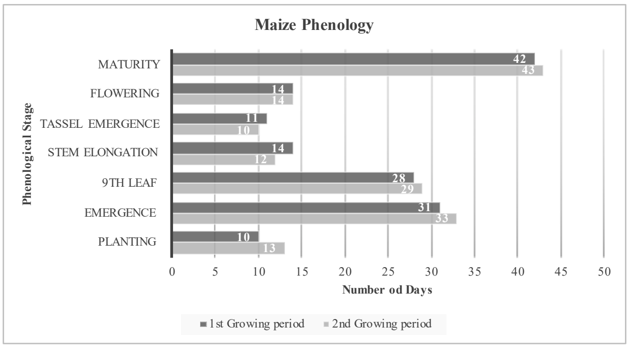

Fig. 9. Phenological stages of maize during two growing periods.
Fig. 9. Stadi fenologici del mais durante i 2 periodi di crescita.

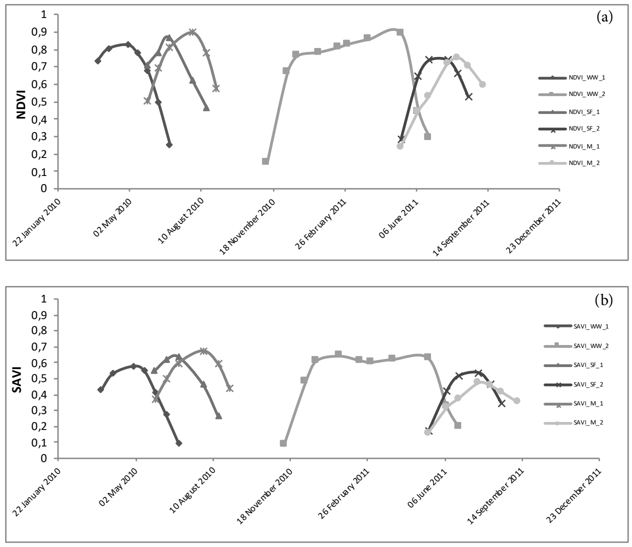

Fig. 10. (a) NDVI for first and second growing seasons (b) SAVI for first and second growing seasons for maize (M), sunflower (SF) and winter wheat (WW).
Fig. 10. (a) NDVI per il primo e secondo ciclo colturale (b) SAVI per il primo e secondo ciclo colturale per mais (M), girasole (SF) e frumento (WW).

widely used for a better understanding of crop health and growth status by making use of that different behaviour of vegetation cover in VIS and NIR bands. In this study, spectral reflectance data measured with a hand type spectroradiometer (Fieldspec., ASD Inc.) which collects data in between 325-1075 nm. Measurements were done biweekly, under a clear and cloudless sky during both periods. SVIs that are shown in the below table calculated (Tab. 1).

Tab. 1. SVIs used in this study.
Tab. 1. SVIs usati in questo studio.

SVI	Equation	References
Normalized Difference Vegetation Index (NDVI)	$\frac{R_{(841-876)} - R_{(841-876)}}{R_{(841-876)} + R_{(841-876)}}$	Rouse *et al.*, 1974
Soil Adjusted Vegetation Index (SAVI)	$(1+L)*\frac{R_{841-876} - R_{620-670}}{R_{841-876} - R_{620-670} + L}$	Huete, 1988

Even though the measurements were done with spectroradiometer are not likely to be affected by atmospheric scattering, there is still a possibility of errors occurring because of technical or systematic issues of the instrument. Therefore, Savitzky-Golay (S-G) filtering was applied in order to reduce any noise that might be encountered. Although there were many SVIs calculated during the study, NDVI and SAVI were chosen to be investigated in terms of their capability to predict G/R_n ratio. NDVI and SAVI variation during both growing periods for maize, sunflower and winter wheat were demonstrated at Fig. 10 a,b.

2.2.4 Energy Budget Components

Net radiation and soil heat flux data measured and recorded during two growing periods for each crop with 10 and 30 min. intervals. Bowen Ratio Energy Balance (BREB) method was used in order to determine latent heat and sensible heat fluxes over crop's surfaces.

Before any further analysis carried out, R_n and G data sets were examined in terms of detecting any outliers and any missing values. Outliers detected using Interquartile Range (IQR) method, also called the Tukey method (Tukey, 1977) by which upper and lower limits determined by first and third quartiles of data sets. The data were filtered by Ohmura (1982) and Perez *et al.* (1999) criteria. Fig. 11 shows data after outliers removed by IQR (only sunflower data was demonstrated here).

As mentioned by other studies as well, G is highly affected by soil wetness as well as vegetation cover and surface temperature (Payero *et al.*, 2005; Kustas and Daughtry, 1990). Payero *et al.* (2005) and others (Camuffo and Bernardi, 1982; Novak, 1993; Domingo *et al.*, 2000) stated hysteresis problem with G data detected on the days after rain and irrigation. They reported that at the cases when wet soil starts to dry out, corresponding R_n-G values differed dramatically compared to dry soil. In order to overcome this problem, the days with and after rain for wheat and the days with and after rain

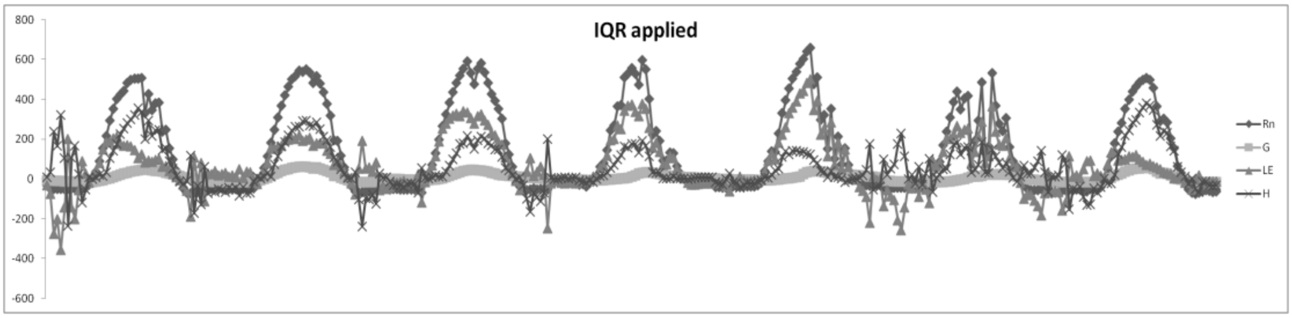

Fig. 11. Energy fluxes data after outliers cleared by IQR.
Fig. 11. Dati di flussi di energia dopo la eliminazione delle anomalie con IQR.

and irrigation for sunflower and maize, G and R_n data were removed from the data set.

In order to understand the apportionment of energy balance components during the day, 30 min. interval data sets for all three crops including two growing periods were used. According to data analysis, G data became dominant after 09:00 and got to its peak around 15:00 then came close to zero afterwards. Therefore 09:00-15:00 interval has been picked as daytime.

In order to make general analysis, after correction and elimination procedures completed, data were considered separately for each growing season. For winter wheat's first growing season G was 10% of R_n during daytime and at the second growing period, it was 15% of Rn, on average. The maximum value recorded for G was 100.4 W/m^2 and R_n was 769 W/m^2 for the first growing season and for the second growing season maximum value of G was 82.1 W/m^2 and maximum R_n value was 800 W/m^2. For sunflower, at first growing season, G was 10% of R_n during the daytime, on average and 8% of R_n for the second growing period. The maximum value recorded for G and R_n were 93.6 W/m^2 and 794.3 W/m^2 for the first growing season and for the second growing season maximum values were 125.3 W/m^2 and 682.6 W/m^2, respectively. For maize, at first growing season, G was 5% of R_n during the daytime, on average and 9% of R_n at the second growing period. The maximum value recorded for G was 131.4 W/m^2 and it was 692.7 W/m^2 for R_n at the first growing season. At the second growing season, maximum values for G and R_n were 131.4 W/m^2 and 692.7 W/m^2, respectively.

G is highly dependent on surface conditions (i.e., wet or dry and bare or vegetated). For bare soil, G may be 20-50% of R_n depending on soil moisture (Idso *et al.*, 1975) whereas, for mature crops, G may be 5-10% of R_n over alfalfa (Clothier *et al.*, 1986), wheat (Choudhury *et al.*, 1987), and soybeans (Baldocchi *et al.*, 1985). Thus, soil heat flux can be a significant portion of R_n ranging from 5% to 50% of R_n depending on soil moisture and fraction of vegetation cover.

Tab. 2. G/R_n midday minimum, maximum and average values according to phenological stages for winter wheat, sunflower and maize.
Tab. 2. valori minimi, massimi e medi di G/R_n nei diversi stadi fenologici per il frumento, il girasole e il mais.

Crop	Phenological Stage	1st Growing Season			2nd Growing Season		
		G/Rn Midday					
		Min	Ave	Max	Min	Ave	Max
Winter Wheat	Emergence-Tillering	0.12	0.26	0.58	0.07	0.13	0.23
	Stem Elongation-Earing	0.03	0.09	0.26	0.02	0.07	0.17
	Flowering-Maturity	0.03	0.07	0.08	0.02	0.04	0.06
	Maturity-Harvest	0.03	0.10	0.39	0.02	0.05	0.15
Sunflower	Emergence-Inflorescence	0.03	0.09	0.22	0.01	0.14	0.42
	Flowering-Maturity	0.03	0.10	0.16	0.01	0.08	0.21
	Maturity-Harvest	0.01	0.05	0.22	0.01	0.05	0.20
Maize	Emergence-Stem Elongation	0.01	0.08	0.22	0.06	0.18	0.33
	Tasselling-Flowering	0.03	0.07	0.34	0.05	0.10	0.19
	Flowering-Maturity	0.03	0.05	0.07	0.02	0.06	0.11
	Maturity-Harvest	0.03	0.05	0.07	0.04	0.07	0.33

In order to better capture G dominancy, midday (09:30-13:30) 30 minutes interval average G/R_n values were examined for each crop considering their phenological stages (Tab. 2).

Although results for each crop were in line with the sense that G/R_n values decreasing with the growing plant, there were differences because of the differing soil moisture, surface temperature, soil content, weather conditions (e.g., precipitation, cloudiness).

3. RESULTS

3.1 Relations between G/Rn and Biophysical Parameters

LAI of each crop was measured biweekly using a plant canopy analyzer (LAI-2000 sensor of LI-COR). Aboveground dry biomass was measured conventional-

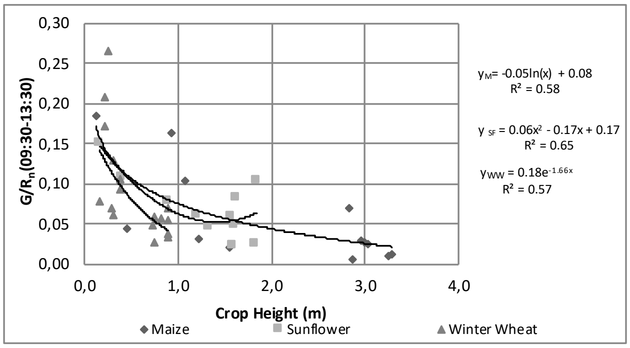

Fig. 12. Relationship between the ratio of G to R_n and crop height for winter wheat, sunflower, and maize.

Fig. 12. Relazione fra G e R_n e l'altezza della coltura in frumento, girasole e mais.

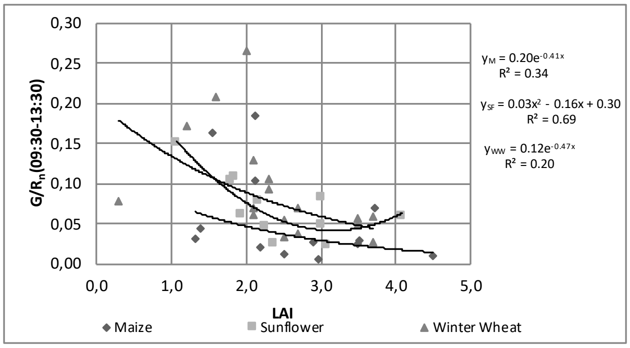

Fig. 13. G/R_n- LAI relationships for winter wheat, sunflower, and maize.

Fig. 13. Relazione tra G/R_n- LAI in frumento, girasole, e mais.

ly by collecting data samples, oven-dry them with 65°C heat and finally measuring the weight. Crop height data was also recorded periodically during the growing periods. There is an obvious negative relationship between G/R_n and crop height for each crop. G/R_n decreased with increasing crop height. The relationship is 2nd order polynomial for sunflower with an r^2 value of 0.65, for maize, it is logarithmic with an r^2 value of 0.58 and for winter wheat it is exponential with an r^2 value of 0.57 (Fig. 12).

Again, with increasing LAI, G/R_n tended to decrease exponentially. However, this time r^2 values were not much significant for winter wheat and maize (0.34 and 0.2) while for sunflower G/R_n seems to be defining LAI very well with 0.69 r^2 value (Fig. 13).

G/R_n relationship with biomass found to be logarithmic for maize and sunflower and 2nd order polynomial for winter wheat with determination coefficients of 0.6, 0.56 and 0.5, respectively (Fig. 14). With growing vegetative mass G/R_n tended to decrease.

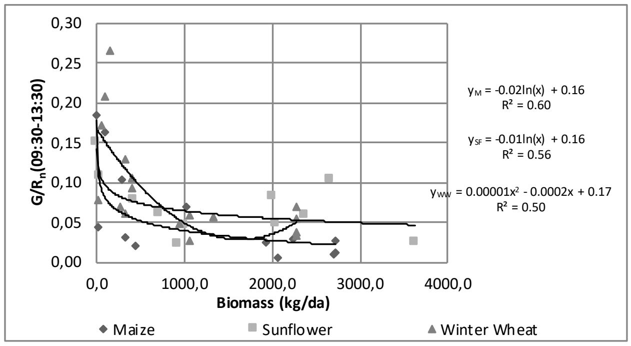

Fig. 14. G/R_n- biomass relationships for winter wheat, sunflower, and maize.

Fig. 14. Relazioni tra G/R_n- biomassa in frumento, girasole e mais.

3.2 Relations between G/Rn and SVIs

NDVI and SAVI increase up to 1.0 with growing vegetation. As G/R_n ratio linearly decreases with increasing vegetative cover, it is expected to have negative linear relations between G/R_n and NDVI and SAVI. Having a good understanding on the relationship between G and SVIs that could easily be obtained such as NDVI and SAVI allows acquiring an estimation for G which has a lot of uncertainty in measurements by depending on many parameters. There are several relationships in the literature in order to estimate G/R_n ratio. They either depend on crop's spectral properties (SVIs) or biophysical properties such as LAI and crop height. The ones with SVIs expressed to be either linear (Clothier *et al.*, 1986, Kustas and Daughtry, 1990), exponential (Jackson *et al.*, 1985, Singh *et al.*, 2008) or power function (Bastiaanssen *et al.*, 1998; Melesse and Nangia, 2005). G/R_n relationships with LAI, on the other hand, found to be exponential (Choudhury *et al.*, 1987; Kustas and Daughtry *et al.*, 1990).

Within this study, LAI and crop height's relationship to G/R_n were already demonstrated. NDVI and SAVI relationships for all three of the crops were shown at Fig. 15 and Fig. 16, respectively. There was no relationship obtained for winter wheat between NDVI and G/R_n, however for maize and sunflower, there were significant relationships with 0.73 and 0.63 r^2 values, respectively. The reason behind no relation detected between NDVI and G/R_n for winter wheat is most probably because most parts of the growing season were in winter. Since G is very sensitive to changes in weather conditions, soil wetness, and soil temperature, etc., the irrelevance can be explained by winter weather conditions.

SAVI and G/R_n were also in a good relationship for maize and sunflower with 0.70 and 0.61 r^2 values. There was a tiny improvement in r^2 (0.23) value compared to

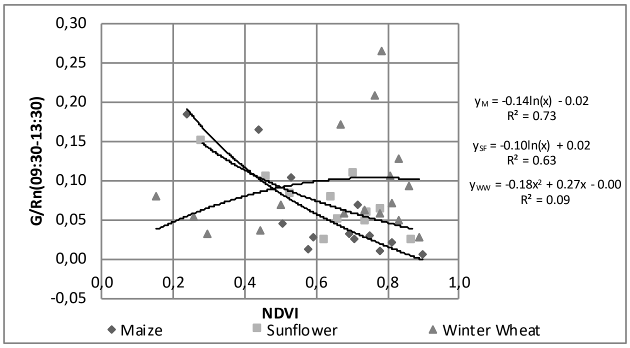

Fig. 15. NDVI-G/R_n relationships for sunflower, maize and winter wheat.
Fig. 15. Relazioni tra NDVI-G/Rn in girasole, mais e frumento.

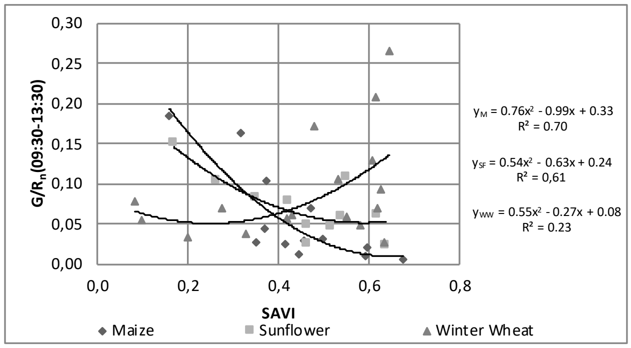

Fig. 16. SAVI-G/R_n relationships for sunflower, maize and winter wheat.
Fig. 16. Relazioni tra SAVI-G/Rn in girasole, mais e frumento.

the NDVI relationship for winter wheat that might be because of the soil adjustment parameter which SAVI included in its equation.

3.3 Assesment of Empirical Equations for G Estimation

Within the alignment of the knowledge obtained with above results, linear and nonlinear regression analysis carried out for determination of G/R_n-SVIs/LAI/CH relationships referring to the models in Tab. 3. Equation 1-4 were the generalized versions of NDVI and SAVI based models in Tab. 3.

$$G = R_n*(Pr_1*e^{(Pr_2*NDVI)}) \quad (1)$$

$$G = R_n*(Pr_1+Pr_2*NDVI) \quad (2)$$

$$G = R_n*(Pr_1*(1-Pr_2*\left(NDVI^{Pr_3}\right) \quad (3)$$

$$G = R_n*\left(Pr_2*\left(Pr_2*SAVI-Pr_3\right)+Pr_4*\left(1-\left(Pr_2*SAVI\right)-Pr_5\right)\right) \quad (4)$$

For LAI based relationships nonlinear regression analysis conducted considering the relation was exponential as shown in Equation 5. And finally crop height G/R_n relationship was assumed to be exponential, power function and linear by using the models shown in Equation 6 and Equation 7.

$$G = R_n*(Pr_1*e^{(Pr_2*LAI)}) \quad (5)$$

$$G = R_n*\left(Pr_1+Pr_2*CH\right) \quad (6)$$

$$G = R_n*(Pr_1*e^{(Pr_2*CH)}) \quad (7)$$

Tab. 3. G estimation models used to evaluate in this study.
Tab. 3. Modelli di stima G usati in questo studio.

G Estimation Models	Ref
$G=R_n*(0.3811*e^{(-2.3187*NDVI)})$	Singh *et al.*, 2008
$G=R_n*(0.3*(1-0.98*NDVI^4))$	Bastiaanssen,1998
$G=R_n*(-0.48*NDVI+0.46)$	Boegh *et al.*, 2004
$G=R_n*(0.1*(1.62*SAVI-0.37)+0.5*(1-(1.62*SAVI-0.37)))$	Boegh *et al.*, 2002
$G=R_n*(-0.49*CH+0.53)$	Payero *et al.*, 2005
$G=R_n*(0.34*e^{(-0.46*LAI)})$	Kustas *et al.*, 1993

Determination coefficients and RMS errors obtained with original G estimation models' parameters which are given in Tab. 3 and, with parameters suggested in this study are demonstrated for each and every crop and for each generalized model are shown in Table 4. Best results for each model and each crop are shown in bold writing.

According to the models' G predictions, overall the best result obtained with an exponential NDVI relationship (Singh *et al.*, 2008) with r^2 equal to 0.831 and RMS error of 20.28 Wm^{-2}. Although determination coefficient values for the Singh model were the best, lowest RMS errors monitored with parameters suggested in this particular study rather than with original ones. The best model for sunflower with respect to determination coefficient value, which was 0.751, was the LAI-based model (Kustas model); whereas for maize best model was an exponential NDVI-based model (Singh Model). For winter wheat on the other hand, generally, all models failed with the lowest determination coefficients and even with no relationships. Nonetheless, SAVI based model represented measured G's with r^2 value as 0.744. Since most of the growing season of winter wheat is in cold weather conditions with heavy rain and snowfall, G might not be

Tab. 4. Results obtained with original parameters and, parameters suggested in this study together with determination coefficients and RMS errors for each crop.
Tab. 4. Risultati ottenuti con i parametric originali e i parametri suggeriti in questo studio insieme ai coefficient di determinazione e gli errori RMS per ciascuna coltura.

Models	Crop Type		pr1	pr2	pr3	pr4	pr5	R²	RMSE
$G = Rn*(Pr_1*(Pr_2*SAVI-Pr_3)+Pr_4*(1-(Pr_2*SAVI-Pr_5)))$	Sunflower	Boegh et al., 2002	0.100	1.620	-0.370	0.500	-0.370	0.709	119.430
		In this study	-0.373	0.436	0.212	0.075	0.125	0.668	13.892
	Maize	Boegh et al., 2002	0.100	1.620	-0.370	0.500	-0.370	0.735	140.804
		In this study	-0.330	0.905	0.431	0.072	0.083	0.688	19.784
	Winter Wheat	Boegh et al., 2002	0.100	1.620	-0.370	0.500	-0.370	0.162	142.795
		In this study	-0.430	-0.053	0.011	0.039	0.038	**0.744**	**9.933**
$G=R_n*(Pr_1*e^{(Pr2*NDVI)})$	Sunflower	Singh et al., 2008	0.381	-2.319	-	-	-	0.729	12.811
		In this study	0.270	-2.102	-	-	-	0.744	**9.933**
	Maize	Singh et al., 2008	0.381	-2.319	-	-	-	**0.831**	20.275
		In this study	0.442	-3.330	-	-	-	0.772	14.934
	Winter Wheat	Singh et al., 2008	0.381	-2.319	-	-	-	0.043	34.9648
		In this study	0.044	0.378	-	-	-	0.320	10.489
$G= R_n*(Pr_1+(Pr_2*NDVI))$	Sunflower	Boegh et al., 2004	-0.480	0.460	-	-	-	0.706	38.592
		In this study	0.194	-0.185	-	-	-	0.746	**9.960**
	Maize	Boegh et al., 2004	-0.480	0.460	-	-	-	**0.791**	48.092
		In this study	0.242	-0.288	-	-	-	0.752	15.011
	Winter Wheat	Boegh et al., 2004	-0.480	0.460	-	-	-	0.038	65.573
		In this study	0.042	0.023	-	-	-	0.323	10.477
$G=R_n*(Pr_1*(1-Pr_2*(NDVI^{Pr3})))$	Sunflower	Bastiaanssen,1998	0.300	-0.980	4.000	-	-	0.739	66.969
		In this study	0.438	0.949	0.284	-	-	0.748	**10.443**
	Maize	Bastiaanssen,1998	0.300	-0.980	4.000			0.596	81.578
		In this study	0.770	1.025	0.220	-	-	**0.775**	15.110
	Winter Wheat	Bastiaanssen,1998	0.300	-0.980	4.000			0.018	75.201
		In this study	0.192	0.676	-0.081	-	-	0.327	10.863
$G=R_n*(Pr_1*e^{(Pr2*LAI)})$	Sunflower	Kustas et al., 1993	0.340	-0.460				0.684	24.087
		In this study	0.311	-0.689	-	-	-	**0.751**	9.906
	Maize	Kustas et al., 1993	0.340	-0.460				0.242	35.055
		In this study	0.144	-0.333	-	-	-	0.280	25.917
	Winter Wheat	Kustas et al., 1993	0.340	-0.460				0.216	20.525
		In this study	0.118	-0.262	-	-	-	0.314	**9.649**
$G=R_n*(Pr_1 +(Pr_2*CH))$	Sunflower	Payero et al., 2005	-0.490	0.530				**0.661**	112.588
		In this study	0.132	-0.050	-	-	-	0.625	11.898
	Maize	Payero et al., 2005	-0.490	0.530				0.395	313.530
		In this study	0.128	-0.034	-	-	-	0.516	20.920
	Winter Wheat	Payero et al., 2005	-0.490	0.530				0.276	57.916
		In this study	0.114	-0.079	-	-	-	0.429	**8.177**
$G=R_n*(Pr_1*e^{(Pr2*CH)})$	Sunflower	In this study	0.154	-0.702	-	-	-	**0.697**	10.782
	Maize	In this study	0.162	-0.614	-	-	-	0.556	20.013
	Winter Wheat	In this study	0.133	-1.227	-	-	-	0.426	**8.079**

estimated very well with other models but SAVI, since SAVI includes soil adjustment parameters. On the other hand, LAI based model worked fine for sunflower however for winter wheat and maize determination coefficients were low. For winter wheat, the reason behind these results might be the same why NDVI based models failed and, for maize the reason might be LAI values during both growing seasons were the highest. Finally, for crop height based G modelling, according to regression results it can be said that the model suggested in this study ($G=R_n*(Pr_1*e^{(Pr_2*CH)})$) worked better than the one suggested by Payero *et al.* (2005) with greater r^2 values together with lower RMS error values.

4. DISCUSSIONS

In this study, energy fluxes measured over three different crop surfaces planted in the Thrace part of Turkey were examined to understand the seasonal and inter-annual variation of the G/R_n ratio by considering spectral and biophysical properties of vegetation together with soil dynamics, meteorological conditions, and land management activities. Among all the components necessary to compute evapotranspiration, R_n is the most crucial one, in terms of its important role in other physical and biological processes (Samani *et al.,* 2007). It stands for the difference between incoming and outgoing radiation at the earth surface and can be used as a proxy data for climate change studies as well as agricultural meteorology (Bisht *et al.*, 2005). Measuring surface energy balance conventionally with direct methods represents only the point where the station is installed and a limited surrounding area. For regional studies locating the sensors properly and trying to determine how many installations needed are critical issues necessary to be considered carefully. Remote sensing techniques provide substantial opportunities to evaluate energy balance components over large areas. In the literature many researchers have tested remote sensing data together with atmospheric and land observations to estimate energy fluxes (Bastiaanssen *et al.*, 1998; Roerink *et al.*, 2000; Bisht *et al.*, 2005; Rimóczi-Paál, 2005; Silva *et al.*, 2005; Samani *et al.*, 2007; Di Pace *et al.*, 2008; Ryu *et al.*, 2008; Wang and Liang, 2009, Santos et al 2011). Obtained results in this study revealed that R_n and G can be estimated by remote sensing data with significantly good relationships. Having these relationships will improve the calibration of crop-climate growth models and therefore results in better estimations. However, to end up with a generalized result, it is crucial to continue collecting data over different soil-crop combinations for longer periods. Therefore, the knowledge of the energy fluxes' estimation for different vegetation cover-soil can be better represented by remote sensing data.

ACKNOWLEDGEMENT

We would like to thank Scientific and Technological Research Council of Turkey (TUBITAK) for supporting this research within the projects entitled as "Determination of Carbon Dioxide, Water Vapour and Energy Fluxes for Winter Wheat" (Project number: 109R006) and "Investigation of Possible Effects of Climate Change to Crop Growth by Crop Growth Models" (Project No: 108O567). We are thankful to Istanbul Technical University (ITU) for providing the opportunity. We would also like to thank Dr Fatih Bakanoğulları and all personnel who put their efforts collecting the data and managing the experimental field studies at Directorate of Atatürk Soil Water and Agricultural Meteorology Research Institute.

REFERENCES

Allen, R., Irmak, A., Trezza, R., Hendrickx, J. M. H., Bastiaanssen. W., Kjaersgaard. J., 2011, Satellite-based ET estimation in agriculture using SEBAL and METRIC. Hydrological Processes, 25, 4011–4027.

Baldocchi, D.B., Verma, S.B., Rosenberg, N.J., 1985, Water use efficiency in a soybean field: Influence of plant water stress. Agric. For. Meteorol. 34, 53–65.

Basso, B., Ritchie, J. T., Pierce, F. J., Braga, R. , & Jones, J. W., 2001, Spatial validation of crop models for precision agriculture. Agricultural Systems, 68, 97–112.

Bastiaanssen, W. G. M., Pelgrum, H., Wang, J., Ma, Y., Moreno, J. F., Roerink, G. J., Van der, W. T., 1998, A Surface Energy Balance Algorithm for Land (SEBAL) 1. Formulation. J. Hydrol., 212, 198-212.

Bastiaanssen, W.G.M., 1995, Regionalization of surface flux densities and moisture indicators in composite terrain, Theses (PhD), Wageningen Agricultural University, Wageningen, Netherlands, 273f.

Bisht G., V. Venturini, S. Islam and L. Jiang, 2005. Estimation of the net radiation using MODIS (Moderate Resolution Imaging Spectroradiometer) data for clear sky days. Remote Sens. Environ. 97, 52-67.

Boegh, E., Soegaard, H., Thomsen, A., 2002, Evaluating evapotranspiration rates and surface conditions using Landsat TM to estimate atmospheric resistance and surface resistance. Remote Sens. Environ., 79, 329-343.

Boegh, E., Soegaard, H., Christensen, J. H., Hasager, C. B., Jensen, N. O., Nielsen, N. W., 2004, Combining weather prediction and remote sensing data for the calculation of evapotranspiration rates: application to Denmark. Int. J. Remote Sens., 25, 2553-2574.

Choudhury, B.J., Idso, S.B., Reginato, J.R., 1987, Analysis of an empirical model for soil heat flux under a growing wheat crop for estimating evaporation by an infrared-temperature based energy balance equation. Agric. For. Meteorol. 39, 283–297.

Clothier, B. E., Clawson, K. L., Pinter, Jr. J., Moran, M. S., Reginato, R. J., Jackson R. D., 1986, Estimation of soil heat flux from net radiation during the growth of alfalfa. Agric. For. Meteor., 37, 319–329.

Camuffo, D., Bernardi, A., 1982, An observational study of heat fluxes and their relationships with net radiation. Boundary-Layer Meteorology 23(3), 359-368.

Di Pace F. T., B. B. Silva, V. R. Silva and S. T. A. Silva, 2008. Mapeamento do saldo de radiação com imagens Landsat 5 e modelo de elevação digital. Revista Bras. Engenharia Agrícola e Ambiental 12, 385-392.

Domingo, F., Villagarcia, L., Benner, A.J., Puigdefabregas, J., 2000, Measuring and modeling the radiation balance of heterogeneous shrubland. Plant and Cell Environment 23(1), 27-38.

Dugas, W. A., R. A. Hicks, Gibbens, R. ,1996. Structure and functions of C3 and C4 Chihuahuan Desert plant communities: Energy balance components. J. Arid Environ. 34, 63-79.

FAO, 2014, Food and agricultural organization of united nations, FAOSTAT, Data. Available at: http://www.fao.org/faostat/en/#data. Accessed on 15 July 2017.

Hsieh, C. I., Huang, C. W., Kiely, G., 2009, "Long-term estimation of soil heat flux by single layer soil temperature, International Journal Of Biometeorology, 53, 113-123.

Huete, A.R., 1988, A soil-adjusted vegetation index (SAVI). Remote Sensing of Environment, 25, 3, 295 – 309.

Idso SB, Aase JK, Jackson RD, 1975, Net radiation–soil heat flux relations as influenced by water content variations. Boundary-Layer Meteorology, 9, 113–122.

Jackson, R.D., Pinter, J., Jr., Reginato, R.J., 1985, Net radiation calculated from remote multispectral and ground station meteorological data. Agric. For. Meteorol., 35, 153 164.

Kumar, K. K., and Rao V. U., 1984, Significance of soil heat flux in the estimation of potential evapotranspiration. Indian J. of Ecology 11, 68-70.

Kustas, W. , Choudhury, B. J., Moran, M. S., Reginato, R. J., Jackson, R. D., and Gay, I. W., 1987, Problems in the estimation of sensible heat flux over incomplete canopy cover with thermal infrared data. In: 18th Conference of Agricultural and Forest Meteorology and 8th Conference on Biometeorology and Aerobiology, Purdue University, 87-90.

Kustas, W. , Daughtry, C. S. T., Oevelen, J. V., 1993, "Analytical treatment of relationships between soil heat flux/ net radiation ratio and vegetation indices", Remote Sensing of Environment, 46, 319 – 330.

Kustas, W. , and C. S. T. Daughtry, 1990: Estimation of the soil heat flux/net radiation ratio from spectral data. Agric. For. Meteor., 49, 205–233.

Kustas, W. , Prueger, J. H., Hatfield, J. L., Ramalingam, K., Hipps L. E., 2000, Variability in soil heat flux from a mesquite dune site. Agric. Forest Meteorol. 103, 249-264.

Melesse, A. M., and Nangia, V., 2005, Estimation of spatially distributed surface energy fluxes using remotely sensed data for agricultural fields. Hydrol. Proc. 19, 2653-2670.

Murray, T., and Verhoef, A., 2007a. Moving towards a more mechanistic approach in the determination of soil heat flux from remote measurements: I. A universal approach to calculate thermal inertia. Agric. Forest Meteorol. 147, 80-87.

Murray, T., and Verhoef, A., 2007b. Moving towards a more mechanistic approach in the determination of soil heat flux from remote measurements: II. The diurnal shape of soil heat flux. Agric. Forest Meteorol. 147, 88-97.

Novak, M. D., 1993, Analytical solutions for two-dimensional soil heat flow with radiation surface boundary conditions. Soil Science Society of America J. 57(1), 30-39.

Núñez, C. M., Varas, E. A, Meza, F. J., 2010, Modeling soil heat flux. Theoretical Applied Climatology, 100, 251-260.

Ogee, J., Lamaud, E., Brunet, Y., Berbigier, , Bonnefond, J. M., 2001, A long-term study of soil heat flux under a forest canopy. Agricultural Forest Meteorology., 106, 173–186.

Ohmura, A., 1982. Objective criteria for rejecting data for Bowen ratio flux calculations. J. Appl. Meteorol. 21, 595–598.

Parker, D. C., and Wolff, M. F., 1965, Remote Sensing. International Science and Technology, 43, 20-31.

Payero, J. O., Neale, C. M. U., Wright, J. L., Allen, R. G., 2003, Guidelines for validating Bowen ratio data. Transactions of the ASAE 46, 1051-1060.

Payero, J., Neale, C., Wright, J., 2005, Estimating soil heat flux for alfalfa and clipped tall fescue grass. Applied Engineering in Agriculture, American Society of Agricultural Engineers, v.21, n.3, 401-409.

Perez, J., F. Castellvi, M. Ibañez, J.I. Rosell, 1999. Assessment of reliability of the Bowen ratio method for partitioning fluxes, Agricultural and Forest Meteorology, 97, 141-150.

Rimóczi-Paál A., 2005. Mapping of radiation balance components for the region of Hungary using satellite information. Phys. Chem. Earth 30, 151-158.

Roerink G. J., Z. Su and M. Menenti, 2000. S-SEBI: A Roerink G. J., Su Z., Menenti M., 2000, S-SEBI: A Simple Remote Sensing Algorithm to Estimate the Surface Energy Balance, Phys. Chem. Earth (B), Vol. 25, No. 2, pp. 147-157.

Rouse, J. W., Haas, R. H., Schell, J. A., Deering, D. W., and Harlan, J. C., 1974, "Monitoring the vernal advancement and retrogradation (green-wave effect) of natural vegetation," _NASA/GSFC Type III Final Report_, Greenbelt.

Ryu Y., S. Kang, S. Moona and J. Kim, 2008. Evaluation of land surface radiation balance derived from moderate resolution imaging spectroradiometer (MODIS) over complex terrain and heterogeneous landscape on clear sky days. Agr. Forest Meteorol. 148, 1538-1552.

Santos C. A. C. D., Nascimento R. L. D., Rao T. V. R. Manzi, A. O., 2011, Net radiation estimation under pasture and forest in Rondônia, Brazil, with TM Landsat 5 images, Atmosfera 24 (4) pp.435-446

Samani Z., Bawazir A. S., Bleiweiss M., Skaggs R., Tran V.D., 2007, Estimating Daily Net Radiation over

Vegetation Canopy through Remote Sensing and Climatic Data, Journal Of Irrigation And Drainage Engineering, DOI: 10.1061/_ASCE_0733-9437_2007_133:4_291

Silva B. B., G. M. Lopes, and V. Azevedo, 2005. Balanço de radiação em áreas irrigadas utilizando imagens Landsat 5 – TM. Rev. Bras. Meteor. 20, 243-252.

Singh, R. K., Irmak, A., Irmak, S., Martin D. L., 2008, Application of SEBAL model for mapping evapotranspiration and estimating surface energy fluxes in south-central Nebraska. J. Irrig. Drain. Eng. 134, 273-285.

Stroppiana, D., Boschetti, M., Brivio, A., Bocchi, S., 2006, Remotely sensed estimation of rice nitrogen concentration for forcing crop groeth models, Italian Journal of Agrometeorology 3, 50-57.

Şaylan, L., Bakanoğulları, F., Çaldağ, B., Çaylak, O., Özkoca, Y., Semizoğlu, E., Karayusufoğlu S. 2010. Investigation of the possible impacts of climate change to crop growth by crop growth models, I. National Soil and Water Resources Congress, 1-4 June, Eskisehir, Turkey.

Şaylan, L., Semizoğlu Ceyhan, E., Bakanoğullari, F., Çaldağ, B., Özkoca, Y.,

Karayusufoğlu Uysal, S., Altınbaş, N., Eitzinger, J., 2018. Analysis of Seasonal Carbon Dioxide Exchange of Winter Wheat Using Eddy Covariance Method in the Northwest Part of Turkey, Italian Journal of Agrometeorology 3, 39-52.

Tasumi, M., 2003, Progress in operational estimation of regional evapotranspiration using satellite imagery. Ph. D. Dissertation, University of Idaho, Moscow, Idaho.

TSMS, 2000, Turkish state meteorological service, Climate classification. Available at: https://mgm.gov.tr/iklim/iklim-siniflandirmalari.aspx?m=KIRKLARELI. Accessed on 10 July 2017.

TSMS, 2016, Turkish state meteorological service, City-based assessment, Available at https://mgm.gov.tr/veridegerlendirme/il-ve-ilceler-istatistik.aspx?m=KIRKLARELI. Accessed on 27 July 2017.

TUIK, Turkish statistical institute, 2016, Agricultural production statistical tables, Available at http://www.turkstat.gov.tr/PreTablo.do?alt_id=1001. Accessed on 15 July 2017.

Tukey, J. W., 1977, Exploratory data analysis. Addison-Wesely.

Van der Tol, C., 2012: Validation of remote sensing of bare soil ground heat flux. Remote Sensing Environment,121, 275-286.

Verhoef, A., 2004, Remote estimation of thermal inertia and soil heat flux for bare soil.Agric.For.Meteor.,123, 221-236.

Verhoef, A., Ottlé, C., Cappelaere, B., Murray, T., Saux-Picart, S., Zribi, M., Maignan, F., Boulain, N., Demarty, J., Ramier, D., 2012, Spatio-temporal surface soil heat flux estimates from satellite data; results for the AMMA experiment at the Fakara (Niger) supersite. Agricultural Forest Meteor., 154, 55-66.

Wang, J., and Bras, R.L., 1999, Ground heat flux estimated from surface soil temperature. Journal of Hydrology, 216, 214-226.

Wang W. and S. Liang, 2009. Estimation of high-spatial-resolution clear-sky longwave downward and net radiation over land surfaces from MODIS data. Remote Sens. Environ. 113, 745-754.

Finito di stampare da
Logo s.r.l. – Borgoricco (PD) – Italia

RIGOROUS PEER REVIEW

Each submission to IJAm is subject to a rigorous quality control and peer-review evaluation process before receiving a decision. The initial in-house quality control check deals with issues such as competing interests; ethical requirements for studies involving human participants or animals; financial disclosures; full compliance with IJAm's data availability policy, etc.

Submissions may be returned to authors for queries, and will not be seen by our Editorial Board or peer reviewers until they pass this quality control check.

Each paper is subjected to critical evaluation and review by Field Editors with specific expertise in the different areas of interest and by the members of the international Editorial Board.

OPEN ACCESS POLICY

The Italian Journal of Agrometeorology provides immediate open access to its content. Our publisher, Firenze University Press at the University of Florence, complies with the Budapest Open Access Initiative definition of Open Access: By "open access", we mean the free availability on the public internet, the permission for all users to read, download, copy, distribute, print, search, or link to the full text of the articles, crawl them for indexing, pass them as data to software, or use them for any other lawful purpose, without financial, legal, or technical barriers other than those inseparable from gaining access to the internet itself. The only constraint on reproduction and distribution, and the only role for copyright in this domain is to guarantee the original authors with control over the integrity of their work and the right to be properly acknowledged and cited. We support a greater global exchange of knowledge by making the research published in our journal open to the public and reusable under the terms of a Creative Commons Attribution 4.0 International Public License (CC-BY-4.0). Furthermore, we encourage authors to post their pre-publication manuscript in institutional repositories or on their websites prior to and during the submission process and to post the Publisher's final formatted PDF version after publication without embargo. These practices benefit authors with productive exchanges as well as earlier and greater citation of published work.

COPYRIGHT NOTICE

Authors who publish with IJAm agree to the following terms:

Authors retain the copyright and grant the journal right of first publication with the work simultaneously licensed under a Creative Commons Attribution 4.0 International Public License (CC-BY-4.0) that allows others to share the work with an acknowledgment of the work's authorship and initial publication in IJAm.

Authors are able to enter into separate, additional contractual arrangements for the non-exclusive distribution of the journal's published version of the work (e.g., post it to an institutional repository or publish it in a book), with an acknowledgment of its initial publication in this journal.

Authors are allowed and encouraged to post their work online (e.g., in institutional repositories or on their website) prior to and during the submission process, as it can lead to productive exchanges, as well as earlier and greater citation of published work (See The Effect of Open Access).

PUBLICATION FEES

Unlike many open-access journals, the Italian Journal of Agrometeorology does not charge any publication fee.

WAIVER INFORMATION

Fee waivers do not apply at Firenze University Press because our funding does not rely on author charges.

PUBLICATION ETHICS

Responsibilities of IJAm's editors, reviewers, and authors concerning publication ethics and publication malpractice are described in IJAm's Guidelines on Publication Ethics.

CORRECTIONS AND RETRACTIONS

In accordance with the generally accepted standards of scholarly publishing, IJAm does not alter articles after publication: "Articles that have been published should remain extant, exact and unaltered to the maximum extent possible". In cases of serious errors or (suspected) misconduct IJAm publishes corrections and retractions (expressions of concern).

Corrections

In cases of serious errors that affect or significantly impair the reader's understanding or evaluation of the article, IJAm publishes a correction note that is linked to the published article. The published article will be left unchanged.

Retractions

In accordance with the "Retraction Guidelines" by the Committee on Publication Ethics (COPE) IJAm will retract a published article if:

- there is clear evidence that the findings are unreliable, either as a result of misconduct (e.g. data fabrication) or honest error (e.g. miscalculation)
- the findings have previously been published elsewhere without proper crossreferencing, permission or justification (i.e. cases of redundant publication)
- it turns out to be an act of plagiarism
- it reports unethical research.
- An article is retracted by publishing a retraction notice that is linked to or replaces the retracted article. IJAm will make any effort to clearly identify a retracted article as such.

If an investigation is underway that might result in the retraction of an article IJAm may choose to alert readers by publishing an expression of concern.

ARCHIVING

IJAm and Firenze University Press are experimenting a National legal deposition and long-term digital preservation service.

SUBMITTING TO IJAm

Submissions to IJAm are made using FUP website. Registration and access are available at: https://riviste.fupress.net/index.php/IJAm/submission

For more information about the journal and guidance on how to submit, please see https://riviste.fupress.net/index.php/IJAm/index

Principal Contact
Simone Orlandini, University of Florence
simone.orlandini@unifi.it

Support Contact
Alessandro Pierno, Firenze University Press
alessandro.pierno@unifi.it

GUIDE FOR AUTHORS

1. Manuscript should refer to original researches, not yet published except in strictly preliminary form.
2. Articles of original researches findings are published in Italian Journal of Agrometeorology (IJAm), subsequent to critical review and approval by the Editorial Board. External referees could be engaged for particular topics.
3. Three types of paper can be submitted: original paper, review, technical note. Manuscript must be written in English, with the exception of technical note that can be both in English or in Italian. All pages and lines of the manuscript should be numbered.
4. First Name, Last Name, position, affiliation, mail address, telephone and fax number of all the Co-Authors are required. Corresponding Authors should be clearly identified.
5. The abstract should be no longer than 12 typed lines and should be written in both English and Italian.
Keywords and title should be written in both English and Italian.
6. Full stop, not comma, must be used as decimal mark (e.g. 4.33 and not 4,33).
7. Figures, tables, graphs, photos and relative captions should be attached in separate files. All images must be vector or at least 300 effective ppi/dpi to ensure quality reproduction.
8. Captions should be written both in English and Italian and should be written as: Fig.x – Caption title, Tab.x – Caption title. Images should be referred to in the text as (Fig.x), (Tab.x). The translation must be written in italic: Fig.x – Caption title, Tab.x – Caption title.
9. For foreign authors, all requested translations into Italian will be made by AIAM.
10. Proof of the paper (formatted according to the Journal style) will be sent to the Corresponding Author for proof reading just one time. Corrections can be made only to typographical errors.
11. All the references in the text must be reported in the "References" section and vice-versa. In the text, only the Author(s) last name must be present, without the name or the first letter of the name (e.g. "Rossi, 2003" and not "Federico Rossi, 2003" or "F. Rossi, 2003"). If two authors are present, refer to them as: "Bianchi and Rossi, 2003" in the text (do not use "&" between the surnames). If more than two Authors are present, refer to them as: "Bianchi et al., 2003" in the text.
For journals, references must be in the following form:
Bianchi R., Colombo B., Ferretti N., 2003. Title. Journal name, number: pages.
For books:
Bianchi R., Colombo B., Ferretti N., 2003. Book title. Publisher, publishing location, total number of pages pp.
Manuscripts "in press" can be cited.

BECOME A REVIEWER

Peer review is an integral part of the scholarly publishing process. By registering as a reviewer, you are supporting the academic community by providing constructive feedback on new research, helping to ensure both the quality and integrity of published work in your field. Once registered, you may be asked to undertake reviews of scholarly articles that match your research interests. Reviewers always have the option to decline an invitation to review and we take care not to overburden our reviewers with excessive requests.

You must login before you can become a reviewer.

If you don't want to be a reviewer anymore, you can change your roles by editing your profile.

COMPETING INTERESTS

You should not accept a review assignment if you have a potential competing interest, including the following:

- Prior or current collaborations with the author(s)
- You are a direct competitor
- You may have a known history of antipathy with the author(s)
- You might profit financially from the work

Please inform the editors or journal staff and recuse yourself if you feel that you are unable to offer an impartial review.

When submitting your review, you must indicate whether or not you have any competing interests.

Italian Journal of Agrometeorology

Rivista Italiana di Agrometeorologia

n. 2 – 2019

Table of contents